

Arckaringa Basin aquifer connectivity

DEWNR Technical report 2015/14



Government of South Australia
Department of Environment,
Water and Natural Resources

*Funding for these projects has been provided
by the Australian Government through the
Bioregional Assessment Programme.*

Arckaringa Basin aquifer connectivity

Tavis Kleinig, Stacey Priestley, Daniel Wohling and Neville Robinson
Department of Environment, Water and Natural Resources

June, 2015

DEWNR Technical report 2015/14



Department of Environment, Water and Natural Resources

GPO Box 1047, Adelaide SA 5001

Telephone National (08) 8463 6946
 International +61 8 8463 6946

Fax National (08) 8463 6999
 International +61 8 8463 6999

Website www.environment.sa.gov.au

Disclaimer

The Department of Environment, Water and Natural Resources and its employees do not warrant or make any representation regarding the use, or results of the use, of the information contained herein as regards to its correctness, accuracy, reliability, currency or otherwise. The Department of Environment, Water and Natural Resources and its employees expressly disclaims all liability or responsibility to any person using the information or advice. Information contained in this document is correct at the time of writing.



This work is licensed under the Creative Commons Attribution 4.0 International License.

To view a copy of this license, visit <http://creativecommons.org/licenses/by/4.0/>.

ISBN 978-1-922255-53-2

Preferred way to cite this publication

Kleinig T, Priestley S, Wohling D and Robinson N, 2015, *Arckaringa Basin aquifer connectivity*, DEWNR Technical report 2015/14, Government of South Australia, through Department of Environment, Water and Natural Resources, Adelaide

Download this document at: <http://www.waterconnect.sa.gov.au>

Foreword

The Department of Environment, Water and Natural Resources (DEWNR) is responsible for the management of the State's natural resources, ranging from policy leadership to on-ground delivery in consultation with government, industry and communities.

High-quality science and effective monitoring provides the foundation for the successful management of our environment and natural resources. This is achieved through undertaking appropriate research, investigations, assessments, monitoring and evaluation.

DEWNR's strong partnerships with educational and research institutions, industries, government agencies, Natural Resources Management Boards and the community ensures that there is continual capacity building across the sector, and that the best skills and expertise are used to inform decision making.

Sandy Pitcher
CHIEF EXECUTIVE
DEPARTMENT OF ENVIRONMENT, WATER AND NATURAL RESOURCES

Acknowledgements

The project team would like to acknowledge the following for their assistance with this project:

- OZ Minerals Limited, in particular Jasmine Richards and Luke Polkinghorne
- Mount Eba Station
- Kent Inverarity – DEWNR
- James Hickey – DEWNR
- Lloyd Sampson – DEWNR for internal peer review
- Andy Love – Flinders University for external peer review
- Vincent Post – Flinders University
- Paul Shand – CSIRO Land and Water, Adelaide

Contents

Foreword	ii
Acknowledgements	iii
Summary	8
1 Introduction	10
1.1 Background	10
1.2 Arckaringa Basin groundwater assessment	12
1.3 Aquifer connectivity investigation	12
1.4 Objectives	13
2 Regional setting	14
2.1 Location and geography	14
2.2 Geology	16
2.3 Hydrogeology	19
2.3.1 Summary of existing knowledge	19
2.3.2 Existing understanding of intra-basin connectivity	21
2.3.3 Existing understanding of inter-basin connectivity – connectivity between the Boorthanna Formation and J-K aquifers	23
3 Methodology	25
3.1 Site selection	25
3.2 Site location	25
3.3 Drilling and construction	25
3.4 Core sampling	29
3.5 Core analysis	30
3.6 Vibrating wire piezometers	31
3.7 Pressure-elevation profile	31
3.8 Modelling	32
3.8.1 Analytical modelling	32
3.8.2 Numerical modelling	32
4 Results and discussion	34
4.1 Drilling program	34
4.2 Site hydrogeology	34
4.3 Physical properties	35
4.3.1 Water potential	35
4.3.2 Gravimetric water content	35
4.3.3 Permeability coefficient	35
4.3.4 Porosity	36
4.3.5 Particle size analysis	37
4.4 Chemistry and environmental tracers	39
4.4.1 Major ion chemistry	39
4.4.2 Stable isotopes of water	42

4.4.2.1	Deuterium ($\delta^2\text{H}$) porewater	43
4.4.2.2	$\delta^{18}\text{O}$ porewater	44
4.4.3	Noble gases	45
4.5	Pore pressure	45
4.6	Modelling	46
4.6.1	Fitting data to the entire aquitard	46
4.6.1.1	Analytical modelling	46
4.6.1.2	Numerical modelling	48
4.6.2	Fitting data as two distinct aquitard layers	50
4.6.2.1	Analytical modelling	50
4.7	Flux estimates	54
5	Up-scaling of aquifer connectivity site results	55
5.1	Palaeohydrogeological systems	55
5.2	Regional aquifer connectivity and groundwater flow	55
5.2.1	Inferred from hydraulics	56
5.2.2	Inferred from environmental tracers	64
5.2.3	Inferred from noble gases	65
6	Conclusions	70
7	Appendices	72
A.	Composite log: unit number 6038-519	72
B.	The transport equation	73
C.	Core descriptions and photographs	76
D.	Physical parameter plots	81
8	Units of measurement	82
8.1	Units of measurement commonly used (SI and non-SI Australian legal)	82
8.2	Shortened forms	82
9	Glossary	83
10	References	85

List of figures

Figure 1-1 Lake Eyre Basin	11
Figure 2-1 Arckaringa subregion location map	15
Figure 2-2 Simplified Cambrian to Cretaceous stratigraphy, hydrostratigraphy and general lithology, Arckaringa subregion	18
Figure 2-3 Intra-basin connectivity in the Arckaringa Basin	22
Figure 2-4 Connectivity between Arckaringa Basin strata and overlying basins and rocks	24
Figure 3-1 Investigation site location map	26
Figure 3-2 Boart Longyear LF90 rig and support vehicles during drilling	27
Figure 3-3 6038-519 VWP datalogger box, with groundwater monitoring well RMS-7 (formerly VMS-2) in the background	28
Figure 3-4 Core sub-portion from interval 47–48.5 m BGS, showing the outer 1–2 mm impacted by drilling fluids (darkened)	30
Figure 4-1 Permeability coefficient depth profile	36
Figure 4-2 Total porosity depth profile	37
Figure 4-3 Particle size (sand and clay) analysis profile	39
Figure 4-4 Chloride depth profile	40
Figure 4-5 Groundwater Cl ⁻ concentration data for Boorthanna Formation well RMD-7	41
Figure 4-6 Groundwater Cl ⁻ concentration data for J-K aquifer well RMS-7	41
Figure 4-7 Stable water isotope composition of aquitard porewater, J-K aquifer and Boorthanna Formation	43
Figure 4-8 Deuterium ($\delta^2\text{H}$) aquitard porewater, J-K aquifer and Boorthanna Formation depth profile	44
Figure 4-9 $\delta^{18}\text{O}$ profile aquitard porewater, J-K aquifer and Boorthanna Formation	45
Figure 4-10 Pressure versus elevation/depth profile	46
Figure 4-11 Single layer aquitard fitting of analytical solution to porewater chloride data	47
Figure 4-12 Measured and initial steady state (4 Ma) modelled chloride concentration in aquitard porewater and groundwater	49
Figure 4-13 Lines of best fit to water potential data	51
Figure 4-14 Two layer aquitard fitting of analytical solution to porewater chloride data	52
Figure 4-15 Diffusive flux and advective flux for two layer aquitard	53
Figure 5-1 Potential leakage pathways through an aquitard	56
Figure 5-2 Location of well nests	62
Figure 5-3 Environmental tracer data for well nests: [a] $^{87}\text{Sr}/^{86}\text{Sr}$ vs $1/\text{Sr}$ (ppm^{-1}) [b] $^{36}\text{Cl}/\text{Cl}$ ($\times 10^{-15}$) vs Cl (mg/L) [c] ^{14}C (pMC) vs $\delta^{18}\text{O}$ [d] $\delta^{13}\text{C}$ (‰) vs $^{87}\text{Sr}/^{86}\text{Sr}$	65
Figure 5-4 Radiogenic ^4He concentrations in the Arckaringa sub-region	68
Figure 5-5 $^3\text{He}/^4\text{He}$ isotope ratios in the Arckaringa sub-region	69

List of tables

Table 2-1	Description of relevant geological and hydrogeological formations within the study extent	17
Table 2-2	Summary of relevant current knowledge of hydrogeology of the Arckaringa Basin	19
Table 3-1	Summary of completion and location details	29
Table 3-2	Model parameters	32
Table 4-1	Formation depths and thickness	34
Table 4-2	Density corrected and uncorrected reduced standing water levels	35
Table 4-3	Permeability coefficients	36
Table 4-4	Laboratory porosities	37
Table 4-5	Particle size analysis	38
Table 4-6	Times and porewater velocities from single layer fitting	48
Table 4-7	Initial concentration and boundary conditions (BC) adopted for chloride simulations	49
Table 4-8	Chloride concentrations and water potentials at, and directly above and below, the 66.38 m BGS sample53	53
Table 4-9	Range of Darcy fluxes	54
Table 5-1	Well nests showing aquifer monitored, RSWL, Stuart Range Formation thickness and calculated vertical flow rates	58

Summary

The Australian Government through the Department of the Environment funded the South Australian Department of Environment, Water and Natural Resources (DEWNR) to collate and ground-truth baseline groundwater, surface water and ecology information to inform the Bioregional Assessment Programme in the Lake Eyre Basin (LEB). Within the LEB bioregion a series of studies forming part of the Arckaringa Basin and Pedirka Basin Groundwater Assessment project have been undertaken. This report documents the investigation of aquifer connectivity in the Arckaringa subregion; and forms a key component of the Arckaringa Basin and Pedirka Basin Groundwater Assessment project.

This project involved the continuous coring of a hole to a depth of 110.4 m below ground surface (BGS) through the Great Artesian Basin (GAB) and into the Arckaringa Basin to provide an assessment of vertical flow in the Arckaringa subregion via hydraulic, hydrogeological, and hydrochemical analysis. Point estimates from the vertical core profile were used to develop 1D analytical and numerical models to simulate the evolution of the measured porewater chemistry profile. Point estimates of aquitard (Stuart Range Formation) hydraulic head were obtained via vibrating wire piezometers (VWPs). Upscaling of groundwater inter-aquifer connectivity to a regional scale was undertaken using regional hydraulic head and hydrochemical data, especially noble gases. This provided an improved understanding of inter-connectivity between the Arckaringa Basin (Permian sequences) and overlying GAB (J-K aquifer).

The investigation utilised the aforementioned multiple investigation techniques to reveal that there is a low degree of connectivity between the Arckaringa Basin and overlying J-K aquifer. It was determined that flow (flux) through the aquitard is small, in the order of millimetres per 1000 years. Aquitard (Stuart Range Formation) physical parameters obtained via laboratory analysis included porosity (12.1 to 26 % volume), particle size analysis (sand 4 to 32 %, silt 23 to 39 %, and clay 39 to 70 %), and permeability coefficients (K_v) (ranging from 4×10^{-13} to 4×10^{-10} m/s, median of 4.5×10^{-12} m/s (3.9×10^{-7} m/d)). One-dimensional (1D) analytical modelling indicated a possible K_v range of 4.8×10^{-13} to 5.3×10^{-12} m/s (4.2×10^{-8} to 4.6×10^{-7} m/d). One-dimensional numerical modelling of the chloride profile suggested an optimal K_v of 1×10^{-12} m/s (8.6×10^{-8} m/d). Given the similarity of measured and modelled results the multi-technique approach provides a K_v value representative of the regional-scale. Further work is recommended using the regional Arckaringa Basin numerical model, to test the impact of K_v 's reported in this investigation which were around four orders of magnitude less than K_v 's previously assigned to the Stuart Range Formation.

Several lines of evidence (porewater chemistry, porewater potential, lithology) indicated aquitard variability and provided justification to simulate profile development using a two-layer analytical solution. Contrary to the overall hydraulic potential for downward flux, and Peclet number suggesting a diffusion dominant system at the investigation site; the two-layer analytical solution provided evidence for an upward flux component from the upper portion of the aquitard profile possibly related to lateral flows in the aquitard, and implied that advection dominates over diffusion. Further work is suggested to investigate the potential for advective flow in the aquitard including; 1) analysis of apparent porewater age and implications for ancient aquitard/aquifer Cl^- concentrations to constrain our regional conceptualisation of groundwater and porewater flow paths, 2) test this conceptualisation through setting of appropriate boundary conditions for analytical or numerical solutions, and 3) implement and test an advection-dominant solution scheme in MT3DMS for future 1D numerical modelling of the aquitard.

Work to upscale aquifer connectivity concluded there was a lack of connectivity between the Boorthanna Formation and J-K aquifer at the majority of assessed locations; although evidence from hydraulics and hydrochemistry suggests localised connectivity between the Boorthanna Formation and J-K aquifer does occur due to secondary permeability in the Stuart Range Formation. There was also evidence for connectivity between the Boorthanna Formation and basement at one location, which likely represents a wider area.

The approach of combining geochemical and isotopic profiling with in-situ hydrodynamics has the benefit of characterising the hydrostratigraphic units at a scale (i.e. regional) that is likely to be of interest for groundwater resource management. These methods have provided a reliable range of estimates for aquitard hydraulic conductivity, enabling the constraint of aquifer connectivity (flux) estimates and increasing confidence in the assessment of aquifer connectivity. Although, additional investigation of aquitard chemistry is warranted, to further understand the differences observed in the Cl^- , $\delta^2\text{H}$ and $\delta^{18}\text{O}$ profiles.

Finally, vertical profiles of aquitard porewater chloride indicate a complex palaeohydrogeology with associated salinity variability. The Cl⁻ profile and associated 1D analytical and numerical modelling enabled an improved understanding of regional palaeohydrogeological conditions in arid areas, which have not been glaciated for hundreds of millions of years, and suggested potential long-term changes in aquifer salinity within the Quaternary period. It is thought that this is one of the few investigations in Australia that has undertaken this type of aquitard assessment.

1 Introduction

1.1 Background

In 2012, the Australian Government established an Independent Expert Scientific Committee (IESC) on Coal Seam Gas (CSG) and Large Coal Mining (LCM) developments to provide independent, expert scientific advice on the future impact these activities may have on water resources. The IESC is a statutory body under the *Environment Protection and Biodiversity Conservation Act 1999* (EPBC Act) which provides scientific advice to Australian governments on the water-related impacts of coal seam gas and large coal mining development proposals. Under the EPBC Act, the IESC has several legislative functions to:

- Provide scientific advice to the Commonwealth Environment Minister and relevant state ministers on the water-related impacts of proposed coal seam gas or large coal mining developments
- Provide scientific advice to the Commonwealth Environment Minister on:
 - Bioregional assessments being undertaken by the Australian Government, and
 - Research priorities and projects commissioned by the Commonwealth Environment Minister
- Publish and disseminate scientific information about the impacts of coal seam gas and large coal mining activities on water resources

The Bioregional Assessment Programme is a transparent and accessible programme of baseline assessments that increase the available science for decision making associated with potential water-related impacts of coal seam gas and large coal mining developments. A bioregional assessment is a scientific analysis of the ecology, hydrology, geology and hydrogeology of a bioregion with explicit assessment of the potential direct, indirect and cumulative impacts of coal seam gas and large coal mining development on water resources. This Programme draws on the best available scientific information and knowledge from many sources, including government, industry and regional communities, to produce bioregional assessments that are independent, scientifically robust, and relevant and meaningful at a regional scale. For more information on bioregional assessments, visit <<http://www.bioregionalassessments.gov.au>>.

The Australian Government through the Department of the Environment funded the South Australian Department of Environment, Water and Natural Resources (DEWNR) to collate and ground-truth baseline groundwater, surface water and ecology information to inform the Bioregional Assessment Programme in the Lake Eyre Basin. The Lake Eyre Basin (LEB) bioregion (Figure 1-1) has been identified as one of six priority areas for a bioregional assessment across Australia. Within the LEB bioregion there are four subregions being the Arckaringa, Pedirka, Cooper and Galilee. This report is part of a series of studies forming part of the Arckaringa Basin and Pedirka Basin Groundwater Assessment project. The Arckaringa Basin and Pedirka Basin Groundwater Assessment project is one of three water knowledge projects undertaken by DEWNR in the western Lake Eyre Basin bioregion, which are:

- Lake Eyre Basin Rivers Monitoring project
- Arckaringa Basin and Pedirka Basin Groundwater Assessment project
- Lake Eyre Basin Springs project

This report documents the investigation of aquifer connectivity in the Arckaringa subregion; and forms a key component of the Arckaringa Basin and Pedirka Basin Groundwater Assessment project.

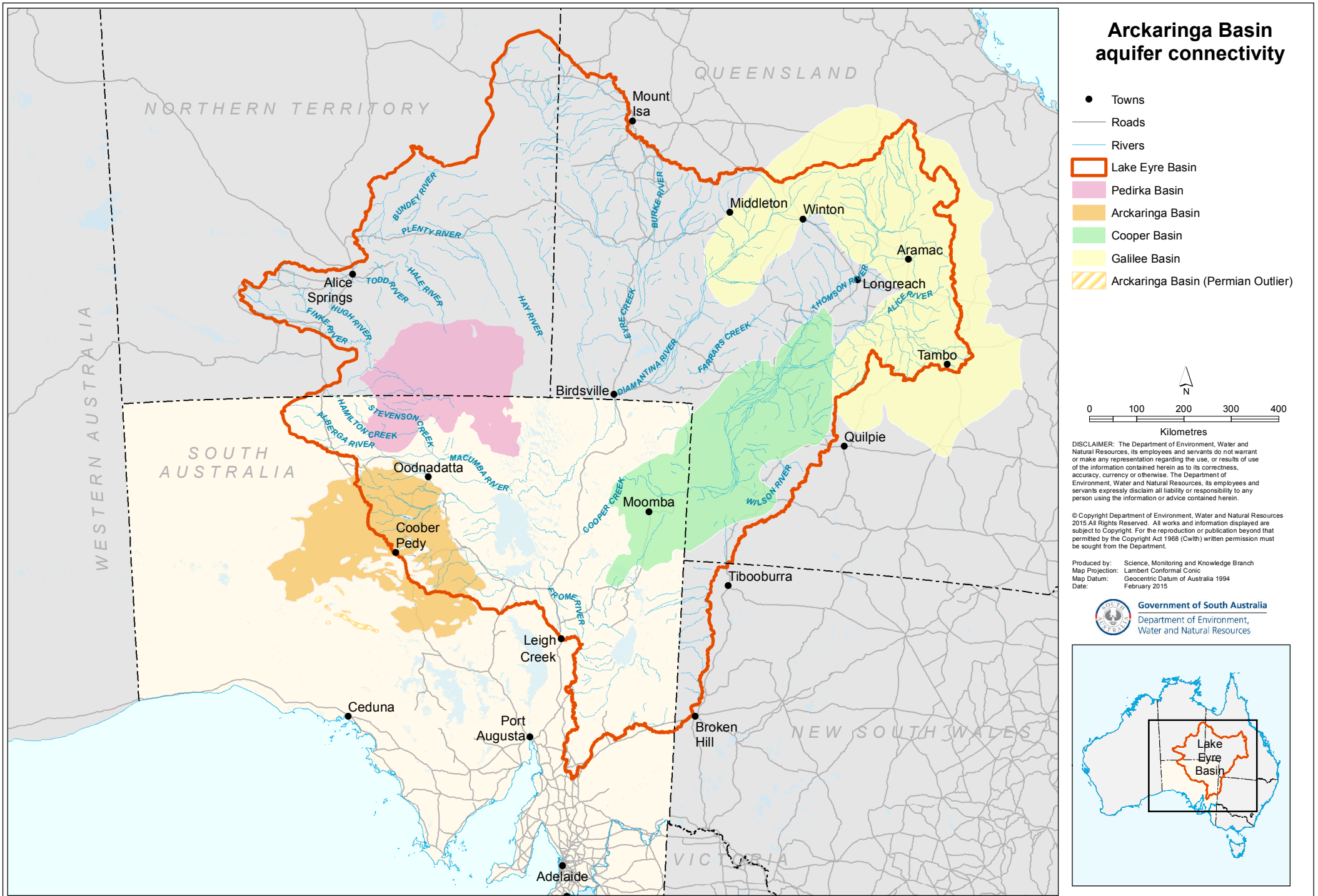


Figure 1-1 Lake Eyre Basin

1.2 Arckaringa Basin groundwater assessment

In 2013, DEWNR undertook a desktop assessment aimed at benchmarking the level of hydrogeological knowledge for the Arckaringa and Pedirka basins (Wohling et al., 2013). The review identified fundamental data gaps in the characterisation of the Arckaringa Basin groundwater system, including:

- Uncertainty surrounding recharge mechanisms, recharge rates and the spatial extent of recharge zones providing inflow to the Arckaringa Basin.
- Limited information on the permeability, transmissivity, hydraulic conductivity and storativity of formations within the Arckaringa Basin
- Uncertainty surrounds the effectiveness of the Stuart Range Formation as an aquitard separating overlying aquifers within the Arckaringa Basin (Mount Toondina Formation) and Great Artesian Basin (GAB) (J-K aquifer) and underlying Boorthanna Formation (Arckaringa Basin), particularly the extent and composition of sediments.
- Paucity of information from which to make confident assessments of the entire basin including spatial and temporal groundwater flow rates.

As part of the Arckaringa Basin Groundwater Assessment project, DEWNR developed an investigation program to address some of these knowledge gaps. The program aims to deliver several targeted studies that will feed into a broader regional assessment of Arckaringa subregion hydrogeology, as well as providing vital information for, and linkage with, the LEB Bioregional Assessment. There are two key themes for targeted investigation: aquifer connectivity, and regional hydrogeological characterisation (Keppel et al., 2015). This report details findings from the aquifer connectivity investigation.

1.3 Aquifer connectivity investigation

The IESC released a background review of aquifer connectivity within the Great Artesian Basin, and the Surat, Bowen and Galilee Basins (Commonwealth of Australia, 2014). The review describes a variety of scientific methods developed to measure and model aquifer connectivity including hydraulic, laboratory, geophysical, as well as analytical and numerical modelling approaches on both spatial and temporal scales. The review recommends, where possible, the application of multiple approaches to improve confidence in the assessment of aquifer connectivity.

Due to the very low permeability of most regional aquitards, many conventional hydraulic and tracer techniques that are applied to study aquitards offer minimal opportunity for determining diffuse recharge in the GAB (Harrington et al., 2013, Love et al., 2013b). The most appropriate techniques for characterising flow and solute transport at the regional scale use natural hydrochemical and isotopic tracers within aquitard porewater (Love et al., 2013b). Tracer-based methods are considered by Smerdon et al. (2014) to be one of the most reliable methods of estimating regional-scale hydraulic conductivity. The interpretation of natural tracer porewater profiles can provide a powerful tool for upscaling solute transport behaviour in space and time (Mazurek et al., 2011). The approach involves (Love et al., 2013b):

1. obtaining a vertical porewater profile
2. creating a conceptual model of profile development over time
3. applying analytical or numerical solute transport models to test conceptual models, and quantify porewater velocity

The application of multiple tracers provides further constraint on the range of fluid flux estimates and, hence, the estimates of aquitard hydraulic properties. Multiple tracers help maximise the knowledge gained from field investigations.

Existing information on the hydrogeology of the Arckaringa Basin and its potential connection with the GAB is limited in spatial extent. A summary of existing information is provided in Keppel et al. (2015). The Arckaringa Basin aquifer connectivity investigation aims to improve our knowledge through the undertaking of a drilling/coring program. This program will allow for the application of hydraulic and geochemical techniques to characterise the connectivity between the Arckaringa Basin and GAB while also establishing a site for longer-term monitoring and future studies.

1.4 Objectives

The Arckaringa Basin aquifer connectivity investigation aims to deliver an improved understanding of aquifer connectivity between Permian formations of the Arckaringa Basin and the overlying GAB sequence, and to advance the conceptual understanding of basin processes to inform future water resource and development activities. The assessment has the following specific objectives:

1. Provide an assessment of aquifer connectivity using a robust methodology that is transferable across this and other basins, including through deep coal bearing units.
2. Continuously core a hole through the GAB and into the Arckaringa Basin sequence in order to create a detailed hydrostratigraphic type section and to provide an assessment of vertical flow in the Arckaringa Basin via hydraulic, hydrogeological, hydrochemical and geophysical analysis. Thus providing an improved understanding of connectivity between the Permian sequence and overlying GAB (J-K aquifer)
3. Provide estimates of hydraulic parameters for the Stuart Range Formation, and other formations if possible
4. Evaluate site specific connectivity findings in the context of the greater Arckaringa Basin

Information on aquifer connectivity (leakage through the Stuart Range Formation aquitard) will be provided using three (scale dependent) techniques:

1. Point estimates from a vertical core profile to develop 1D numerical and analytical models to simulate the evolution of the measured porewater chemistry profile. This may serve as an archive for past hydrogeological conditions and provide useful information for transient modelling.
2. Point estimate of aquitard hydraulic head via use of vibrating wire piezometers (VWPs). Installation of VWPs will provide longer-term assessment of pressure response in the aquitard, including any natural decline in pressure in the GAB, and any potential changes from pumping activity at our investigation scale.
3. Upscaling groundwater inter-aquifer connectivity to a regional scale using regional hydraulic head and hydrochemical data, particularly noble gases.

The new knowledge gained will provide baseline hydrogeological information to allow for advancement of the conceptual understanding of hydrodynamic processes within the Arckaringa Basin, and inform numerical groundwater modelling.

2 Regional setting

The location, geography, geology and current understanding of the hydrogeology have been recently described by Wohling et al. (2013), and Keppel et al. (2015). A summary of information from these sources with direct relevance to this report is provided below.

2.1 Location and geography

The Arckaringa subregion is in northern South Australia, approximately 600 km north–north-west of Adelaide. The subregion area is based on the subsurface extent of the main part of the Arckaringa Basin, which covers an area of approximately 100 000 km² and is bordered by a series of ranges, ridges and plateaus (Figure 2-1). The climate of the subregion is arid, with weather patterns dominated by persistent high pressure systems. Rainfall is predominantly sourced from weak winter cold fronts originating from the Southern Indian Ocean or sporadic summer monsoon rainfall that originates in north-west Australia; rainfall for the region averages 150 mm/y, although this can vary significantly from year to year. The landscape is largely flat-lying, desert-dominated, consisting of sand dunes and gibber plains. Vegetation of the region is composed of species adapted for survival in arid climates.

Coober Pedy is the largest town in the area, with a population of approximately 2000. Other towns in the vicinity include Roxby Downs, Marla and Oodnadatta. Parts of the Pitjantjatjara, Yankunytjatjara and Ngaanyatjarra (or Anangu) Aboriginal freehold lands are situated within the Arckaringa subregion.

The pastoral industry represents the predominant land use across the subregion, while mining and tourism are increasingly important industries. The OZ Minerals Prominent Hill copper-gold mine, Arrium Peculiar Knob iron ore and Cu-River Mining Cairn Hill iron ore mine (formerly owned by Termite Resources and recently placed into 'care-and-maintenance') are in the south-eastern portion of the Arckaringa subregion. The majority of water supplies for domestic, pastoral, commercial and industrial purposes in the subregion are derived from groundwater as surface water resources are limited and unreliable. Most groundwater is sourced from the GAB due to quality (salinity, which ranges from 500 to 72 000 mg/L total dissolved solids (TDS), but typically groundwater quality is towards the lower end of the range) and shallower depth, with some supplies derived from the underlying Arckaringa Basin. Prominent Hill is the largest user of water in the region and sources water from the Arckaringa Basin (Boorthanna Formation).

The Prominent Hill copper-gold mine is comprised of the Malu open pit mine, Ankata underground mine, a grinding and flotation processing plant, permanent village, haulage road, power line and borefields. The site is dependent on the supply of groundwater to sustain its operation. Groundwater is extracted from the Boorthanna Formation within the Arckaringa Basin, primarily from the Aries Borefield. OZ Minerals occasionally use groundwater from the Virgo Borefield, despite it being more saline. OZ Minerals, who own and operate the mine, have licence to extract 26.6 ML/d from the Boorthanna Formation aquifer. In 2014, Prominent Hill mines total groundwater use was 5919 ML <http://www.ozminerals.com/2014-sustainability-report/Environmental/Water_management/water_management.htm>. Other extraction from Permian aquifers is minimal across the Arckaringa Basin.

There are a number of pastoral and mining production wells within the Arckaringa subregion that extract groundwater from aquifers within the GAB. Volumes of groundwater extracted from aquifers within the GAB in the study extent are not known with certainty, largely due to being unmetred stock and domestic use.

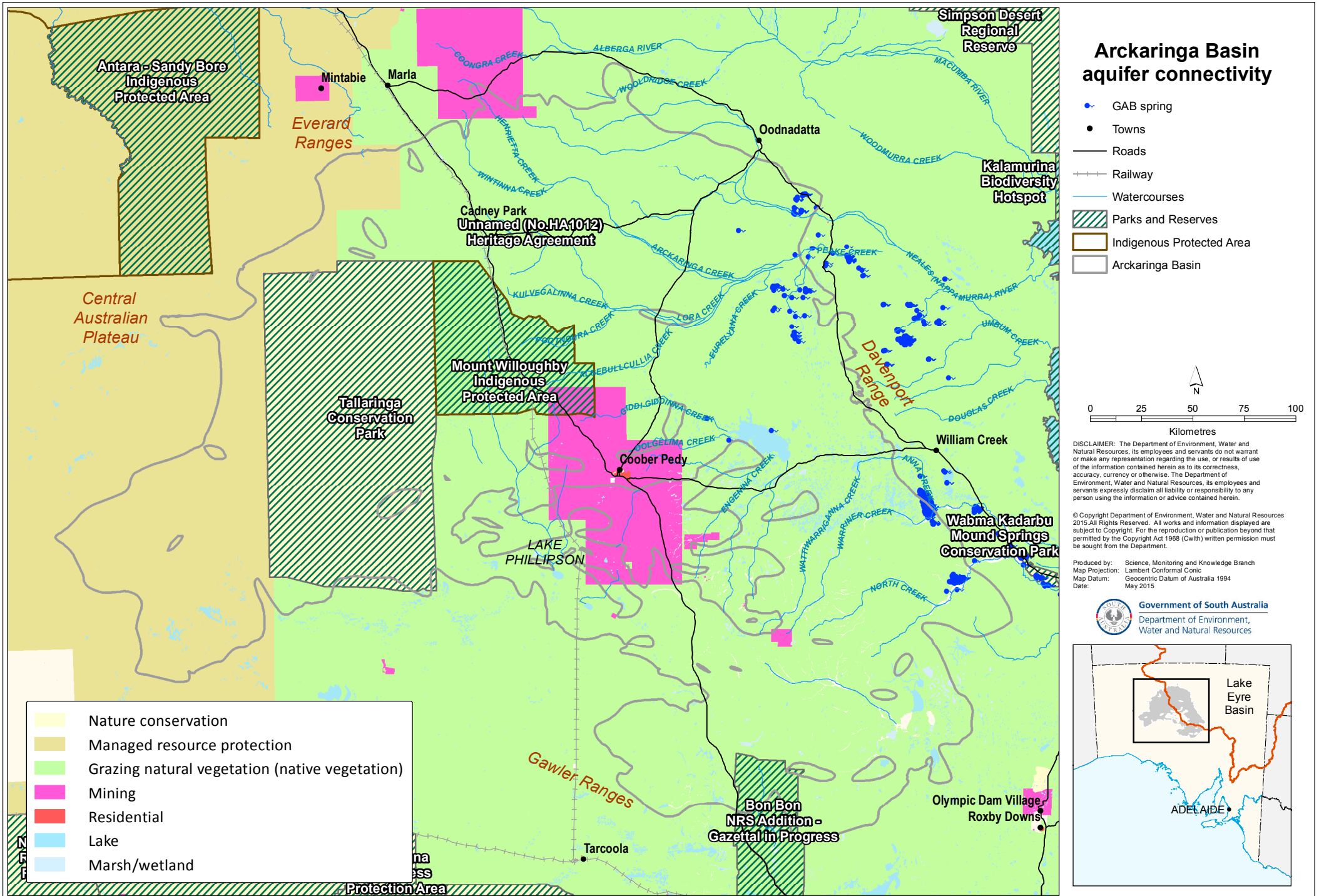


Figure 2-1 Arckaringa Subregion location map

2.2 Geology

The Arckaringa Basin is a sedimentary basin comprising Carboniferous to Permian sediments, the majority of which are sub cropping. The basin unconformably overlies the Warburton and Officer basins and Proterozoic basement rock. The Arckaringa Basin unconformably underlies the Mesozoic Eromanga Basin, synonymous with the Great Artesian Basin. The western portion of the Arckaringa Basin is thin, geologically simple and moderately faulted, whereas the eastern portion of the basin is more geologically complex, with structure influenced by faulting and glacial scouring (Wohling et al., 2013).

There are three major recognised hydrogeological formations within the Arckaringa Basin: Mount Toondina Formation, Stuart Range Formation and the underlying Boorthanna Formation. Table 2-1 provides a summary of the geological and hydrogeological formations encountered with depth within the Arckaringa Basin study extent. A summary of the stratigraphy of the Arckaringa Basin as well as overlying and underlying formations is provided in Figure 2-2. This summary is based on more detailed descriptions provided in Wohling et al. (2013) and Keppel et al. (2015). In addition, Appendix A presents a borehole composite log and Appendix B a detailed description and photographs from the continuous core drilled as part of this work program.

Table 2-1 Description of relevant geological and hydrogeological formations within the study extent (after Purczel, 2015)

Geological Basin	Hydro-stratigraphy	Geological Unit(s)	Age	Depositional Environment	Description of Lithology	Hydrogeological Characteristics
Great Artesian Basin	-	Bulldog Shale	Cretaceous	Low energy marine	Marine shaley mudstone and silt	Aquitard
	J-K aquifer	Cadna-owie Formation Algebuckina Sandstone	Mid-Cretaceous to Jurassic	Marine transitional and terrestrial	Fine to coarse grained sandstone and siltstone	Aquifer
Arckaringa Basin	-	Mount Toondina Formation	Permian (195 – 290.1 Ma)	Non-marine lagoons and swamps with intermittent fluvial	Carbonaceous shale, coal and interbedded sandstones and siltstone	Potential aquifers and aquitards within the one formation
	-	Stuart Range Formation	Permian (298.9 – 290.1 Ma)	Brackish restricted marine with periods of anoxic, bottom water conditions	Marine mudstones, siltstones and shales	Potential aquitard
	-	Boorthanna Formation	Permian (298.9 – 295.0 Ma)	Marine and glacial	Upper unit a marine conglomerate and sandstone; lower unit is boulder clays (diamictite)	Potential aquifers and aquitards within the one formation

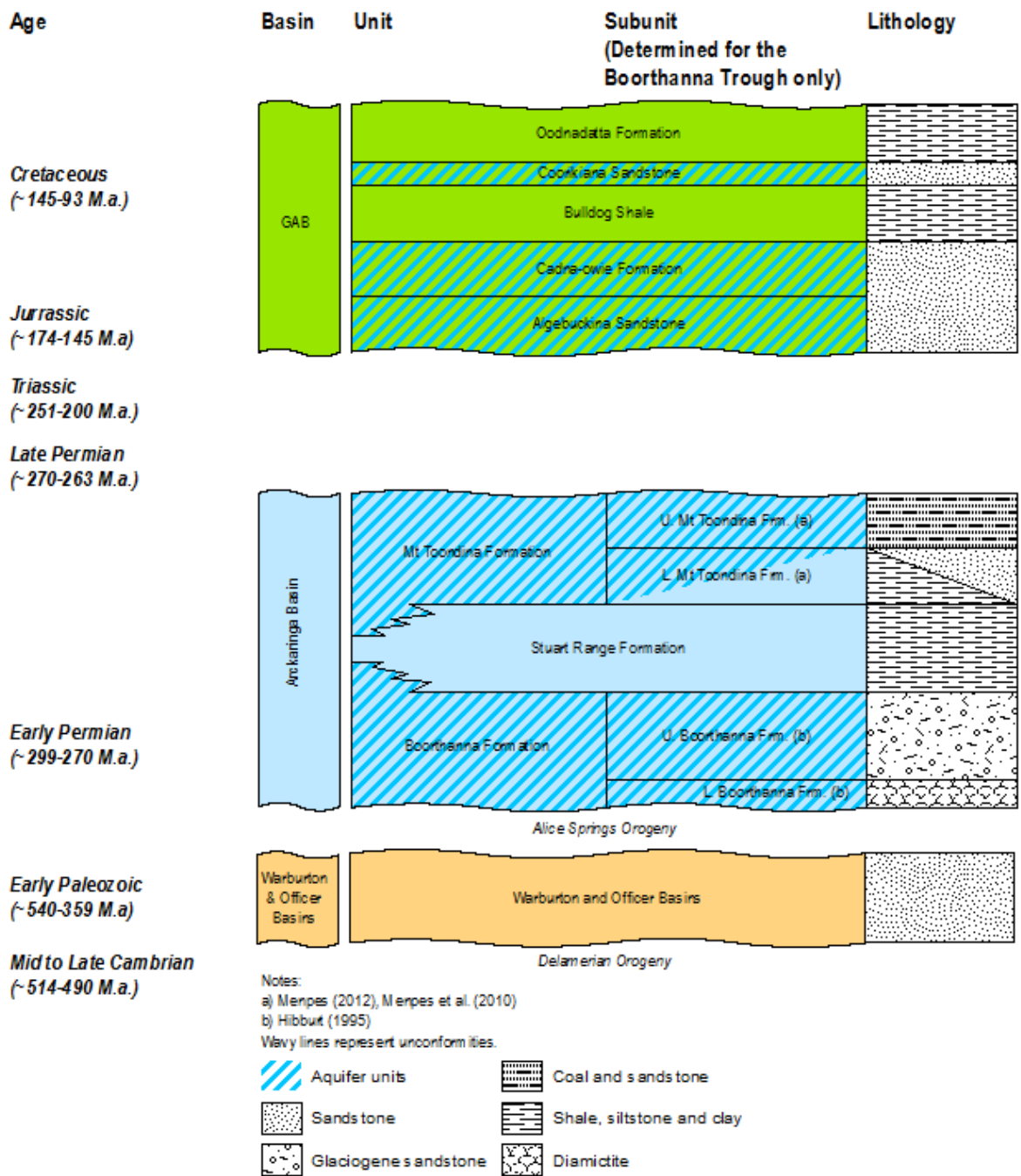


Figure 2-2 Simplified Cambrian to Cretaceous stratigraphy, hydrostratigraphy and general lithology, Arckaringa subregion. From Keppel et al. (2015).

2.3 Hydrogeology

2.3.1 Summary of existing knowledge

A summary of previous knowledge concerning the hydrogeology of the Arkaringa Basin has been provided in Wohling et al. (2013) and Keppel et al. (2015). A summary of hydrogeology knowledge in the Arkaringa Basin relevant to this project is provided in Table 2-2. It should be noted that many of the hydraulic parameters provided for the formations in this table are based on very limited data and/or from studies with a very specific focus. Consequently care should be taken when applying such parameters at a regional scale.

Table 2-2 Summary of relevant current knowledge of hydrogeology of the Arkaringa Basin

Hydrogeological property/process	Component	Summary of current information
Recharge	Recharge zones and mechanisms	Recharge to the Arkaringa Basin aquifers within the Mount Toondina and Boorthanna formations is most likely to occur in regions where aquifers within the overlying GAB, the Cadna-Owie Formation and Algebuckina Sandstone referred to herein as J-K aquifer, are unsaturated and confining layers, such as the Cretaceous Bulldog Shale and Permian Stuart Range Formations are either thin or absent. Kellett et al. (1999) proposed that recharge in the south-east portion of the Arkaringa Basin occurs via diffuse discharge through the J-K aquifer. Howe et al. (2008) suggested possible direct recharge to the Boorthanna Formation where the formation sub-crops near the southern basin margin and north of the Boorthanna Fault. Additional recharge zones include freshwater stream and wetland environments located near the south-eastern margin of the basin. In the western Arkaringa Basin, based on limited hydraulic head data, recharge is thought to occur along the western margin of the Arkaringa Basin, in the vicinity of the Musgrave and Everard ranges and Central Australian Plateau.
	Recharge rates	Diffuse recharge rate estimated between 0.05 and 0.5 mm/y using Chloride Mass Balance (CMB) approach. Aquaterra REM (2005b) used a constant recharge rate of 0.18 mm/y for numerical modelling the south-eastern Arkaringa Basin based on reported recharge rates for the overlying GAB.
Aquifer parameters	Transmissivity	Boorthanna Formation: 2-150 m ² /d (Howe et al., 2008; SKM, 2009)
	Storativity	Stuart Range Formation: 1 x 10 ⁻⁴ (Howe et al., 2008) Boorthanna Formation: 1 x 10 ⁻⁴ – 1 x 10 ⁻⁵ (Howe et al., 2008)
	Permeability and hydraulic conductivity	<u>Permeability</u> Boorthanna Formation: 2.96 x 10 ⁻⁹ - 1.97 x 10 ⁻⁸ cm ² ((Tucker, 1997) <u>Hydraulic Conductivity</u> Stuart Range Formation: K _v : 1 x 10 ⁻⁴ m/d (Howe et al., 2008) Boorthanna Formation: K _i : 1-5 m/d (Howe et al., 2008)
	Porosity	Boorthanna Formation: 3.6-25 % (CRAE, 1987; DMITRE, 2011, Tucker, 1997) Kellett et al. (1999) suggests that secondary porosity development is important in assessing the unit's viability as a reliable groundwater supply.
Hydrodynamics	Aquifer composition and extents	SKM (2009) suggested that productive aquifer units may occur as relatively isolated semi-discontinuous "pods" related to sporadic turbidite flows within an otherwise quiescent glacio-marine environment and that further discontinuity may arise from syn and post depositional faulting. Large drawdowns (>50 m) observed within borefields located within the western half of the basin was interpreted by REM (2007) and presented in SKM (2009) as evidence for a limited lateral aquifer extent.
	Groundwater flow and flow scale	It is possible that the Arkaringa Basin is partitioned into a series of semi-discrete sub-basinal areas that may be isolated from the regional groundwater flow system that is assumed to exist. These sub-basinal areas are expected to have localised groundwater flow-systems with intra-basinal recharge and discharge zones.

Hydrogeological property/process	Component	Summary of current information
Hydrodynamics		<p>The most well-understood of these sub-basinal areas is the south-east corner of the Arckaringa Basin where groundwater flow is generally eastward toward the Stuart Shelf and a number of salt pan and saline environments near the margin of the Arckaringa Basin (Kellett et al., 1999; Aquaterra REM, 2005; Howe et al., 2008; SKM, 2009; Lyons et al., 2010). In addition, a deep groundwater flow path from the Boorthanna Trough south into the south-east corner of the Arckaringa Basin has been inferred (Aquaterra REM, 2005).</p> <p>Another hydrogeological sub-basinal area is thought to occur south of the Mount Woods Inlier and west of the Stuart Range, on the basis of differences in hydrochemical evolution and radiocarbon results. Based on limited hydraulic head data, groundwater within the western Arckaringa Basin is speculated to flow in an easterly direction from the basin margin towards the Stuart Range. Also, headward erosion contributing to the development of the Stuart Range and the subsequent development of the Lake Eyre (hydrological) Basin may be associated with a zone of recharge for the eastern Arckaringa Basin. Subsequent flow associated with this conjectural zone of recharge is interpreted to be eastward toward the Boorthanna Trough.</p> <p>An average groundwater velocity of 1.4 m/y and a residence time up to 200 000 years was estimated by Kellett et al. (1999) for the Boorthanna Formation.</p>
	Potentiometric surface	<p>Uncorrected groundwater levels for the Boorthanna Formation aquifer in the south of the basin suggest a general flow direction of west and south west from the Mount Woods Inlier, and from the southern margin of the Arckaringa Basin to the eastern margin of the basin. There is insufficient data to interpret a potentiometric surface at a more regional scale for the Boorthanna Formation aquifer. An average hydraulic gradient of 6×10^{-4} was observed across the south east portion of the Boorthanna Formation.</p> <p>Groundwater in the J-K aquifer flows to the east with an estimated hydraulic gradient of 7×10^{-4} in the south eastern portion of the Arckaringa subregion, although in this area there are a number of zones where the GAB has been interpreted to be unsaturated.</p>
	Cross-formational flow	<p>The limited scope and spatial extent of previous studies of the hydrogeology of the Arckaringa Basin has resulted in contradictory results or interpretations. Kellett et al. (1999) and Belperio (2005) described the Stuart Range Formation as a leaky aquitard that separates the J-K and Boorthanna Formation aquifers. SKM (2009) and Aquaterra (2009) suggest that the Stuart Range Formation potentially provides sufficient leakage to enable drawdown stability in Boorthanna Formation screened production wells. Conversely, Aquaterra REM (2005) and SKM (2009) infer that the Stuart Range Formation acts as an effective aquitard. Pumping test data in SKM (2009) and Lyons et al. (2010) indicated limited connectivity between Boorthanna Formation and unconfined GAB aquifers.</p> <p>For the deeper Boorthanna Formation aquifer, the removal of younger sedimentary horizons (in particular the Stuart Range Formation) by erosion prior to the deposition of the GAB or younger sedimentary units, provides potential for inter-connectivity between the Boorthanna Formation and overlying GAB aquifer units. This potential largely occurs in the south-eastern and south-western margins of the basin.</p> <p>Faulting potentially contributes to the variable thickness of Permo-carboniferous formations. Evidence of seismic activity and active springs near fault zones in the eastern Arckaringa Basin suggests that faulting may be contributing to changes in hydrodynamics and hydrogeological properties at local and regional scales.</p>
	Hydrochemistry	<p>Groundwater from aquifers within the Arckaringa Basin is generally described as brackish to hypersaline, although fresh supplies are known in parts of the south-eastern corner. Major ion hydrochemistry from Arckaringa Basin aquifers is very similar to that found within the overlying GAB, being predominantly Cl^- and $\text{Na}^+ + \text{K}^+$ dominant, with relatively high Mg^{2+} and SO_4^{2-}. Although trends in major ion hydrochemistry are evident, the trends may be more closely related to spatial distribution rather than hydrostratigraphy.</p> <p>Jack (1923) and Habermehl (1980) suggested there are two predominant GAB groundwater types, notably a $\text{Na}^+ + \text{Cl}^- + \text{HCO}_3^-$ type from the eastern GAB and a $\text{Na}^+ + \text{Cl}^- + \text{SO}_4^{2-}$ type from the west.</p> <p>There are broad evolutionary trends towards hypersalinity, with added complexity via features such as localised recharge and discharge characteristics, variations in aquifer connectivity and possible heterogeneities with aquifer types.</p>

Hydrogeological property/process	Component	Summary of current information
		<p>The discrepancy between the hydrochemistry (major ion, stable isotope and radiocarbon) and hydraulic data has been noted previously (e.g. Howe et al., 2008, REM 2007b), with explanations including localised recharge or palaeoclimate. Another possible explanation is the existence of a historical pressure head in which pressure and therefore potentially flow from the north-east and east was once far greater than at present and operable under conditions insufficiently different from modern day to reverse the hydrochemical signature. Radiocarbon dating appears to be highlighting a groundwater palaeo-flow that contrasts significantly from modern conditions.</p> <p>Some differences between GAB and Boorthanna Formation groundwater are suggested via use of ³⁶Cl and stable isotopes (e.g. Lyons et al., 2010).</p>
Discharge	Discharge zones and mechanisms	<p>Discharge from the south-east corner of the Arckaringa Basin is interpreted to occur into the Andamooka Limestone on the Stuart Shelf (Kellett et al., 1999; Howe et al., 2008; Lyons et al., 2010). Aquaterra REM (2005) and SKM (2009) also indicate that upward leakage from the Boorthanna Formation aquifer into the overlying J-K aquifer, salt pan and saline environments near the eastern margin of the Arckaringa Basin is possible on the basis of hydraulic gradient data. However, the Stuart Range Formation may limit this capacity. Beyond this, discharge from the Arckaringa Basin is poorly understood, although conditions similar to those described for the south-east corner of the Arckaringa Basin occur to the west of the Peake and Denison Inlier.</p>
	Discharge rates	No information available on discharge rates from the Permian formations

Source: modified from Wohling et al. (2013) and Keppel et al. (2015)

2.3.2 Existing understanding of intra-basin connectivity

Areas of potential regional-scale intra-basinal aquifer connectivity (Figure 2-3) are influenced by the extent and characteristics of the Stuart Range Formation. In particular, in areas where the erosion of the Stuart Range Formation prior to deposition of younger sedimentary units occurred, interconnectivity between the Boorthanna Formation aquifer and overlying aquifers in the Mount Toondina Formation is possible (Keppel et al., 2015).

The Arckaringa Basin may be defined into a series of sub-basinal areas. These sub-basinal areas are considered to have been formed either before Permian sedimentation by glacial erosion, or via faulting before, during or after Permian sedimentation. Although not readily mapped, faulting may also be actively contributing to changes in regional hydrodynamics and hydrogeological properties, particularly with respect to secondary porosity and permeability characteristics (Keppel et al., 2015). Furthermore faulting can provide an avenue for the movement of water and solutes between different aquifers (Cherry and Parker, 2004).

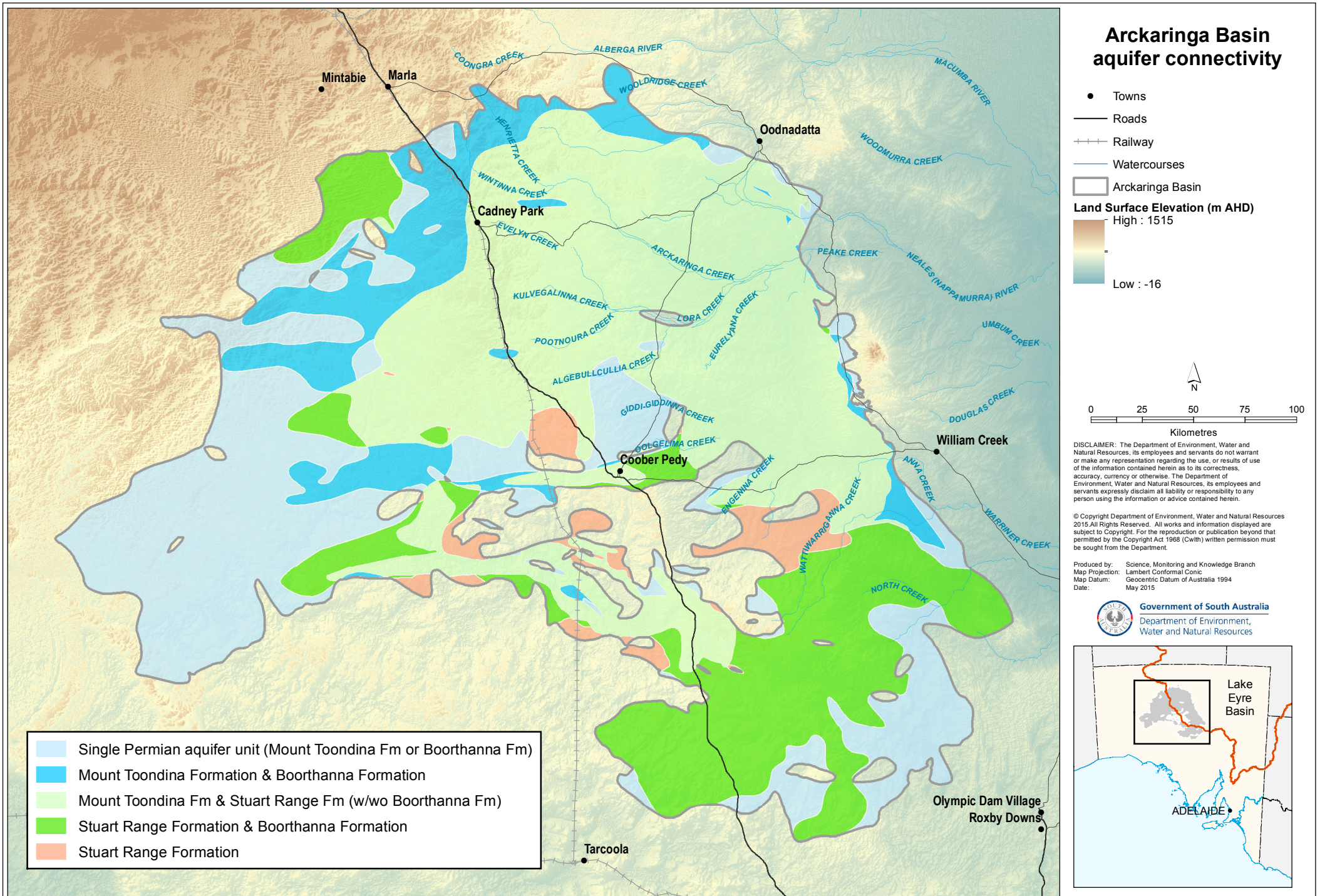


Figure 2-3 Intra-basin connectivity in the Arckaringa Basin

2.3.3 Existing understanding of inter-basin connectivity – connectivity between the Boorthanna Formation and J-K aquifers

The erosion of younger sediments (in particular the Stuart Range Formation) prior to the deposition of the GAB or younger sedimentary units, provides potential for interconnectivity between the Boorthanna Formation and overlying GAB aquifers. This potential interconnectivity occurs in the south-eastern and south-western basin margins (Figure 2-4) (Keppel et al., 2015).

Keppel et al. (2015) identified areas of aquifer connectivity, groundwater flow and mixing in the Arckaringa subregion using environmental tracers (e.g. $^{87}\text{Sr}/^{86}\text{Sr}$, ^{14}C and $\delta^{13}\text{C}$). Keppel et al. (2015) suggested a difference in the Sr isotope ratios at nested piezometer sites represents a lack of connectivity at a localised scale, which is in contrast to mixing identified between two end member water types. A mixing trend between end members may indicate regional-scale inter-aquifer connectivity. Finally, Keppel et al. (2015) identified a radiogenic Sr isotope signal as the result of upward leakage from the Boorthanna Formation into the J-K aquifer in a well in the regional discharge area.

3 Methodology

3.1 Site selection

DEWNR completed a desktop review to identify a suitable site for the aquifer connectivity drilling by applying the following selection criteria. The:

1. Bulldog Shale, J-K aquifer, Mount Toondina Formation, Stuart Range Formation and Boorthanna Formation underlie the site. The J-K aquifer, Mount Toondina Formation, Stuart Range Formation and Boorthanna Formation are saturated, and each have a minimum expected thickness of 20 m.
2. expected depth to the Boorthanna Formation was less than 125 m.
3. site was located outside the artesian (flowing) portion of the GAB.
4. site has an open, flat area and good access roads.
5. site was adjacent to groundwater monitoring wells screened in the J-K aquifer, Mount Toondina Formation and Boorthanna Formation.

Estimates of formation extents and thicknesses were drawn from the Arkaringa Basin Hydrogeological Map (Sampson et al. 2015), developed as part of the Arkaringa Basin and Pedirka Basin desktop assessment (Wohling et al., 2013). Information on expected artesian conditions within the J-K aquifer was sourced from the South Australia and Northern Territory Hydrogeological Map of the Great Artesian Basin Part 2 (Sampson et al., 2012). Four potential sites were identified in the southern portion of the Arkaringa Basin, with the selected location chosen primarily for the shallow Boorthanna Formation depth and relative ease of site access. The upper unit of the Arkaringa Basin (Mount Toondina Formation) was absent at the selected location. Budget constraints precluded site selection with all formations present due to drilling depths.

3.2 Site location

The drilling site was located on Mount Eba Station approximately 750 km north-west of Adelaide and 130 km south-east of Coober Pedy. The site was located near OZ Minerals Prominent Hill mine site, and adjacent to monitoring wells constructed as part of the OZ Minerals Virgo borefield (Figure 3-1). Access was from the Stuart Highway, via the OZ Minerals Prominent Hill access road. From the mine, the site was located approximately 30 km south along the Virgo borefield access track.

The drilling pad (Figure 3-2) was situated on a rocky, gibber plain. The immediate area surrounding the drilling pad was flat lying, while mesas were located further to the south and west. The landscape was chenopod shrubland sparsely vegetated with saltbush. The mine site and associated infrastructure was distantly visible to the north.

3.3 Drilling and construction

The drilling program commenced on 11 March 2015 and concluded on 18 March 2015. The drilling works were completed under contract by Rockbeare Drilling Contractors Pty Ltd trading as Underdale Drillers Oz. Site supervision and logging were undertaken by DEWNR hydrogeologists. The hole was drilled using a Boart Longyear LF90 rig crewed by a team of three drillers under the supervision of site foreman, Darrin Noll. The Boart Longyear LF90 was equipped to drill using rotary air and rotary mud drilling methods. Water for the drilling process was sourced from the OZ Minerals Prominent Hill mine as desalinated (reverse osmosis) water, originating from the Aries borefield.

For this investigation, one hole was drilled (cored) using HQ diamond (60 mm inner diameter, 95 mm outer diameter) and mud rotary methods to 110.4 m BGS. Although the hole was continuously cored from the surface, 100% recovery was not achieved as sample was mixed in with circulating muds or too unconsolidated for the core barrel and catcher to recover. No core recovery was obtained from the intervals 21.4–23.4 m, 24.2–26.4 m, and 29.9–31.4 m.

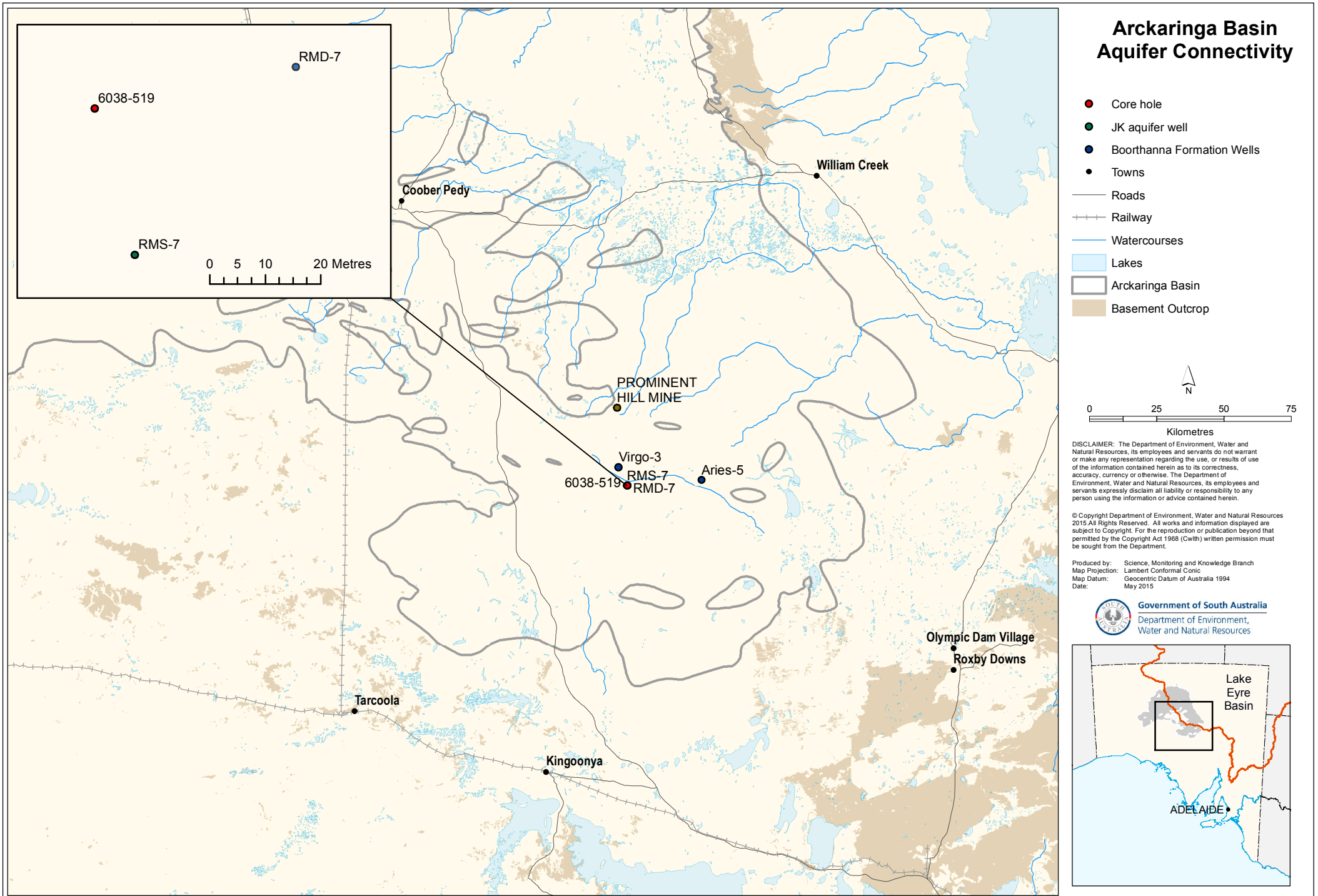


Figure 3-1 Investigation site location map



Figure 3-2 Boart Longyear LF90 rig and support vehicles during drilling

Other issues included the drill bit being worn down by abrasive sands or rock, core recovery tool and split spoon becoming stuck on clays, core lifter not deploying due to clay blockages, blockage (by clay) of the mud holes in the drill bit, damage of the wireline cable, and seizure of the mud pump. These issues, in most cases, required the tripping out of the drilling string. Collapsing sands (predominantly) and clay required redrilling, in particular after being left overnight (particularly due to swelling clays). Due to the unstable nature of the hole it was decided not to deploy downhole geophysics tools due to the risk of tools becoming stuck.

Core was able to be recovered in 3 m lengths using wireline diamond core drilling, however variable depth coring runs (< 3 m) were employed dependent on the geology. Core was placed in a core tray for logging and sampling by the site hydrogeologist. Small cutting samples were collected in chip trays for future reference.

The hole was drilled to a depth of 110.4 m BGS under DEWNR well permit number (P/No) 239388, Unit number 6038-519. The hole was completed with an outer steel standpipe set in concrete. A smaller diameter threaded steel standpipe was installed inside the outer standpipe, allowing the vibrating wire piezometer (VWP) data logger to be screw-mounted at approximately 1.6 m above ground surface (AGS) (Figure 3-3).



Figure 3-3 6038-519 VWP datalogger box, with groundwater monitoring well RMS-7 (formerly VMS-2) in the background

The adjacent groundwater monitoring wells screened in the J-K aquifer and Boorthanna Formation aquifer were approximately 30 m from 6038-519 and provided depth control for the drilling. However, depth differences of lithology boundaries between historic drilling and drilling for this program were up to 3 m.

A borehole composite log including VWP installation details is provided in Appendix A. A summary of the site monitoring infrastructure is provided in Table 3-1.

Table 3-1 Summary of completion and location details

Well ID	Easting GDA94 Z53	Northing GDA94 Z53	Monitored depth (m BGS)	Formation monitored	SWL (m BTOC)	RSWL (m AHD)
6038-185 (RMS-7)	560165	6686401	39-56	J-K aquifer	40.54	113.61
6038-187 (RMD-7)	560194	6686435	108-138	Boorthanna	55.05	99.29
6038-519 VWP 1			50.8			
6038-519 VWP 2			63.8			
6038-519 VWP 3	560152	6686404	76.8	Stuart Range	N/A	N/A
6038-519 VWP 4			89.8			
6038-519 VWP 5			102.8			

3.4 Core sampling

Samples for major ion and stable isotope of water analysis were taken at approximately 2 m intervals. Samples for permeability and particle size analysis were taken at approximately 10 m intervals, or at any lithological change.

Core samples were collected for physical and chemical analysis by first shaving and discarding the outer core (approximately 2 mm) to avoid drilling fluid contamination, as evidenced by Figure 3-4. The major ion and particle size analysis samples were vacuum sealed in two Food Saver® bags then placed in a large Ziploc® bag (26.8 x 27.3 cm). The stable isotopes of water samples were sealed in a small Ziploc® bag (17 x 19 cm) with all the air expelled then placed in a second large Ziploc® bag (26.8 x 27.3 cm) using the method outlined by Wassenaar et al. (2008). Permeability samples were wrapped in thin plastic wrap and labelled with the depth interval and an arrow to indicate direction to top of core, then placed in PVC pipe for protection and vacuum sealed in a Food Saver® bag. All samples were stored in insulated coolers.



Figure 3-4 Core sub-portion from interval 47–48.5 m BGS, showing the outer 1–2 mm impacted by drilling fluids (darkened)

3.5 Core analysis

Major ion and stable isotopes of water analysis of core porewater and core porewater potential measurements were undertaken at Flinders University. It was not possible to obtain a sufficient amount of porewater from the core by squeezing or centrifuging. A minimum of 5 mL is necessary for anion and stable isotopes of water analysis. Instead the porewaters were extracted with 1:5 dilution based on the method outlined in Sacchi et al. (2001). The actual anion and cation concentrations in the porewaters are back calculated using the gravimetric water content of the samples.

The gravimetric water content of the core sample was determined by oven drying a portion of the sample at 105°C for 24 hours. The sample was weighed prior to and following drying to determine the water content with the equation (1) below:

$$\% \text{ water} = \frac{[(\text{wet soil weight}) - (\text{dry soil weight})]}{(\text{dry soil weight})} \times 100 \quad (1)$$

The 1:5 dilution was undertaken on air dried soil samples, so there was no free water in the sample but there was no irreversible precipitation of minerals due to high temperature drying. The air dried samples were weighed and oven dried at 40°C for 24 hours. Twenty grams of air dried sample was then added to 100 mL of ultra-pure water and shaken for 24 hours to thoroughly mix and extract the free porewater. These mixed samples were then centrifuged at 3500 rpm for 2 hours, to settle sediment out of solution, prior to 0.45 µm filtration. Filtered samples were then analysed on a Metrohm 883 Basic IC plus ion chromatograph (IC) using in-house standard solutions to generate calibration graphs following standard analytical techniques (standard method 4110; APHA, 2000). Precision for anion analysis was ≤ 2.5 %.

Stable isotopes of water ($\delta^2\text{H}$ and $\delta^{18}\text{O}$) samples were analysed on a Picarro L21302-i using the vapor equilibration method outlined in Wassenaar et al. (2008). The difference between repeated measurements for $\delta^2\text{H}$ and $\delta^{18}\text{O}$ was ≤ 5 %.

Core porewater potential measurements were undertaken on an AquaLab Dew Point Water Activity Meter 4TE using the method outlined in Gee et al. (1992).

Permeability and porosity measurements were undertaken by Ground Science Engineering testing laboratory, Victoria. The permeability of the sample was measured using a triaxial cell, with the pressure at depth replicated by the laboratory. Porosity of the samples was measured using two tests, 1) specific gravity, and 2) bulk density and moisture content. The specific gravity test determined the density of particles making up the sample, while the bulk density and moisture content gave the volume and mass of the material.

Particle size analysis was arranged by Apal Agricultural Laboratory, with analysis undertaken via the pipette method (Gee and Bauder, 1986).

3.6 Vibrating wire piezometers

The borehole was instrumented with a multi-point (total of five) vibrating wire piezometer (VWP) string (HMA Geotechnical Systems Australia Model 1200) that was fully grouted into the borehole without a sandpack. Vibrating wire piezometers were zeroed on the ground before installation and inverted as part of the installation to ensure no air is trapped against the diaphragm. The five VWPs were spaced 13 m apart from 50.8 to 102.8 m BGS. The VWP string was secured to a 32 mm PN 12.5 (nominal working pressure rated) high density polyethylene tremie pipe (blue stripe) that was lowered into the borehole through the drilling rods. The borehole was closed by pumping a 20:1 cement/bentonite grout through the tremie pipe until the borehole was completely filled and the grout mixture flowed to ground surface. The piezometer string was connected to a ten channel data logger (RST Instruments Model DT2055B), comprising five vibrating wire sensors and their associated thermistors.

The fully grouted installation is simplified compared to groundwater monitoring wells, especially where measurements are required at different depths (Smerdon et al., 2014). A VWP will detect changes in pore pressure through 8 cm of cement-bentonite grout within a few minutes (Smerdon et al., 2014).

The benefit of multi-point VWP strings are that the temporal resolution and vertical extents create a data record of response to driving forces across different timeframes (Smerdon et al., 2014). This data could be used as transient data when modelling regional scale groundwater flow, or when evaluating data from aquifers and aquitards. Long-term pore pressure measurement via VWPs provides a link between laboratory-scale data and regional-scale data.

3.7 Pressure-elevation profile

Pressure-elevation profiles provide an estimate of current day vertical communication between aquifers in a multi-layered aquifer-aquitard system (van der Kamp, 2001; Love et al. 2013a). Pressure-elevation profiles represent the fluid pore pressure versus elevation along a vertical line, and they show the vertical gradient of pore pressure, which is the change in pore pressure per unit of vertical length (van der Kamp, 2001; Love et al. 2013a). Where a vertical pressure gradient exists, it may be smaller or larger than the hydrostatic pressure, which indicates a force driving the fluid downward or upward, respectively (Love et al., 2013a). The pressure distribution is a function of the surrounding rock, with abrupt changes usually due to changes in rock permeability or a reflection of the presence of different driving forces (e.g. pumping) (Love et al., 2013a).

It was possible to use the difference in hydraulic heads between aquifers (and other parameters as detailed in equations (2) and (3)) to calculate the groundwater flow rate through the Stuart Range Formation (equations (2) and (3)):

$$q_z = \Delta h/c \quad (2)$$

$$c = b/K_v \quad (3)$$

where q_z is the flow rate, Δh is the difference in hydraulic head of the aquifers, b is the thickness of the aquitard and K_v is the vertical hydraulic conductivity.

3.8 Modelling

3.8.1 Analytical modelling

Of the well studied aquitards in Canada (Hendry and Wassenaar, 1999; 2011) and Europe (Mazurek et al., 2011), that of the King aquitard, Saskatchewan, Canada, provides a profile of deuterium porewater concentrations very similar to that of Cl^- in this study. In both the Canadian and European examples, a 1D transport equation was used to assess likely values of porewater velocity and age of aquitard formation. Both assumed diffusive transport to be more significant than advective transport.

A 1D transport equation was used in this investigation to fit aquitard Cl^- data, with the solution being in time dependent analytical form (Appendix B).

3.8.2 Numerical modelling

The finite difference groundwater flow model MODFLOW-2005 (Harbaugh, 2005) was used, via the graphical user interface Visual MODFLOW (Schlumberger Water Services, Visual MODFLOW, Version 2011.1 Pro), to undertake numerical simulations of the site using a one-dimensional advection-diffusion model. MT3DMS was used in Visual MODFLOW to undertake solute transport simulations.

A steady-state flow field was produced by assigning specified head boundary conditions at the top (J-K aquifer) and bottom (Boorthanna Formation) of the model domains, with constant values corresponding to measured groundwater levels in March 2015. The sequence was represented in the MODFLOW-MT3DMS model as a single row and single column of cells comprising 80 layers with a uniform thickness of one metre. This was comprised of four J-K aquifer layers, 58 Stuart Range Formation layers and 19 Boorthanna Formation layers. Aquifer layers were included to allow incorporation of groundwater end-member data. End-member depths were assigned screened interval mid-point depths. Cells were assigned constant hydraulic parameters, including hydraulic conductivity (K) and total porosity (Table 3-2). No recharge or evapotranspiration was applied to the model.

The assumption of steady state flow was on the basis that long-term erosional rates for the western Lake Eyre Basin are likely to be 0-2 m/Ma over (geologically) recent times, thus any reduction of hydraulic heads in the middle of the aquitard can be considered negligible (Harrington et al., 2013). This is supported by porewater pressure data from VWP's installed in the aquitard, which showed no evidence of considerable heterogeneities in the rock matrix (Section 4.5). The downward hydraulic gradient that exists between the J-K aquifer and Boorthanna Formation may have remained relatively constant over recent (geological) time, with water table depths varying slightly in response to different hydrological conditions (Harrington et al., 2013).

Table 3-2 Model parameters

Parameter	J-K aquifer	Source	Stuart Range Formation	Source	Boorthanna Formation	Source
K_h (m/s)	2.31×10^{-4}	Purczel, 2015	$10 \times K_v$	-	1.45×10^{-5}	Purczel, 2015
K_v (m/s)	2.31×10^{-5}		Varied for sensitivity analysis	-	1.45×10^{-6}	
S_s (-/m)	1×10^{-5}		1×10^{-6}	Calculated from Howe et al. (2008)	1×10^{-5}	
Porosity (%) volume)	0.281	Average of 2 samples (this project)	0.216	Average of 8 samples (this project)	0.201	One sample (this project)

One-dimensional vertical flow and transport was considered appropriate because the vertical hydraulic gradient through the aquitard (0.17) was more than two orders of magnitude greater than the horizontal hydraulic gradient in the aquifers (0.0006–0.0007) (Keppel et al., 2015). The steady-state flow across individual aquitard layers was constant, hence a single value of K_v was applied for the core.

Based on estimates of K , and similar work undertaken elsewhere in the GAB (Harrington et al., 2013), it was anticipated that transport of Cl^- and $\delta^2\text{H}$ would be dominated by diffusion rather than advection and that mechanical dispersion would be negligible compared to diffusion. Hence dispersivity was set at zero. Following the method of Harrington et al. (2013), the Upstream Finite Difference Scheme was used in MT3DMS rather than more commonly used schemes in advection-dominated systems.

Following the rationale of Harrington et al. (2013), the effective diffusion coefficient, D_e , (required in MT3DMS) was equivalent to D_p , i.e. D_e/η_e (where D_p is the porewater diffusion coefficient, and η_e is effective porosity). The effective porosity was assumed to be equal to the average value of total porosity (i.e. $\eta_e = \eta = 0.216$). The effective diffusion coefficient was estimated via equation (4) using free water diffusion coefficients (D_0) of $1.71 \times 10^{-9} \text{ m}^2\text{s}^{-1}$ for Cl^- at 18 °C and $2.27 \times 10^{-9} \text{ m}^2\text{s}^{-1}$ for $\delta^2\text{H}$ at 25 °C:

$$D_e = \eta^m D_0 \quad (4)$$

where m is an empirical exponent (value of 2.3 used, as per Harrington et al. (2013)).

Effective diffusion coefficients of $5.038 \times 10^{-11} \text{ m}^2\text{s}^{-1}$ for Cl^- at 18 °C and $1.128 \times 10^{-9} \text{ m}^2\text{s}^{-1}$ for $\delta^2\text{H}$ at 25 °C were derived. Average temperature-corrected D_e values were calculated via equation (5) and an average measured in-situ temperature of 25.4 °C measured via the VWP thermistors:

$$\frac{D_{e,T_2}}{D_{e,T_1}} = e^{\frac{E_A}{R} \left(\frac{1}{T_1} - \frac{1}{T_2} \right)} \quad (5)$$

where E_A is activation energy ($20 \pm 1 \text{ kJ mol}^{-1}$ for Cl^- and deuterium), R is Boltzmann's constant ($8.31451 \text{ J mol}^{-1} \text{ K}^{-1}$), and T_1 (18 °C for Cl^-) and T_2 (25 °C) are temperatures for a given solute and porous medium.

Average temperature-corrected D_e values were obtained for Cl^- ($6.183 \times 10^{-11} \text{ m}^2\text{s}^{-1}$) and $\delta^2\text{H}$ ($1.128 \times 10^{-9} \text{ m}^2\text{s}^{-1}$), which were converted to D_p ($2.863 \times 10^{-10} \text{ m}^2\text{s}^{-1}$ and $5.222 \times 10^{-9} \text{ m}^2\text{s}^{-1}$, respectively) for input to MT3DMS.

The modelling approach included various steady-state flow simulations with head boundary conditions as described and a range of possible values for vertical K (K_v), based on previous estimates obtained via laboratory measurements and from other authors (Howe et al., 2008, and Purczel, 2015). Flow velocities from these simulations were used as initial conditions for transport simulations to determine the most appropriate value of K_v . η_e and D_e were not altered in the solute transport simulations due to uncertainties associated with their values.

4 Results and discussion

4.1 Drilling program

The following section summarises the stratigraphy encountered during drilling of borehole 6038-519. An interpretation of the sequence from drill core is provided in a composite log (Appendix A), and a detailed description and photographs from the continuous core is provided (Appendix C).

Bulldog Shale (Kmb) (0–17.8 m). Dark grey-brown, silty clay with trace sand. Low to medium plasticity increasing to medium to high plasticity with depth. Highly weathered, friable and gypsiferous (from 1.3–15.4 m). The lower 2–3 m becomes sandier, with fine to coarse grained sand, and appears to be a transitional zone.

J-K aquifer (17.8–46.6 m). Generally medium to coarse grained sand, however often poorly sorted with fining and coarsening sequences. Light grey in colour, with hard and soft alternating layers in the upper 9 m. Sand is predominantly quartz in composition with subrounded to subangular quartz and sandstone gravels to 50 mm. Minor interbeds of sandstone and claystone.

Stuart Range Formation (P-s) (46.6–104 m). Grey consolidated claystone, except between 62.8 m and 71.5 m, where the formation was minimally consolidated, softer and plastic. Minor fine to medium grained sand and sub-rounded to sub-angular quartz and sandstone gravels to 50 mm. From 86-104 m depositional features including very fine layering, swirls, and vitreous appearance are apparent. Generally thin (<50 mm) sandstone interbeds and gradational sequences from 91 m, with a 1m thick interbed from 91-92 m. Variable grey and brown in colour from 91 m.

Boorthanna Formation (CP-b) (104–110.4 m (end of hole)). Grey sandstone with poorly sorted sand and moderate percentage of pyritic gravels. More permeable zones of (unconsolidated) fine to coarse grained sand, and rare thin (10 mm) claystone interbeds are apparent.

Table 4-1 Formation depths and thickness

Formation	Basin	Depth intersected (m)	Thickness (m)
Bulldog Shale	GAB (Eromanga Basin)	Surface	17.8
J-K aquifer	GAB (Eromanga Basin)	17.8	28.8
Stuart Range	Arckaringa Basin	46.6	57.4
Boorthanna	Arckaringa Basin	104.0	~131*

*based on Sampson et al. (2014)

4.2 Site hydrogeology

One selection criterion for the aquifer connectivity investigation drilling site was to be in close proximity to groundwater wells screened in the J-K aquifer and Boorthanna Formation. Drilling for borehole 6038-519 was undertaken adjacent (approximately 30 m) to groundwater monitoring wells RMS-7 (formerly VMS-2) (unit number 6038-185) and RMD-7 (unit number 6038-187).

The reduced standing water level (RSWL) in each well has been density corrected to account for variable groundwater temperature and salinity through the profile. Corrections have been undertaken according to the following method detailed in Post & von Asmuth (2013):

$$h_{f,r} = z_r + \frac{\rho_i}{\rho_f} (h_i - z_i) - \frac{\rho_a}{\rho_f} (z_r - z_i) \quad (6)$$

where: h_{fr} is freshwater head, h_i is point water head measured relative to z_r , z_r is reference level, z_i is elevation head of the screen mid-point, ρ_a is average water density between z_i and z_r , ρ_f is freshwater density, ρ_i is density of water surrounding the screen.

The corrected freshwater heads are presented with the uncorrected RSWL measurements for comparison in Table 4-2. The vertical hydraulic gradient was downwards between the J-K aquifer and Boorthanna Formation. The density correction changed the hydraulic head in well 6038-185 (J-K aquifer) by 0.05 m and well 6038-187 (Boorthanna Formation) by 1.4 m. The vertical hydraulic gradient calculated on corrected hydraulic heads was downward (0.17).

Table 4-2 Density corrected and uncorrected reduced standing water levels

Well ID	Aquifer	Screen mid-point (m BGS)	Uncorrected RSWL (m AHD)	Corrected freshwater head RSWL (m AHD)	Direction of vertical groundwater flow
6038-185 (RMS-7)	J-K aquifer	47.5	113.61	113.66	Downward
6038-187 (RMD-7)	Boorthanna Formation	123	99.29	100.69	

4.3 Physical properties

4.3.1 Water potential

Laboratory determined water potential varied from -0.18 MPa (40.75 m BGS) to -8.62 MPa (104.45 m BGS), with a general decreasing trend with depth as expected. Water moves from an area of higher water potential to lower water potential, with solutes acting to lower the water's potential. A water potential plot is provided in Appendix D.

4.3.2 Gravimetric water content

Gravimetric water content (GWC) ranged from 4.3 % (91.78 m BGS) to 47.7 % (10.88 m BGS). GWC was high (47.7 %) for the near surface Bulldog Shale (clay), and significantly lower in the sandy J-K aquifer (4.6–18.9 %), which was expected based on the higher porosity and a rainfall moisture source for the Bulldog Shale. The GWC slightly decreased with depth in the Stuart Range Formation from 13 % to 9 % from ~48 to ~81 m BGS, however from ~81 to 104 m water content increased to 12 %. The increase was possibly due to the increased percentage of clay in this section of the aquitard, from 39 % to a maximum of 70 %. Boorthanna Formation (sandstone) had low GWC at ~7 %. A gravimetric water content plot is provided in Appendix D.

4.3.3 Permeability coefficient

Permabilities were reported as the coefficient of permeability, or permeability coefficient, in accordance with Australian Standard AS1289 6.7.3. Permeability coefficient is used synonymously with hydraulic conductivity (Aubertin et al., 1996). Permeability coefficients (Table 4-3) are low and range over three orders of magnitude for the Stuart Range Formation. Lowest permeability coefficients (10^{-13} m/s) are encountered in the middle of the aquitard at 77.3 m BGS and 84.2 m BGS (Figure 4-1), with the highest permeability coefficient (4×10^{-10} m/s) for the aquitard at ~68 m BGS, corresponding to a softer area with minimal consolidation and fine to medium grained sand. The Boorthanna Formation permeability coefficient was lower than anticipated (based on the minimally consolidated sample), however the Boorthanna Formation displayed variable geology over the short interval encountered in this investigation, with unconsolidated sand lenses interspersed with occasional claystone interbeds, sand and gravel.

Table 4-3 Permeability coefficients

Formation	Median permeability coefficient (m/s)	Median permeability coefficient (m/d)	Permeability coefficient range (m/s)	Permeability coefficient range (m/d)	No. of samples
Bulldog Shale	-	-	2×10^{-10}	1.7×10^{-5}	1
J-K aquifer	-	-	1×10^{-8} to 6×10^{-6}	8.6×10^{-4} to 0.5	2
Stuart Range	4.5×10^{-12}	3.9×10^{-7}	4×10^{-13} to 4×10^{-10}	3.5×10^{-8} to 3.5×10^{-5}	8
Boorthanna	-	-	5×10^{-12}	4.3×10^{-7}	1

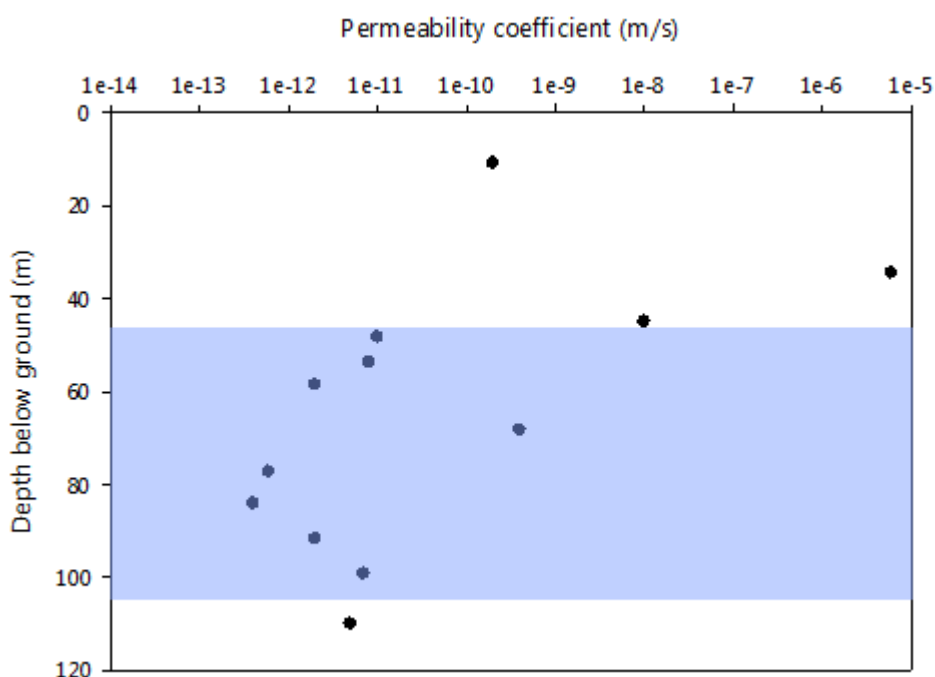


Figure 4-1 Permeability coefficient depth profile. Shaded zone corresponds to the location of the Stuart Range Formation.

4.3.4 Porosity

Porosity was estimated from measurements of GWC and specific gravity. Total porosities ranged from 12.1 % vol. (Stuart Range Formation, 91.8 m BGS) to 58.1 % vol. (Bulldog Shale, 10.9 m BGS) (Table 4-4, Figure 4-2). Specific gravity ranged from 2.649 t/m³ (46 m BGS) to 2.719 t/m³ (62.23 m BGS) (for brevity, data not shown). Porosity within the Bulldog Shale was at the upper end of that expected for clay, with the fine to medium grained sand of the J-K aquifer fitting the expected porosity range (26-53%) (Domenico and Schwartz, 1998). The low porosities reported for the second J-K aquifer sample and for the Boorthanna Formation were from consolidated claystone and sandstone zones respectively, thus a lower porosity was expected (5-30%). Stuart Range Formation porosities were low, as per typical claystones (Domenico and Schwartz, 1998).

Table 4-4 Laboratory porosities

Formation	Total porosity average (% vol.)	Total porosity range (% vol.)	No. of samples
Bulldog Shale	58.1	58.1	1
J-K aquifer	28.1	13.3 to 42.8	2
Stuart Range	21.6	12.1 to 26	8
Boorthanna	20.1	20.1	1

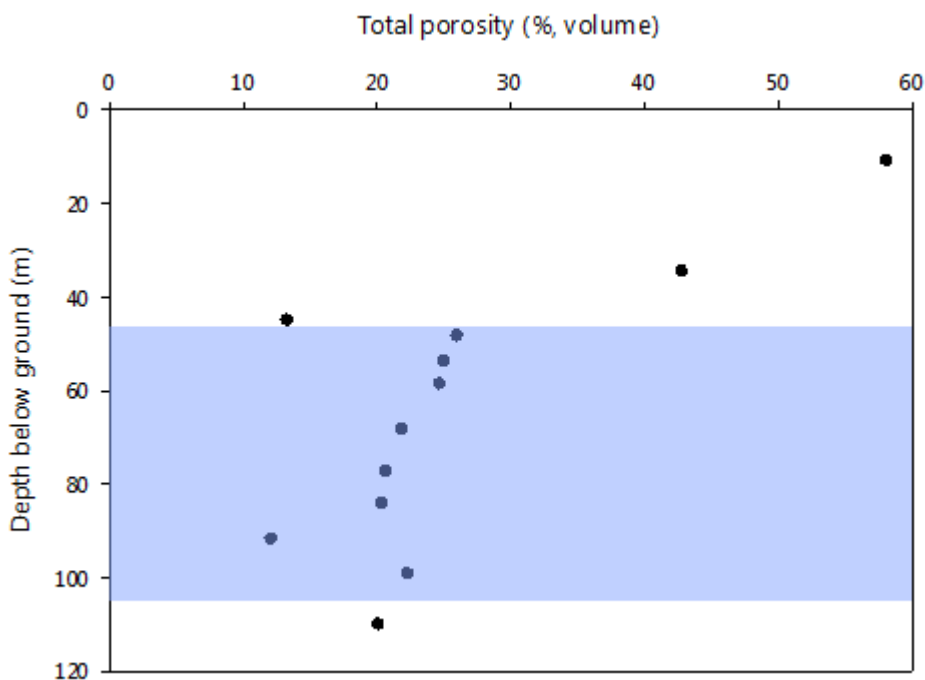


Figure 4-2 Total porosity depth profile. Shaded zone corresponds to the location of the Stuart Range Formation.

4.3.5 Particle size analysis

Particle size analysis of eleven samples provided useful insights, in particular with respect to other physical parameters assessed (Table 4-5). Of note was the distinct compositional change between the upper (<~80 m BGS) and lower aquitard (>~80 m BGS), with a moderate sand and clay percentage in the upper aquitard changing to a low sand and high clay percentage in the lower aquitard (Figure 4-3).

Table 4-5 Particle size analysis

Formation	Ave. depth (m BGS)	Geology	Sand %	Silt %	Clay %
Bulldog Shale	11.13	CLAY, dark grey-brown with increased yellow and red-brown mottling, medium to high plasticity, friable, but becoming less friable with depth, blocky, less frequent white gypsum crystal veining <3mm, trace sand	2	59	39
J-K aquifer	28.88	SAND, light grey with orange-brown mottling, medium to coarse grained, trace fine grains, sub-rounded to sub-angular quartz and red-brown semi-consolidated to consolidated sandstone gravel <50mm, trace clay, trace sub-rounded to sub-angular quartz gravel <50mm	91	5	4
	43.43	SAND, white-light grey, medium to coarse grained, trace sub-angular quartz gravels <20mm, trace clay	88	7	5
Stuart Range	51.53	CLAYSTONE, grey with trace orange-brown mottling, consolidated, trace sand, trace sub-rounded to sub-angular quartz and sandstone gravels <10mm	29	31	40
	69.73	CLAYSTONE, grey, little consolidation, softer, medium to high plasticity, fine to medium grained sand, trace sub-rounded to sub-angular quartz, claystone and sandstone gravels <10mm	30	30	39
	75.35	CLAYSTONE, grey, consolidated, increase in fine to medium grained sand, trace sub-rounded to sub-angular quartz, claystone and sandstone gravels <10mm	32	29	39
	86.63	CLAYSTONE, dark grey, consolidated, variably trace fine to coarse grained sand and sub-rounded to sub-angular quartz and granitic (?) gravels <30mm, vitreous in appearance, very fine layering and flaking apparent (indicative of fining sequence?), swirls visible	8	26	66
	92.28	CLAYSTONE, grey-brown, fine to medium grained sand, 5mm thick sandstone interbeds	7	38	55
	95.53	CLAYSTONE, grey, fine to medium grained sand, trace gravel <3mm, wavy/swirly depositional features	4	39	57
	101.33	CLAYSTONE, dark brown-grey, trace fine to coarse grained sand, trace sub-rounded to rounded gravels <40mm, wavy/swirly depositional features, poorly sorted	7	23	70
Boorthanna	105.55	SANDSTONE, grey, fine to medium grained sand, moderate clay and silt, trace gravel <5mm	17	26	57

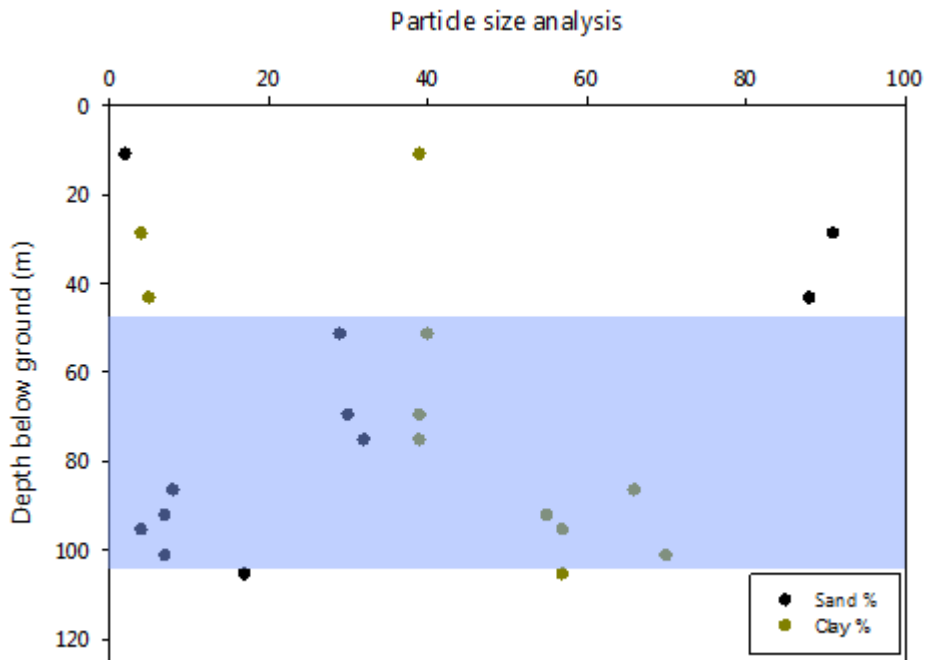


Figure 4-3 Particle size (sand and clay) analysis profile. Shaded zone corresponds to the location of the Stuart Range Formation.

4.4 Chemistry and environmental tracers

4.4.1 Major ion chemistry

It was assumed that Cl^- is chemically conservative and as a result was used to model flux through of the aquitard. The Cl^-/Br^- molar ratio provides an indicator of whether halite dissolution has occurred and therefore contributed to the high Cl^- concentrations. The ratios ranged from 226 to 872 for the porewater samples, suggesting no halite dissolution occurred at these depths.

Porewater chloride data ranged from 2605 mg/L (66.4 m BGS) to 12 953 mg/L (106.7 m BGS) and exhibits a non-linear trend with a saline shift in the upper part of the profile (Figure 4-4). The uppermost and lowest data points are groundwaters, while the remaining data points are porewater. The J-K aquifer (groundwater sample) was the most saline area of the upper profile (6390 mg/L). Deviation of the profile away from a linear trend occurs in the upper part of the aquitard (<66 m BGS), suggesting this portion of the aquitard may have some control on solute transport. The saline shift of the profile may be the result of a change in climatic conditions. The measured groundwater Cl^- concentration in the Boorthanna Formation (21 500 mg/L) was much higher than that of porewater in the lower portion of the aquitard and the upper part of the Boorthanna Formation. This suggests that the Boorthanna Formation could be more saline, i.e. > 21 500 mg/L, now than in the past.

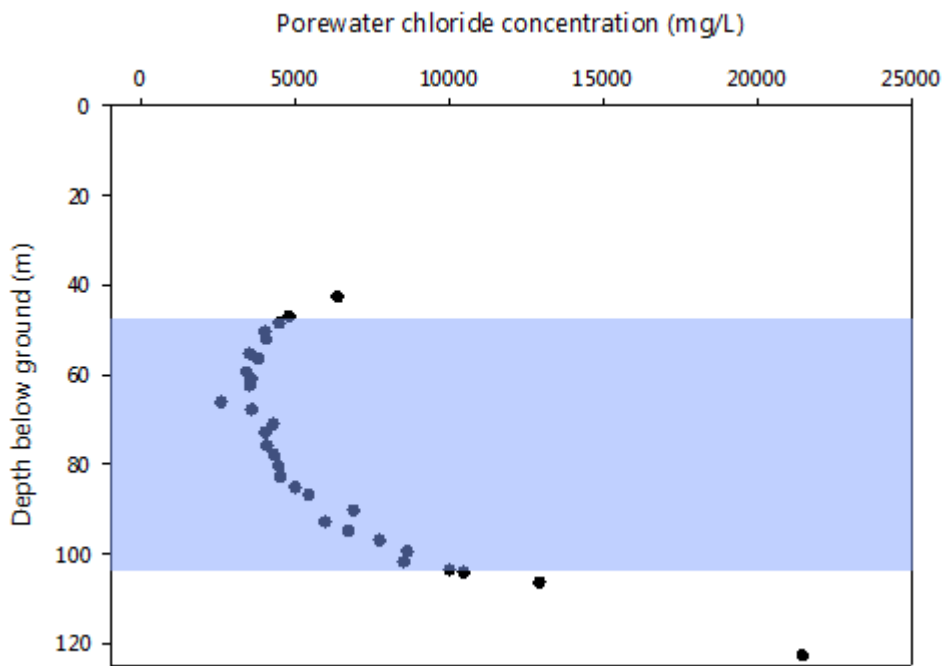


Figure 4-4 Chloride depth profile. Shaded zone corresponds to the location of the Stuart Range Formation.

Variability was observed in groundwater Cl^- concentrations from the Boorthanna Formation screened well assessed in this study (well RMD-7). Groundwater Cl^- concentration data since 2006 (Figure 4-5) indicates a wider concentration range than expected, with potential influencing factors including different sampling methodologies, sampling undertaken above the screened interval, different laboratories, uncertain quality assurance/quality control (QA/QC) procedures and potential effects of nearby Virgo borefield pumping. Pumping from the borefield for mine process water/dust suppression commenced in late 2006. Chloride concentrations in well RMD-7 range from 14 000 mg/L (December 2008) to 21 500 mg/L (June 2014), with an average concentration of 18 300 mg/L. It was noted that porewater Cl^- concentrations in the upper part of the Boorthanna Formation are 10 494 mg/L (104.45 m BGS) and 12 953 mg/L (106.73 m BGS).

The lower portion of the Cl⁻ depth profile within the Stuart Range Formation is roughly linear, suggesting a long-term and possibly steady-state diffusion profile. The upper portion of the profile may have been affected by alternating fresh and saline phases in the shallower J-K aquifer. This hypothesis was explored by Harrington et al. (2013), with their study sites ~200 km north-east of this investigation site. Magee et al. (2004) reported that the ephemeral playa Kati Thanda-Lake Eyre, approximately 155 km north-east of 6038-519, has undergone the following phases:

1. 150–130 ka before present – greatest aridity
2. 130–110 ka – deepest perennial lake
3. 100–75 ka – brief drying, refilling
4. 75–70 ka – drying and deflation
5. 65–60 ka – lacustrine conditions
6. 60–40 ka – drying and significant deflation
7. ~40 ka – minor low-level perennial lake
8. 35–12 ka – drying and minor deflation
9. 12–4 ka – low-level perennial lake
10. 4–0 ka before present – modern ephemerally flooded playa.

It should be noted that during the highstand phase (130–110 ka before present) Kati Thanda-Lake Eyre was thought to have covered nearly 35 000 km², greater than three times the current area (Magee et al., 2004).

4.4.2 Stable isotopes of water

Deuterium ($\delta^2\text{H}$) and $\delta^{18}\text{O}$ porewater concentrations range from -32.76 ‰ to -21.04 ‰ VSMOW and -3.24 ‰ to -1.05 ‰ VSMOW, respectively. The samples roughly cluster on a conventional $\delta^2\text{H}$ - $\delta^{18}\text{O}$ plot to the right of the Alice Springs local meteoric water line (LMWL) (IAEA/WMO 2015, Crosbie et al, (2012)) with no distinguishable trend (Figure 4-7). Despite being highly variable, the $\delta^2\text{H}$ composition of spiked drilling mud (-15.4 ‰ to 107.4 ‰ VSMOW) was significantly more enriched than porewater compositions (for brevity, not shown), indicating that the core was not contaminated during drilling.

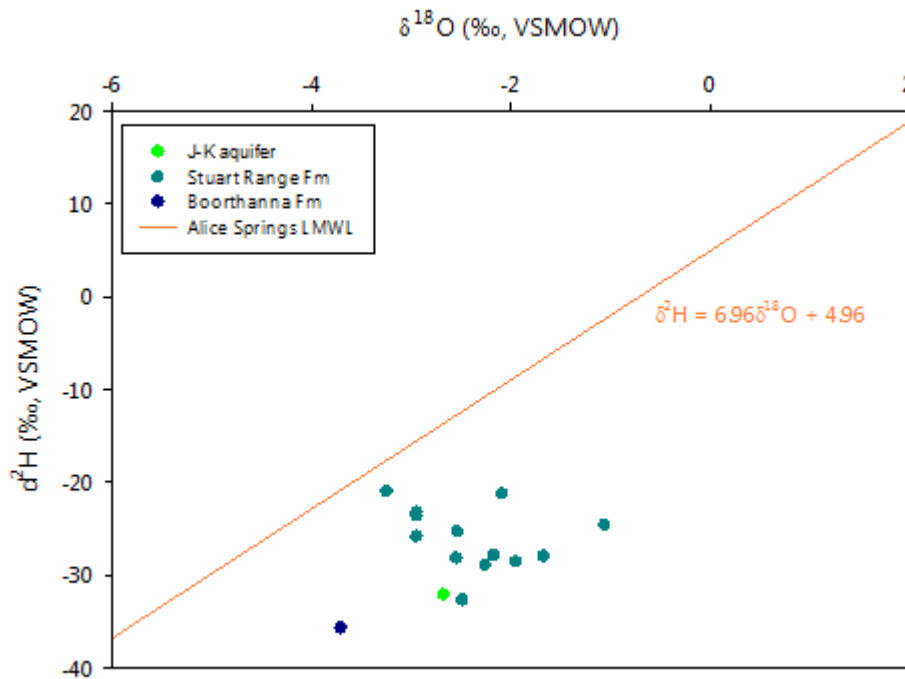


Figure 4-7 Stable water isotope composition of aquitard porewater, J-K aquifer and Boorthanna Formation

4.4.2.1 Deuterium ($\delta^2\text{H}$) porewater

The deuterium (and $\delta^{18}\text{O}$) porewater profile exhibits a different shape to the Cl^- profile, with greater data scatter (noise) and a resulting in difficulty in determination of an overall trend (Figure 4-8). It was expected that the stable isotopes of water profiles would exhibit similar shapes to the Cl^- profile, however there was an apparent decoupling of the profiles. The $\delta^2\text{H}$ and $\delta^{18}\text{O}$ profiles unexpectedly demonstrate differing profiles, although overall trend determination was difficult for both profiles. The relatively small range of $\delta^2\text{H}$ values (less than a factor of two) compared with Cl^- concentrations (factor of five, not including the Boorthanna Formation data) and significantly narrower range than most ranges observed in aquitard studies in North America and Europe (Harrington et al., 2013) adds to the difficulty of trend determination. The lower part of the aquitard is slightly more enriched than the upper part of the Stuart Range Formation aquitard and Boorthanna Formation groundwater. This suggests that Boorthanna Formation groundwater had a more depleted $\delta^2\text{H}$ composition in the recent past.

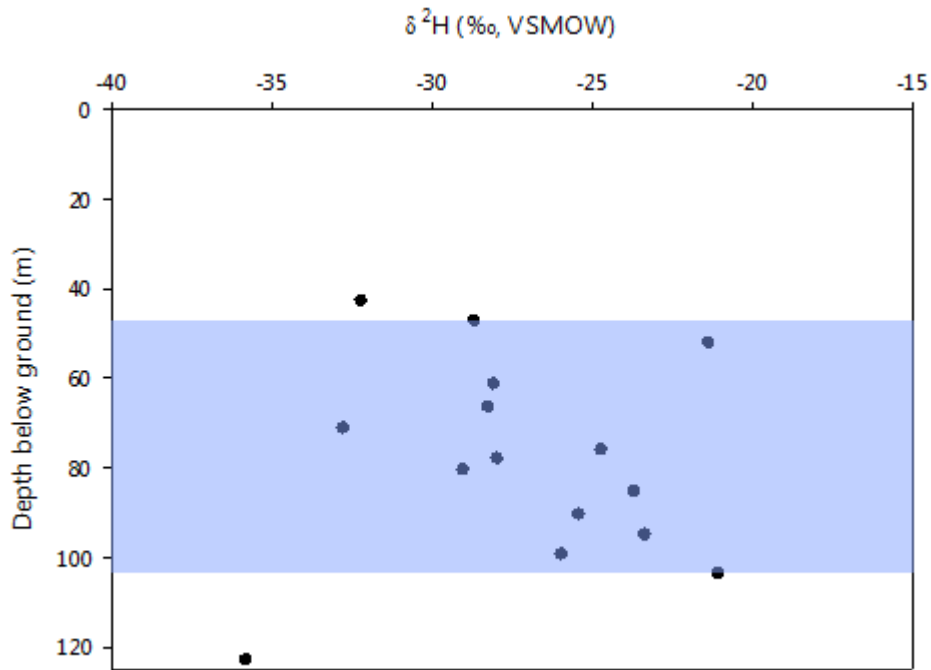


Figure 4-8 Deuterium ($\delta^2\text{H}$) aquitard porewater, J-K aquifer and Boorthanna Formation depth profile. Shaded zone corresponds to the location of the Stuart Range Formation.

4.4.2.2 $\delta^{18}\text{O}$ porewater

Most of the $\delta^{18}\text{O}$ porewater data plots in a narrow range (-1.5 ‰ to -3 ‰), which together with standard error ranges results in the difficulty of trend determination (Figure 4-9). The lower part of the aquitard and the Boorthanna Formation are more depleted than the upper portion of the aquitard, with a (linearly) depleting $\delta^{18}\text{O}$ trend with depth. This suggests that the lower part of the aquitard and the Boorthanna Formation had more depleted $\delta^{18}\text{O}$ composition in the recent past.

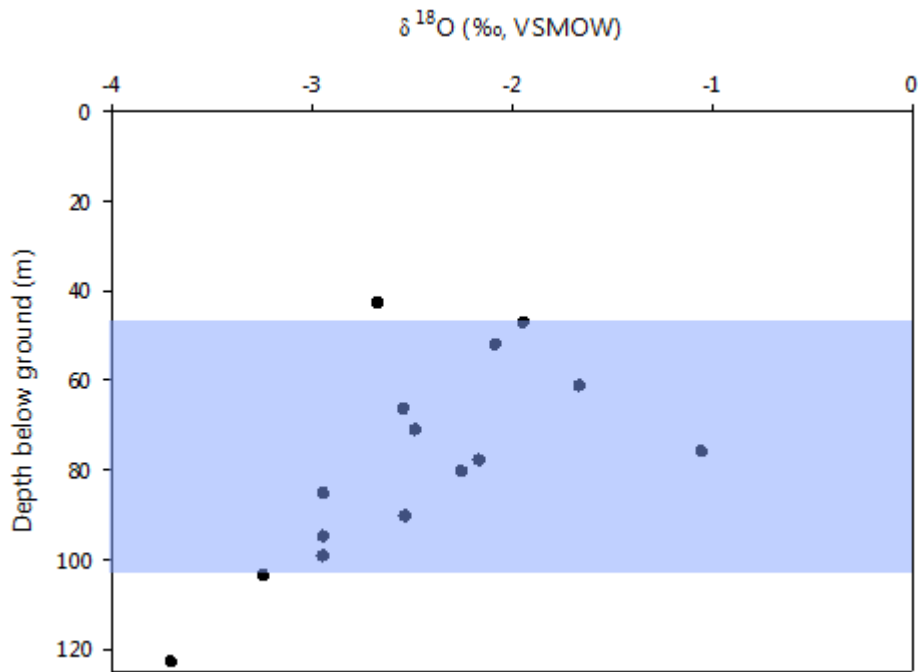


Figure 4-9 $\delta^{18}\text{O}$ profile aquitard porewater, J-K aquifer and Boorthanna Formation. Shaded zone corresponds to the location of the Stuart Range Formation.

4.4.3 Noble gases

The results and discussion for the noble gas investigation are included in Section 5.2, as this work directly relates to upscaling from the local (site) scale to regional scale.

4.5 Pore pressure

Five VWP were successfully installed in the Stuart Range Formation aquitard, with data manually downloaded 34 days after VWP installation to allow for pressure equilibration. Aquitard pore pressures at this time ranged from 64.67 kPa for the shallowest VWP (50.8 m BGS) to 512.58 kPa for the deepest VWP (102.8 m BGS). Temperatures varied from 24.89 °C for the shallowest VWP (50.8 m BGS) to 25.96 °C for the deepest VWP (102.8 m BGS).

Pressure data was temperature and salinity corrected using data from the VWPs and chloride profiles to provide understanding as to whether the magnitude of the correction was significant with respect to flow direction. An estimation of vertical flow was obtained using corrected and uncorrected heads (pressures). Groundwater elevations for the J-K aquifer and Boorthanna Formation were converted to pressures to allow further assessment of the pressure-elevation profile. The pressure gradient was less (8.17 kPa/m) than the hydrostatic line (10.20 kPa/m), thus the pressure values reflect subhydrostatic pressure and imply downward flow potential (Figure 4-10). The continuous pressure decrease with depth suggests no considerable heterogeneities in the rock matrix over the depth interval assessed, and no observed driving forces (e.g. pumping).

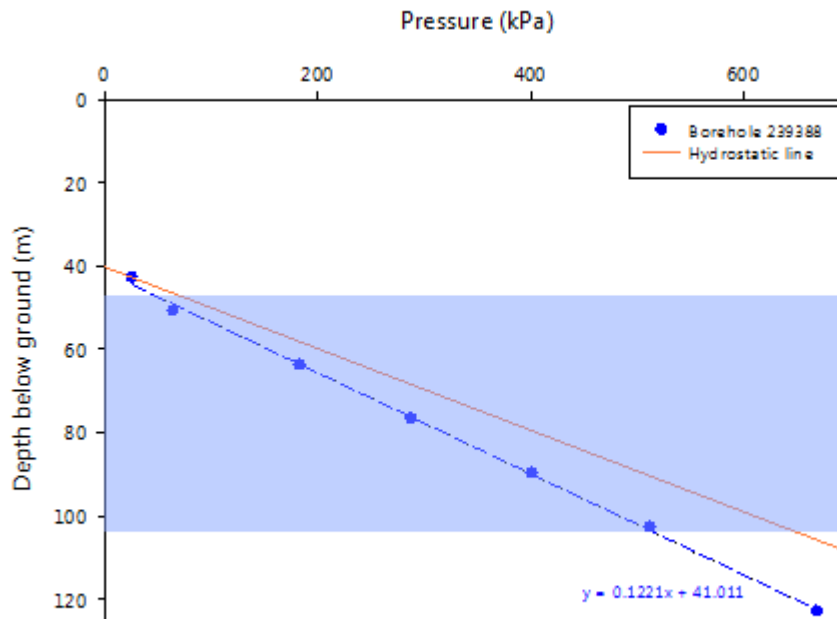


Figure 4-10 Pressure versus elevation/depth profile. Shaded zone corresponds to the location of the Stuart Range Formation.

4.6 Modelling

4.6.1 Fitting data to the entire aquitard

4.6.1.1 Analytical modelling

First an attempt was made to conceptualise the aquitard as a single layer. Note that all concentrations were from the aquitard, as the analytical modelling considers only the aquitard and the sample depths used were the average over the sampling interval. In order to use the transport equation solution of equation (B16), values were required for the four parameters D_e , C_0 , C_1 , C_2 as well as V and t , both of which were the main quantities to be determined from fitting. As per equation (4), Archie's Law gives $D_e = D_0 \eta_e^m$, where D_0 is the free water diffusion coefficient with a value of $1.71 \times 10^{-9} \text{ m}^2/\text{s}$ at 18°C , η_e is the measured porosity and m is an empirical constant in the range 2.0 to 2.5 (Mazurek et al., 2011). Here $m = 2.3$ was the chosen base case, so that $D_e = 6.183 \times 10^{-11} \text{ m}^2/\text{s} = 1.951 \text{ m}^2/\text{yr}$ including a temperature correction for the average aquitard temperature of 25.4°C . For C_0 , C_1 , C_2 there is no guidance, and so the procedure of Hendry and Wassenaar (1999) was adopted. That was by taking present day values ($C_1 = 4824 \text{ mg/L}$ and $C_2 = 10\,031 \text{ mg/L}$) holding for all time since $t = 0$ of, where the initial value of C_0 was taken at the present day 'nose' of the Cl^- data with approximate value $C_0 = 3500 \text{ mg/L}$. With a single layer depth, $L = 56.65 \text{ m}$ ($103.88 - 47.23 \text{ m}$) the time constant $t_0 = L^2 / D_e = 1\,645\,000 \text{ yrs}$ was well below the interpreted age of the aquitard at 270-263 Ma (Drexel and Preiss, 1995).

With the parameters above, a best fit was made to find both t and V , resulting in the values shown in Table 4-6 of $t = 40,600 \text{ yrs}$ and $V = -9.221 \times 10^{-5}$. This value of t was well below steady state and V was negative and upwards despite what the overall potential gradient shows. However, the fit to the data as seen in Figure 4-11 was not good. The measure of fit generated by ODRPACK is the least sum of squared errors for all data points, which was modified to the root mean square (RMS) value (equation (7)),

$$\text{RMS} = \left[\frac{\sum_{i=1}^{NREC} (C - C_{data})_i^2}{NREC} \right]^{1/2}, \quad (7)$$

which in turn was modified to a measure suitable for comparing any two data sets with different numbers of record pairs, $NREC : RMS_{AV\%} = RMS / (C_{data})_{AV} \times 100$. A series of fits were made holding $C_0 = 3500$ mg/L and fixing t to find V . As t increased towards steady state, which, from Table 4-6 can be approximated at 500 000 yrs, the fits became worse and the velocities increased to become a maximum of 2.5×10^{-4} m/yr. By decreasing C_0 down to a zero value, with variable t and V , the fits improved, and the velocities became positive with a maximum of 1.324×10^{-5} m/yr. Values of Peclet number, P_e , and diffusion length α_d are provided in Table 4-6. Overall the Peclet number suggests that diffusion transport dominates advection. However, the diffusion length was moderate to very large for $t < 150$ 000 yrs, suggesting that different values of C_0, C_1, C_2 could have a large influence on the predicted concentration values, provided the actual conditions are well below steady state.

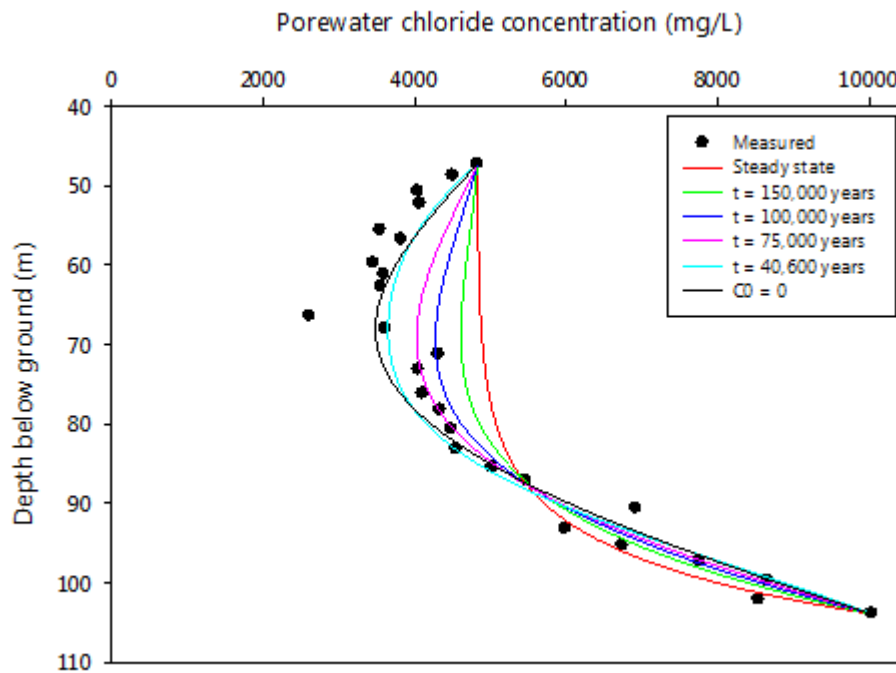


Figure 4-11 Single layer aquitard fitting of analytical solution to porewater chloride data)

Note: $C_0 = 3500$ mg/L, except where stated $C_0 = 0$

Table 4-6 Times and porewater velocities from single layer fitting

C_0 (mg/L)	t (yrs)	V (m/yr)	RMS _{Av%}	P_e	α_d (m)
3500	∞	2.484×10^{-4}	17.95	7.21	7.86
3500	500 000	2.471×10^{-4}	17.94	7.17	7.90
3500	150 000	1.348×10^{-4}	15.18	3.91	14.5
3500	100 000	7.747×10^{-5}	12.36	2.25	25.2
3500	75 000	3.383×10^{-5}	10.59	0.982	57.7
3500	50 000	-4.223×10^{-5}	9.15	1.23	46.2
3500	40 600	-9.221×10^{-5}	8.97	2.68	21.2
3000	65 000	-2.890×10^{-5}	8.83	0.838	67.5
2500	87 250	-5.830×10^{-6}	8.81	0.169	334.7
2000	106 200	3.633×10^{-5}	8.79	0.105	537.0
1000	137 500	1.080×10^{-5}	8.76	0.31	180.7
0	163 400	1.324×10^{-5}	8.75	0.385	147.3

In summary, none of the modelled fits to data were good (fitted curves from selected pairs of t and V values, Table 4-6 and Figure 4-11). The optimum fit at 40 600 years showed a time considerably less than t_0 and the interpreted geological age of 270 to 263 Ma. The optimum fit had an overall negative velocity despite the overall potential difference indicating a downward velocity; and decreasing C_0 from a value of 3500 mg/L improved the fit to positive velocities to the best fit at the unlikely $C_0 = 0$.

4.6.1.2 Numerical modelling

Chloride

One-dimensional numerical modelling simulated the Stuart Range Formation as a single layer aquitard. The procedure utilised was to start with a steady-state model of the Cl⁻ profile to represent the lower portion of the profile. Constant head and constant concentration upper and lower boundary conditions were assumed, to generate the curvilinear profile (Table 4-7). Constant concentration boundaries are justifiable due to long groundwater flow paths and therefore expected long-term water quality stability.

The Boorthanna Formation lower boundary condition depth was taken as the screened interval mid-point for well RMD-7 (123 m BGS). Although porewater chloride concentrations were obtained in the upper Boorthanna Formation, these values were not utilised as lower boundary conditions due to greater confidence that the groundwater sample was representative of free water, and that the porewater samples from the upper Boorthanna Formation are from the aquitard-aquifer (geological) transition zone and not ideal representative end-members. However the selection of the screened interval mid-point as the depth of the lower boundary condition is a potential source of error. It is noted that the approach to include groundwater data in addition to porewater data in the numerical modelling is different to that of the analytical modelling, which only models aquitard (porewater) data.

An optimal value for K_v of 1×10^{-12} m/s was determined by trial-and-error, which compares well with laboratory values ranging from 4×10^{-13} to 4×10^{-10} m/s (median of 4.5×10^{-12} m/s). Solute transport in this system was assumed to be diffusion-dominated and any advective transport will be controlled by the least permeable zone. Hence the modelling assumed a single, bulk value for K_v for the aquitard. Using a K_v of 1×10^{-12} m/s, the lower part of the Cl⁻ profile was allowed 4 Ma to evolve from

a constant initial condition (Figure 4-12). Following the rationale of Mazurek et al. (2011), the initial conditions and starting point for the model were set at a stage of post-depositional evolution at which time reasonable assumptions about solute composition and hydrogeological changes up to the present can be made. 4 Ma was considered sufficient time for the lower part of the steady state profile to develop, based on the work of Harrington et al. (2013).

Table 4-7 Initial concentration and boundary conditions (BC) adopted for chloride simulations

Time BP	Initial concentration (mg/L)	Upper BC (J-K)		Lower BC (Boorthanna)	
		Flow (m AHD)	Transport (mg/L)	Flow (m AHD)	Transport (mg/L)
	3500	Fixed Head	Constant Conc.	Fixed Head	Constant Conc.
4 Ma		113.61	5500	99.29	30 000

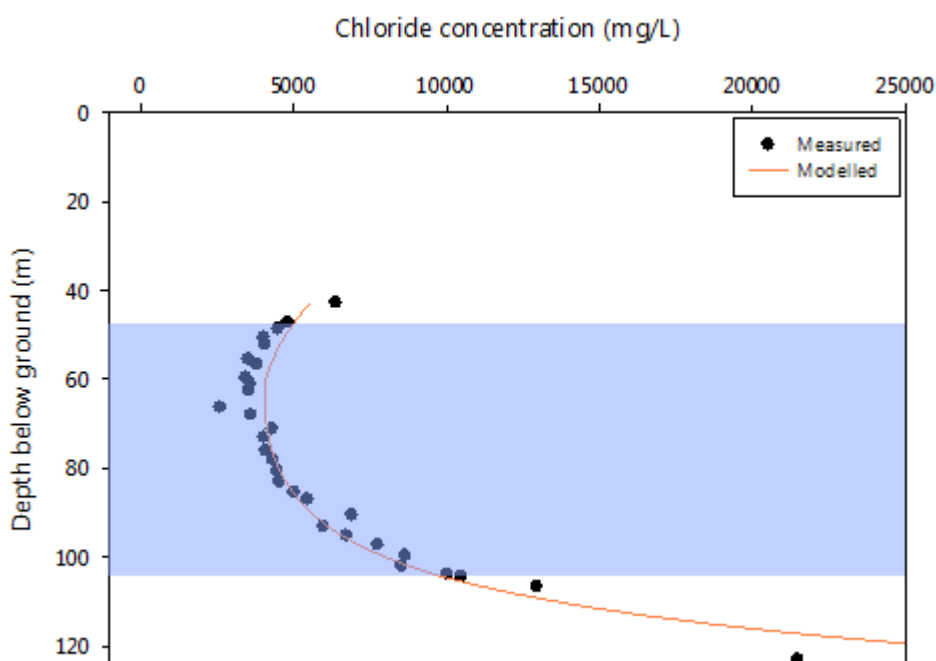


Figure 4-12 Measured and initial steady state (4 Ma) modelled chloride concentration in aquitard porewater and groundwater. Groundwater data for well RMS-7 (J-K aquifer) was the upper data point (42.8 m BGS), with depth taken as the mid-point of the J-K aquifer screened portion. Groundwater data for well RMD-7 (Boorthanna Formation) was the lowest data point (123 m BGS), with depth taken as the mid-point of the screened interval. Shaded zone corresponds to the location of the Stuart Range Formation.

When modelling the evolution of the Cl⁻ profile it was necessary to specify a constant concentration in the J-K aquifer of 5500 mg/L, which is fresher than the present day value (6400 mg/L). This suggests Cl⁻ concentration in the J-K aquifer changed relatively recently (compared to up to 4 Ma timeframe for the profile development).

Variability in groundwater Cl⁻ concentrations from the Boorthanna Formation (well RMD-7) and J-K aquifer (well RMS-7) is discussed in Section 4.4.1. It was probable that there had been variation in Cl⁻ (and δ²H and δ¹⁸O) concentrations since

formation deposition. This, and other identified geochemical changes to the aquitard, supports the observations of Mazurek et al. (2011) that the aquitard was dynamic over geological time, always adjusting to evolving boundary conditions.

The greatest potential source of error in the modelled tracer profile was the effective diffusion coefficient (D_e). Underestimation of D_e causes an overestimation in the time for profile development, and vice versa, although the shape of the profile will not be altered (Harrington et al., 2013). Harrington et al. (2013) report that uncertainty in D_e was the result of the selection of the power term 'm', with the selected value in this study ($m = 2.3$, Section 3.8.2) leading to an error of approximately 20 % in D_e . This error results in a 17–25 % error in the simulation time, comparable to errors associated with constant concentration boundary conditions (Harrington et al., 2013).

The evolution times simulated are sensitive to the initial concentrations assumed in the model. The uncertainties in initial concentrations are one of the main limitations on the accuracy of simulated evolution times (Mazurek et al., 2011).

Stable isotopes of water

Due to the $\delta^2\text{H}$ and $\delta^{18}\text{O}$ profiles exhibiting far greater noise than the Cl^- profile, the relatively small range of the data, and difficulty in ascertaining definitive trends, the stable water isotope profiles were not modelled.

4.6.2 Fitting data as two distinct aquitard layers

4.6.2.1 Analytical modelling

The two data sets used as a basis for modelling as a two layer aquitard were those of Cl^- and water potential, shown in Figures 4-4 and 4-13 respectively.

For Cl^- , there was a transition between depths 51 and 75 m BGS which also coincides with changes identified in the aquitard physical properties. The data point at 66.38 m BGS lies in this region, and it was probably either an outlier when considering the aquitard as a single layer or a point of significance in a zone of division if the aquitard was better considered as two distinct layers. The water potential data showed the same groupings of upper and lower values relative to this point. Least squares data fitting by straight lines has been made using the Levenberg-Marquardt method within a robust computer software package ODRPACK (Boggs et al., 1992). The least squares was done using orthogonal distance between data points and the fitted lines. This was simple here, but is important for the fitting of the model concentrations to the Cl^- data where measurement errors are likely to occur in both depths and concentrations. The fitted values of the straight lines are shown on Figure 4-13. The main point was that the fitting of the lower group shows that the average potential difference over the group section provides a definite downward porewater velocity, whereas the trend for the upper group velocity was possibly upwards.

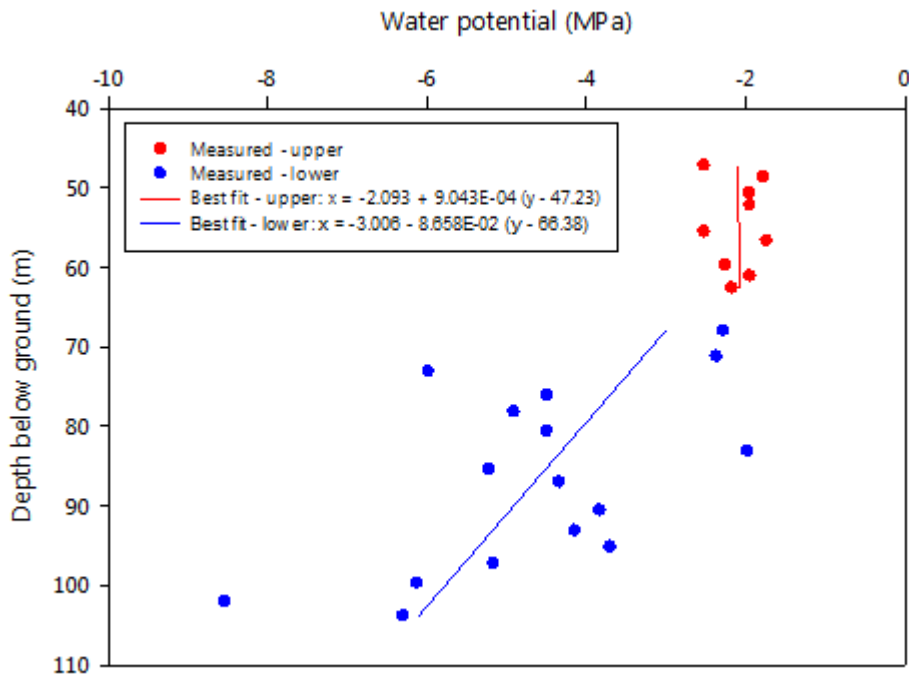


Figure 4-13 Lines of best fit to water potential data

From this brief overview of data and reference to geological properties, it is likely that the aquitard needs to be considered as two separate layers as was done with the King aquitard in Canada (Hendry and Wassenaar, 1999). The single layer was divided into two layers, the upper layer from 47.23 to 62.63 mBGS, with a thickness of 15.40 m, and a lower layer from 68.00 to 103.88 m BGS, with a thickness of 35.88 m. The section between 62.63 and 68.00 m BGS, containing the data (sample) at 66.38 m BGS, is not included.

The lower layer was studied first. The average temperature of the lower layer was 25.7 °C, providing a temperature corrected $D_e = 6.233 \times 10^{-11} \text{ m}^2/\text{yr}$. Other parameters for the model are $L = 35.88 \text{ m}$, $C_0 = 3500 \text{ mg/L}$, $C_1 = 3812 \text{ mg/L}$, $C_2 = 10\,031 \text{ mg/L}$ and $t_0 = 654\,491 \text{ yrs}$.

Attempting to fit both t and V with the analytical solution produced a stable $V = 1.221 \times 10^{-4} \text{ m/yr}$ but an unstable t . By fixing t at various values and determining V , it was found that for $t = 100\,000, 200\,000, 300\,000, 400\,000$ and $500\,000 \text{ yrs}$, the corresponding V values were $V = 7.681 \times 10^{-5}, 1.154 \times 10^{-4}, 1.209 \times 10^{-4}, 1.216 \times 10^{-4}, 1.221 \times 10^{-4} \text{ m/yr}$, meaning that essentially the data corresponds to steady state values and t_0 is a good estimate. Then, $P_e = 2.227$ and $\alpha_d = 16.1 \text{ m}$. The curve fitted to the data is shown in Figure 4-14, with an $\text{RMS}_{AV\%} = 6.38 \%$.

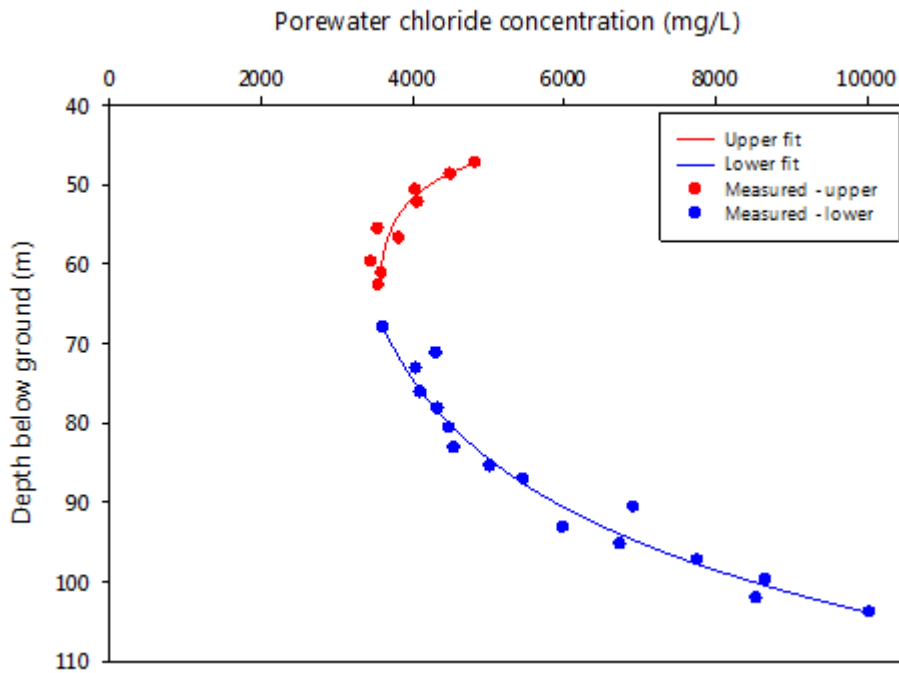


Figure 4-14 Two layer aquitard fitting of analytical solution to porewater chloride data

For the upper layer the average temperature is 24.9 °C, providing a temperature corrected $D_e = 6.100 \times 10^{-11} \text{ m}^2/\text{yr}$. Other parameters are $L = 15.40 \text{ m}$, $C_0 = 3500 \text{ mg/L}$, $C_1 = 4824 \text{ mg/L}$, $C_2 = 3549 \text{ mg/L}$ and $t_0 = 123 \text{ 199 yrs}$. Fitting the model to the data presented the same situation of a stable $V = -4.269 \times 10^{-4} \text{ m/yr}$ and an unstable t . As before, fixing t at various levels and finding V , it was found that for $t > 110 \text{ 000 yrs}$, this stable value of V was achieved, so that there was essentially steady state and t_0 was a good estimate for it. Then, $P_e = 3.415$ and $\alpha_d = 4.51 \text{ m}$. The fitted curve is shown (Figure 4-14), with an $\text{RMS}_{\text{AV}\%} = 2.65 \%$.

The porewater velocity in the upper layer was negative and upwards and almost 4 times the magnitude of the downward velocity of the lower layer. In this upper level the gradient dC/dz is negative and an average overall diffusive flux (equation (B1)) was then positive downwards. This suggests that the overall advective flux dominates the diffusive flux. This was contrary to the expectation of diffusion dominance with a $P_e = 3.415 < 5$.

To investigate the relative important of flux components, plots of these are shown in Figure 4-15, where expression (B17) has been used for the diffusive flux and (B18) for the total flux. Arrows on the various curves show the effective flux directions. For both upper and lower layers, the advective components dominate the diffusive components with combined values constant at -1.496 mg/L m/yr in the upper layer and 0.346 mg/L m/yr in the lower layer. It was noted that the diffusive fluxes in both layers are nearly zero near the 'nose' of the data where dC/dz was zero.

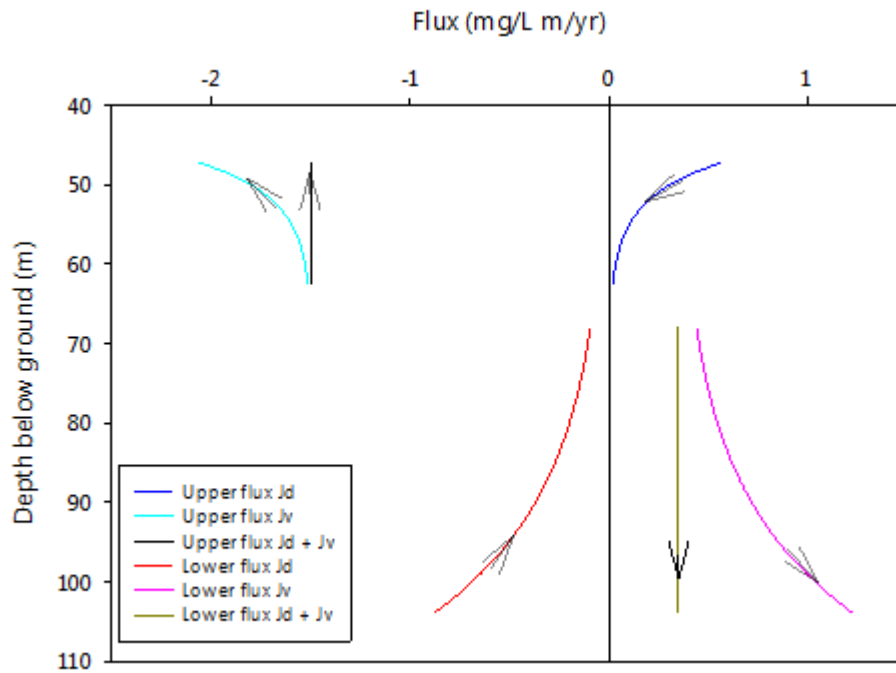


Figure 4-15 Diffusive flux and advective flux for two layer aquitard

The implication from these results is that, provided C_1 and C_2 at present day values have held for all time, then there must be an additional lateral inflow of water in the zone between the two layers to provide the upward vertical flow in the upper layer.

Considering the Cl^- concentrations and water potentials at the excluded level at 66.38 m BGS, it can be seen that they would support the idea of lateral water inflow. Extracting the data values on either side of this depth is shown in Table 4-8.

Table 4-8 Chloride concentrations and water potentials at, and directly above and below, the 66.38 m BGS sample

Depth (m BGS)	Chloride concentration (mg/L)	Water Potential (mPa)
62.63	3549	-2.16
66.38	2605	-1.09
68.00	3612	-2.28

The value of water potential -1.09 mPa (at 66.38 m BGS) is not only higher than its neighbours but the highest at all levels and suggests inflowing water which would dilute the neighbouring Cl^- concentrations to the low 2605 mg/L.

Changes in velocities for different diffusion coefficients can be easily calculated (at steady state) by noting that D_e and V appear as the fixed ratio V/D_e in equation (B15) for C_∞ . By changing the values of the exponent m in Archie's Law for diffusion coefficients from $m = 2.3$ to 2 and 2.5. The upper layer has values of $D_e = 9.871 \times 10^{-11}$, 6.233×10^{-11} , 4.588×10^{-11} m^2/s corresponding to a $V = 1.934 \times 10^{-4}$, 1.221×10^{-4} , 0.899×10^{-4} m/yr and $m = 2.0$, 2.3 and 2.5. Likewise in the lower layer, $D_e = 9.660 \times 10^{-11}$, 6.100×10^{-11} , 4.489×10^{-11} m^2/s corresponding to a $V = -6.76 \times 10^{-4}$, -4.269×10^{-4} , -3.142×10^{-4} m/yr and $m = 2.0$, 2.3 and 2.5.

On the assumption that a 1D transport model with diffusive and advective components is applicable and that the Cl^- concentrations for the top and bottom of the aquitard hold for all time, then the most likely outcome from the modelling is that there is lateral flow of water near the depth 66.38 m BGS. Although there is leakage from the bottom of the aquitard with

a possible range of porewater velocities 0.899×10^{-4} to 9.871×10^{-4} m/yr (1.528×10^{-5} to 1.678×10^{-4} m/yr, Darcy velocities), the leakage was most likely coming from a steady state subsurface lateral flow rather than from the top of the aquitard.

4.7 Flux estimates

Groundwater flux through the Stuart Range Formation was estimated using the adopted value of K_v from the modelled Cl^- profile, the laboratory determined median K_v , the porewater velocity range determined from analytical modelling and equation (2) (Table 4-9).

Table 4-9 Range of Darcy fluxes

Hydraulic Conductivity, K_v (m/s)	Hydraulic Conductivity, K_v (m/d)	Source of K_v Value	Darcy Flux (m/year)	Darcy Flux (mm/1000 years)
1×10^{-12}	8.6×10^{-8}	Cl^- profile modelling	5.36×10^{-6}	5
4.5×10^{-12}	3.9×10^{-7}	Median laboratory value	2.41×10^{-5}	24
4.8×10^{-13} to 5.3×10^{-12}	4.2×10^{-8} to 4.6×10^{-7}	Analytical modelling	1.53×10^{-5} to 1.68×10^{-4}	15 to 168

5 Up-scaling of aquifer connectivity site results

Coring, and 1D analytical and numerical modelling provided an understanding of inter-connectivity between the Arckaringa Basin and GAB at a point scale. Translating local-scale findings to regional scale is required if the results are for an improved understanding of basin processes and to inform management decisions. Commonwealth of Australia (2014) documents several approaches for assessing aquifer connectivity at a regional scale including geophysical methods, hydraulic techniques, environmental tracers and numerical modelling.

5.1 Palaeohydrogeological systems

Environmental tracer profiles (in this case Cl^-) and associated 1D analytical and numerical modelling provide a basis for furthering our understanding of regional palaeohydrogeological conditions in arid areas. The observed porewater Cl^- profile provided insights to the palaeohydrology of the region within the Quaternary period (2.59 Ma to present).

Comparison of Cl^- and $\delta^2\text{H}$ values from the Boorthanna Formation and the lower part of the Stuart Range Formation reveal that the Boorthanna Formation was more saline (higher Cl^-) and more depleted (lower $\delta^2\text{H}$) in the past. Comparison of Cl^- and $\delta^2\text{H}$ values from the J-K aquifer and the upper part of the Stuart Range Formation indicate that the J-K aquifer was fresher (lower Cl^-) and more enriched ($\delta^2\text{H}$) in the past. Both of these conclusions suggest potentially different historic recharge mechanisms to current day.

5.2 Regional aquifer connectivity and groundwater flow

Studies of porewater composition conducted on cored aquitard material do not provide a comprehensive picture of inter-aquifer connectivity on a regional scale. Aquitard porewaters provide information about local-scale flow through aquitard pore spaces, whereas on a regional scale, leakage is generally controlled by secondary permeability such as fractures, discontinuities and sand lenses etc. (Figure 5-1) (Neuzil 1986, Konikow and Arevalo 1993, Hendry et al., 2004).

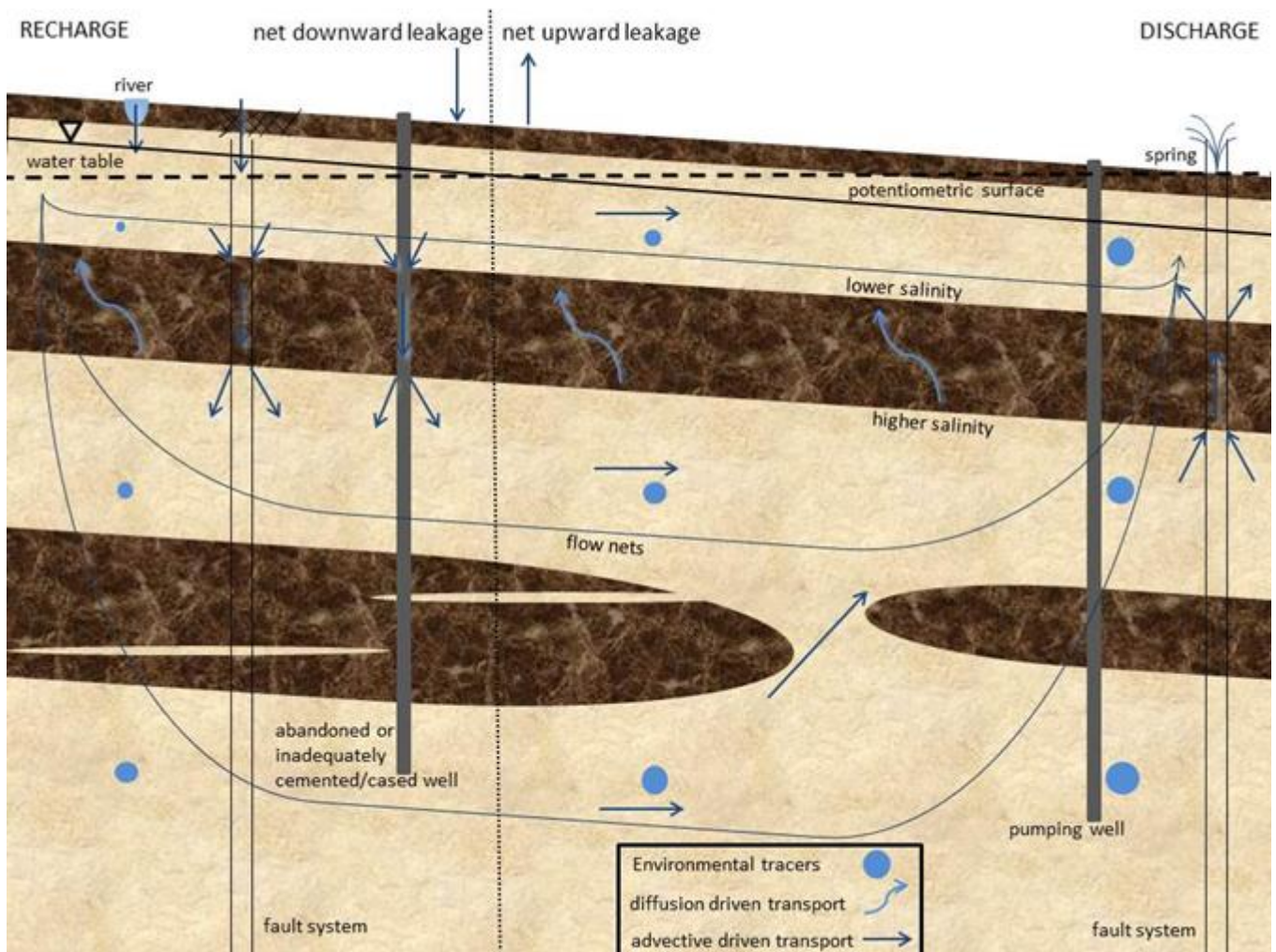


Figure 5-1 Potential leakage pathways through an aquitard (adapted from Cherry and Parker, 2004)

Multiple methods exist to investigate leakage. Pumping tests with monitoring wells in aquifers above and below, as well as within the aquitard can be used to investigate the permeability of aquitards (Hantush 1966, Hantush 1967, Neuman and Witherspoon 1969, Neuman and Witherspoon 1972). Regional hydraulic head patterns provide the flow direction and infer recharge and discharge locations under today's conditions. In addition, hydraulic head measurements within aquitards can be used to investigate vertical groundwater flow (Meyboom 1966). When hydraulic head measurements are analysed in conjunction with environmental tracers it is possible to identify past processes (Love et al., 1993).

Regional scale investigations can infer secondary permeability features in aquitards by using hydraulic head measurements and environmental tracers in aquifers, for example where environmental tracer signatures are similar in aquifers above and below an aquitard. Love et al. (1993, 1994), Herczeg et al., (1996) and Dogramaci and Herczeg (2002) all identified groundwater leakage using environmental tracers including major ions, stable water isotopes, ^{14}C , ^{36}Cl and Sr isotopes. Love et al. (1993, 1994) identified inter-aquifer connectivity in the Otway Basin by comparing current day hydraulic head measurements with variations in major ion and stable isotopes of water composition and the apparent age of groundwater via ^{14}C analysis. Herczeg et al. (1996) were able to use $^{234}\text{U}/^{238}\text{U}$ and ^{36}Cl to identify inter-aquifer mixing in the Otway Basin, while Dogramaci and Herczeg (2002) calculated the fraction of water exchanged between aquifers in the Murray Basin using Sr isotopes. Noble gases can be used in addition to the aforementioned environmental tracers, and have been used to examine groundwater flow, palaeo-climate and inter-aquifer leakage (Clark et al., 1997, Althaus et al., 2009).

5.2.1 Inferred from hydraulics

Inter-aquifer connectivity can be identified by comparing hydraulic heads between aquifers at one location. Regional hydraulic heads and flow paths in the Boorthanna Formation and J-K aquifer indicate groundwater flow to the east toward the Stuart

Shelf (Figure 5-2) (Keppel et al., 2015). Well nests were identified to infer inter-aquifer connectivity at a regional scale in the Arckaringa sub-region (Figure 5-2, Table 5-1). Ideally, heads are compared at the same location where multiple wells exist but for the purpose of this study well nests are wells completed in the J-K aquifer and Boorthanna Formation adjacent to or within a 5 km radius.

Comparison of hydraulic heads in well nests show downward potential for groundwater flow in all locations except well nests 16 and 18, where the head difference indicates upward flow potential from the Boorthanna Formation to the J-K aquifer. These locations are located in a regional discharge area associated with springs. At well nests 11 and 13 one of the two Boorthanna Formation wells has RSWLs 30–40 m lower than the adjacent. The lower RSWLs reflect the influence from pumping by Prominent Hill Mine whereas the higher RSWLs represent pre-pumping and thus reflect flow potential prior to the development of the Prominent Hill borefield.

The head difference provides an indication of the potential flow direction but not the flow rate. Where the Stuart Range Formation was present, especially where it is thick, flow rates may be extremely low (less than a fraction of a millimetre per year). In the south-eastern portion of the Arckaringa sub-region the Stuart Range Formation was absent. At these locations the J-K aquifer and Boorthanna Formation are in direct contact and head differences in most wells indicate downward flow. The head difference in well nest 4 indicates a potential for both upward or downward flow to the nearby Boorthanna Formation wells.

Where the Stuart Range Formation was present it was possible to calculate the groundwater flow rate through the Stuart Range Formation using the hydraulic head of the Boorthanna Formation and J-K aquifer, and using Darcy's Law, equation (2) described in Section 3.7. Flow rates were calculated using the maximum (4×10^{-10} m/s) and minimum (4×10^{-13} m/s) measured vertical hydraulic conductivity for the well nests (Table 5-1). The vertical flow rates range between 7.7×10^{-2} – 1.8×10^{-9} m/y and are extremely low flow rates, in the order of only mm-cm's per 1000 years. Therefore any leakage on a significant scale will most likely be due to secondary permeability.

Table 5-1 Well nests showing aquifer monitored, RSWL, Stuart Range Formation thickness and calculated vertical flow rates

Well nest no.	Well name	Unit Number	Aquifer	Uncorrected RSWL (m AHD)	Corrected RSWL (m AHD)	Potential vertical groundwater flow	Stuart Range Formation thickness (m)	Flow rate (m/y)
1	RMS 4	6138-90	J-K	59.28	59.30	downward	0	N/A
	New Mudla MONWELL	6138-99	J-K	62.29	62.30		0	N/A
	Tuckers Bore	6138-25	J-K	60.75	60.76		0	N/A
	RMD 4	6038-198	Boorthanna	48.08	48.36		0	N/A
2	Watchie Well (New)	6138-38	J-K	79.59	79.59	downward	0	N/A
	Watchie Well 1108	6138-85	Boorthanna	67.03	67.05		0	N/A
3	6137-77	6137-77	J-K	72.64	72.63	downward	0	N/A
	Homestead MONWELL	6137-92	Boorthanna	71.11	71.11		0	N/A
4	WSC-4B	6137-90	J-K	76.42	77.82	downward	0	N/A
	WSC-4A	6137-93	J-K	77.29	77.63		0	N/A
	6137-38	6137-38	Boorthanna*	73.82	73.82		0	N/A
	NO 20A Bore	6137-78	Boorthanna*	78.99	79.02		0	N/A
5	ASMW 4	6038-211	J-K	98.84	99.01	downward	61	$3.4 \times 10^{-6} - 3.4 \times 10^{-3}$
	Aries-BA	6038-170	Boorthanna	82.35	83.54		78	
6	Nickel Well 2	6038-26	J-K	117.98	118.26	downward	65	$3.7 \times 10^{-6} - 3.7 \times 10^{-3}$
	Nicholl 2	6038-93	Boorthanna	98.80	99.15		87	
7	6138-40	6138-40	J-K	91.11	91.11	downward	4	$7.7 \times 10^{-5} - 7.7 \times 10^{-2}$
	AMD 3	6138-91	Boorthanna	66.85	68.25		8	

Well nest no.	Well name	Unit Number	Aquifer	Uncorrected RSWL (m AHD)	Corrected RSWL (m AHD)	Potential vertical groundwater flow	Stuart Range Formation thickness (m)	Flow rate (m/y)
8	AMS 2	6038-199	J-K	90.86	90.89	downward	120	$4.6 \times 10^{-6} - 4.6 \times 10^{-3}$
	Aries 9A	6138-120	Boorthanna	53.00	54.83		104	
	Aries-E2	6138-74	Boorthanna	60.13	62.09		104	
9	ASMW 3	6038-210	J-K	94.64	94.56	downward	65	$1.2 \times 10^{-6} - 1.2 \times 10^{-3}$
	New No.1 Bore	6038-29	J-K	95.01	95.03		63	
	Millers Creek 1	6038-25	Mt Toondina	92.99	93.07		57	
	Aries-C	6038-219	Boorthanna	89.21	90.12		65	
10	ASMW 4	6038-211	J-K	98.84	99.01	downward	61	$5.8 \times 10^{-6} - 5.8 \times 10^{-3}$
	AMD 2	6038-177	Boorthanna	70.63	71.97		47	
11	AMS 2	6038-199	J-K	90.86	90.89	downward	120	$5.9 \times 10^{-6} - 5.9 \times 10^{-3}$
	BFMW 2	6038-147	Boorthanna	47.19	47.28		93	
	Aries-1	6038-190	Boorthanna	77.51	78.10		93	
12	TSF-D6	6038-207	J-K	118.54	118.59	downward	30	$4.3 \times 10^{-7} - 4.3 \times 10^{-4}$
	TSF-D4	6038-232	Boorthanna	117.52	117.55		20	
13	VMS-1	6038-248	J-K	113.54	113.47	downward	84	$5.5 \times 10^{-6} - 5.5 \times 10^{-3}$
	Virgo-E4	6038-184	Boorthanna	77.13	79.61		84	
	Virgo-4	6038-240	Boorthanna	106.44	108.88		39	
	Virgo-E5	6038-244	Boorthanna	107.84	110.42		91	
14	VMS 2 (now RMS 7)	6038-185	J-K	114.48	114.86	downward	54	$4.6 \times 10^{-6} - 4.6 \times 10^{-3}$

Well nest no.	Well name	Unit Number	Aquifer	Uncorrected RSWL (m AHD)	Corrected RSWL (m AHD)	Potential vertical groundwater flow	Stuart Range Formation thickness (m)	Flow rate (m/y)
	RMD 7	6038-187	Boorthanna	94.86	96.83		54	
	Rankins Bore No 3	6036-35	J-K	115.95	115.96		17	
15	Clemens	6036-195	Boorthanna	113.02	113.20	downward	29	$1.3 \times 10^{-6} - 1.3 \times 10^{-3}$
	Clemens Bore	6036-36	Boorthanna	113.20	113.28		29	
16	RMS 3	6139-47	J-K	60.82	60.80	upward	277	$1.8 \times 10^{-9} - 1.8 \times 10^{-6}$
	RMD 3	6139-46	Boorthanna	60.78	61.96		277	
	RMS 2	6137-86	J-K	93.06	93.03		59	
17	RMD 2	6137-04	Basement	66.23	66.58	downward	59	$6.4 \times 10^{-6} - 6.4 \times 10^{-3}$
	Millers CK 9 BORE	6137-85	Boorthanna	63.28	63.43		56	
	Hunts Bore	6138-36	J-K	50.58	50.61		30	
18	RMS 1	6138-71	J-K	51.88	52.02	upward	25	$8.2 \times 10^{-6} - 8.2 \times 10^{-4}$
	RMD 1	6138-70	Boorthanna	52.52	53.84		25	
19	Aries JS	6038-212	J-K	98.24	98.46	downward	5	$5.9 \times 10^{-5} - 5.9 \times 10^{-2}$
	Aries JD	6038-206	Basement	65.66	66.69		5	
20	NO.6 MONWELL-S	6038-176	J-K	92.53	92.63	downward	78	$2.9 \times 10^{-6} - 2.9 \times 10^{-3}$
	NO.6 MONWELL-D	6038-175	Boorthanna	74.69	74.87		78	
21	ASMW 3	6038-210	J-K	94.64	94.56	downward	64	$2.7 \times 10^{-6} - 2.7 \times 10^{-3}$
	Aries-Q	6038-222	Boorthanna	81.12	81.86		104	

* No 20A BORE and 6137-38 are completed in the Boorthanna Formation, however they appear to be outside of the Boorthanna Formation extent (Figure 5-2). This was due to the geologic extent being mapped prior to bore logs being available.

As discussed in Section 3.7 the flow rate is dependent on the head difference (Δh), the thickness of the aquitard (b) and the vertical hydraulic conductivity of the aquitard (K_v). When the vertical hydraulic conductivity is low or the Stuart Range Formation is thick, a larger head difference is required to drive the same flow rate as where the formation is thinner or more permeable. In other words, a large hydraulic head difference between the aquifers can be taken as an indication that there is an effective barrier in place to maintain head differences between aquifers.

Well nests 3, 4, 9, 12, 15, 16 and 18 have very similar hydraulic heads. Most of these locations have a potential downward flow direction except well nests 16 and 18 with a potential for upward flow. A small head difference may be interpreted as the Stuart Range Formation being thin or having a high hydraulic conductivity, potentially due to secondary permeability. The head difference for well nests 16 and 18 are of the same magnitude as the freshwater head corrections so it was not possible to interpret vertical flow direction because of the uncertainty involved (Post et al., 2007). Alternatively this could be where there is a cross-over of the hydraulic heads between the Boorthanna Formation and J-K aquifer in a hinge-zone that separates regional recharge to discharge areas. Therefore, to ascertain if inter-aquifer connectivity occurs at these locations it was necessary to look at environmental tracers in addition to the hydraulics.

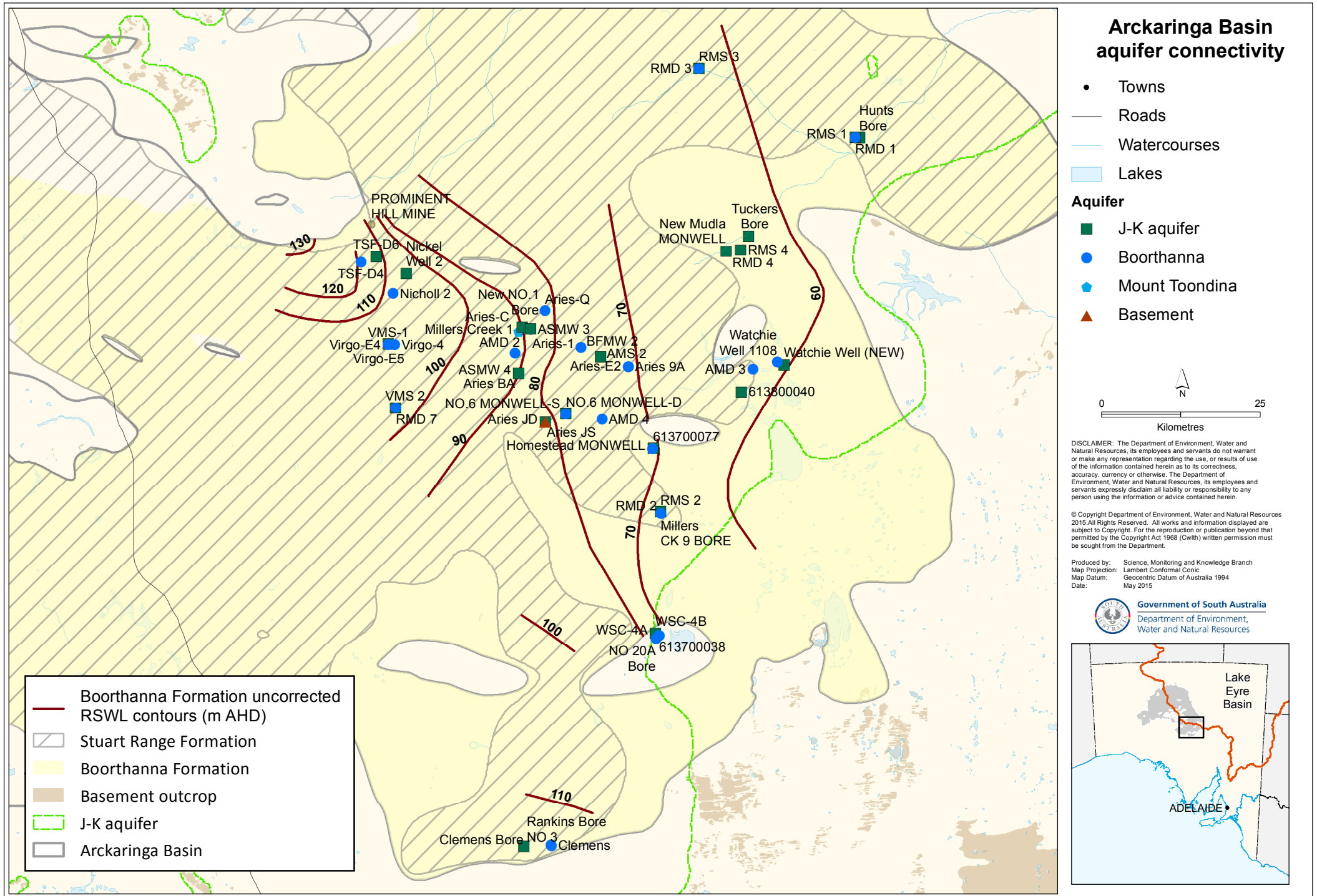


Figure 5-2 Location of well nests

Well nests where aquifer connectivity may be occurring:

Well nest no.	Well name	Stuart Range Formation thickness (m)
3	6137-77	0
	Homestead MONWELL	0
4	WSC-4B	0
	WSC-4A	0
	6137-38	0
	NO 20A Bore	0
	ASMW 3	65
9	New No.1 Bore	63
	Millers Creek 1	57
	Aries-C	65
	TSF-D6	30
12	TSF-D4	20
	Rankins Bore No 3	17*
15	Clemens	29*
	Clemens Bore	29*
16	RMS 3	277
	RMD 3	277
18	Hunts Bore	30*
	RMS 1	25*
	RMD 1	25*

* Near southern margin of the basin and shallow

5.2.2 Inferred from environmental tracers

Inter-aquifer connectivity between the well nests was examined using $^{87}\text{Sr}/^{86}\text{Sr}$ ratios, $\delta^{13}\text{C}$, ^{14}C and ^{36}Cl data (Keppel et al., 2015). Available data is presented in Figure 5-3, with the well nests plotted in similar colours and aquifers distinguished by shape for easier identification. Well nests 19 and 20 are combined due to the lack of available data and the very close proximity of the wells within these two nests. Well nests with similar tracer signatures in each aquifer provide a line of evidence to support connection between aquifers.

The majority of the well nests show variation in environmental tracers (Figure 5-3) suggesting a lack of complete connectivity. The exceptions to this were well nest 9, 19 and 20. Well nest 19 and 20 show similar ^{14}C , $\delta^{13}\text{C}$ and $^{87}\text{Sr}/^{86}\text{Sr}$ ratios for No 6 Monwell D (Boorthanna Formation) and Aries JD (basement), corresponding to previous findings that the Boorthanna Formation and basement aquifers can be in hydraulic contact (Keppel et al., 2015). Well nest 9 shows very similar values for all plotted environmental tracers (Figure 5-3). The similarity of the age tracers, ^{14}C and ^{36}Cl , could indicate that the groundwater in the J-K aquifer and Boorthanna Formation have had similar residence times. The $\delta^{13}\text{C}$ and $^{87}\text{Sr}/^{86}\text{Sr}$ ratios provide an indication of the water-rock interactions. The similarity of the $^{87}\text{Sr}/^{86}\text{Sr}$ ratios and $\delta^{13}\text{C}$ results for the nested wells indicate that the groundwater has been in contact with the same rocks. Keppel et al. (2015) states that the Sr isotope ratios within the J-K aquifer are consistently between 0.7145 and 0.7119 and the values at Aries-C (Boorthanna Formation) fits within this trend. Therefore it seems plausible that there was leakage from the J-K aquifer to the Boorthanna Formation at this location. Considering the Stuart Range Formation is ~ 90 m thick at this location, any inter-aquifer leakage at this location would be due to flow along secondary permeability features such as fractures.

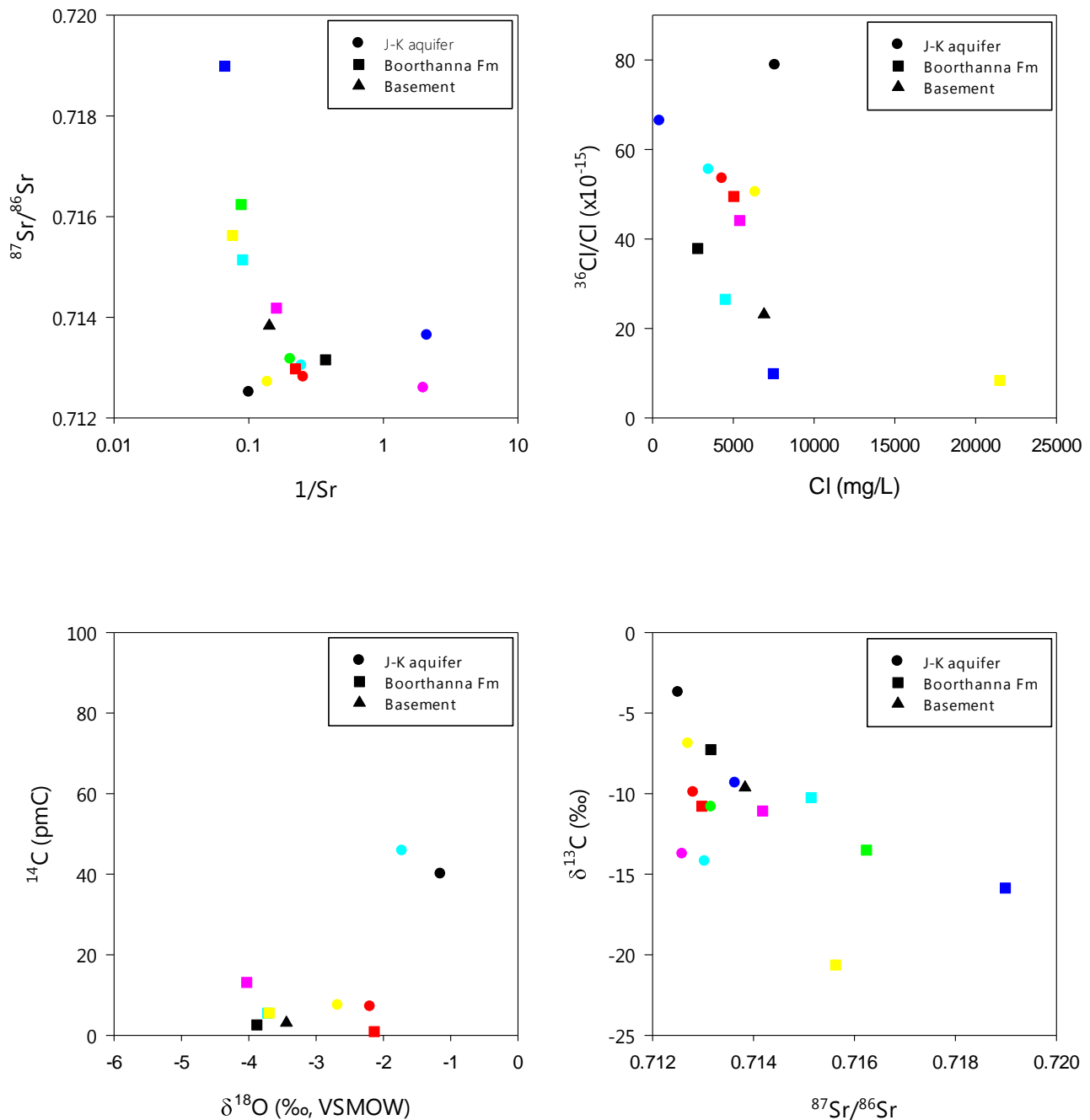


Figure 5-3 Environmental tracer data for well nests: [a] $^{87}\text{Sr}/^{86}\text{Sr}$ vs $1/\text{Sr}$ (ppm⁻¹) [b] $^{36}\text{Cl}/\text{Cl}$ (x10⁻¹⁵) vs Cl (mg/L) [c] ^{14}C (pMC) vs $\delta^{18}\text{O}$ [d] $\delta^{13}\text{C}$ (‰) vs $^{87}\text{Sr}/^{86}\text{Sr}$. Well nest 1 is light blue, well nest 9 is red, well nest 13 is green, well nest 14 is yellow, well nest 16 is blue, well nest 17 is pink, well nest 19 and 20 are black.

5.2.3 Inferred from noble gases

Noble gas concentrations in groundwater can provide information on residence times, conditions during recharge and inter-aquifer mixing (Mazor and Bosch 1987, Kipfer et al., 2002). They are particularly useful tracers to investigate inter-aquifer mixing and leakage because they are chemically inert and have multiple origins (Marty et al., 2003). Atmospheric derived noble gases comprise the majority of natural waters and are only fractionated by well understood physical/chemical mechanisms, although there are also terrigenous and radiogenic (crustal and mantle) contributions (Mazor and Bosch 1987, Ballentine et al.,

2002, Kipfer et al., 2002). Noble gas dissolution in water is dependent on temperature, pressure and salinity. The concentrations in groundwater are commonly in excess of the expected atmospheric equilibrium, which is termed 'excess air' (Heaton and Vogel 1979, 1981, Kipfer et al., 2002).

Helium isotopes are used in groundwater studies to determine groundwater residence times. Radiogenic ^4He concentrations increase with groundwater residence time and can be used to infer apparent groundwater age up to thousands or millions of years (Osenbruck et al., 1998, Mazor and Bosch 1987, Beyerle et al., 2000, Kipfer et al., 2002). Multiple sources and variable production rates can make interpretation of ^4He groundwater ages complicated. ^3He is produced by the decay of tritium and can be used to date young groundwaters with a residence time of up to 50 years. $^3\text{He}/^4\text{He}$ ratios are high ($^3\text{He}/^4\text{He} > 10^{-7}$) in recharge areas and low elsewhere ($^3\text{He}/^4\text{He} < 10^{-7}$). ^3He can also migrate from volatiles transported from the mantle in regions that have been tectonically active ($^3\text{He}/^4\text{He} > 10^{-5}$) (Kipfer et al., 2002).

Marty et al. (2003) were able to demonstrate the confining nature of the upper Trias-Lias aquitard in the Paris Basin through lack of corresponding high ^3He isotope concentrations in the aquifer above. Many studies have identified groundwater mixing using noble gases combined with other environmental tracers (Mazor et al., 1986, Clark et al., 1997, Althaus et al., 2009, Sultenfuss et al., 2011, Gardner and Heilweil 2014).

Noble gas samples were collected from pastoral production wells as well as mining borefield monitoring and production wells within the Arckaringa Basin between November 2013 and May 2014. The radiogenic ^4He concentrations are presented in Figure 5-4 and $^3\text{He}/^4\text{He}$ ratios are presented in Figure 5-5. It is expected that radiogenic ^4He concentrations increase (and the $^3\text{He}/^4\text{He}$ ratios decrease) along inferred flow paths, demonstrated schematically in Figure 5-1.

The J-K aquifer has the lowest radiogenic ^4He concentrations and highest $^3\text{He}/^4\text{He}$ ratios (but not high enough to infer a mantle contribution) with the high $^3\text{He}/^4\text{He}$ ratios indicative of potential recharge areas. Further to this, radiogenic ^4He concentrations are lowest and the $^3\text{He}/^4\text{He}$ ratios are highest near surface water features. Wells VMS 2, Aries JS, RMS 2, RMS 3 and RMS 4 have very low radiogenic ^4He concentrations and high $^3\text{He}/^4\text{He}$ isotope ratios indicating the J-K aquifer receives some recharge from the nearby surface water features, a finding consistent with Keppel et al., (2015). Well ASMW 3 has the second lowest radiogenic ^4He concentration and a high $^3\text{He}/^4\text{He}$ isotope ratio, indicating some recharge may occur to the J-K aquifer at this location. ASMW3 is in the centre of the basin and may be receiving recharge from an area subject to inundation (the nearest outcropping basement is ~60 km north-west). Wells No 2 Monwell and Millers Creek No2. are located adjacent to a basement high toward the discharge area and had higher radiogenic ^4He concentrations. Wells PMB 02, UTP005-P01 and PK WB 01 have similar radiogenic ^4He concentrations and low $^3\text{He}/^4\text{He}$ ratios. These samples are highly saline from evapotranspiration and water/rock interactions (Keppel et al., 2015). Finally, RMS 1 had the highest radiogenic ^4He concentration and lowest $^3\text{He}/^4\text{He}$ ratio from the J-K aquifer. This well was located close to a regional discharge area near Margaret Springs.

The Boorthanna Formation and basement aquifers show higher radiogenic ^4He concentrations and lower $^3\text{He}/^4\text{He}$ ratios than the J-K aquifer which was expected with increased depth and residence time. RMD 3, No 6 Monwell D, RMD4, 1281 and RMD 7 (Boorthanna Formation) as well as Aries JD and RMD 2 (basement) have high radiogenic ^4He concentrations and low $^3\text{He}/^4\text{He}$ ratios and show a large difference compared to the nested J-K aquifer wells indicating limited connectivity between aquifers at these locations. No 6 Monwell D (Boorthanna Formation) and Aries JD (basement) have similar radiogenic ^4He concentrations and $^3\text{He}/^4\text{He}$ ratios indicating possible connection, consistent with Keppel et al. (2015).

No 20 A, Virgo E5 and Aries C (Boorthanna Formation) and PMB 01 (basement) show the lowest radiogenic ^4He concentrations. PMB 01 has similar radiogenic ^4He concentrations and $^3\text{He}/^4\text{He}$ ratios as the above PMB 02 (J-K aquifer) indicating a potential connection between aquifers. No 20 A Bore has low radiogenic ^4He concentration and had a high $^3\text{He}/^4\text{He}$ ratio and was located next to a basement high, where the Boorthanna Formation was absent, indicating preferential recharge from the J-K aquifer. Virgo E5 and Aries C are both located closer to the inferred recharge area (Keppel et al., 2015) so it would be expected that the radiogenic ^4He concentrations are lower and $^3\text{He}/^4\text{He}$ ratios are higher due to the shorter residence time of the water. Indeed, Virgo E5 has a low ^4He concentration but also the lowest $^3\text{He}/^4\text{He}$ ratios in the Boorthanna Formation which could be explained if the tritiogenic ^3He has had sufficient time to decay. Aries C, located further along the inferred flow path, actually had the lowest radiogenic ^4He concentration and one of the higher $^3\text{He}/^4\text{He}$ ratios for the Boorthanna Formation. This could be an area of aquitard leakage from the J-K aquifer to the Boorthanna Formation which would be consistent with the Sr isotope data in Section 5.2.2. The Stuart Range Formation is ~ 65 m thick at this location so any leakage would most likely be due to secondary permeability.

In summary, the helium isotope signatures in the J-K aquifer reflect proximity to surface water features, indicating recharge may be entering the J-K aquifer through thin or fractured sections of the Bulldog Shale around surface water features. The Boorthanna Formation close to basement highs appear to have recharge occurring. There was connection between the Boorthanna Formation and basement aquifers which likely represents a wider area considering the Boorthanna Formation and basement are in contact throughout the basin. There was minimal connectivity between the Boorthanna Formation and J-K aquifer at the majority of locations, however there appears to be connectivity between Aries C (Boorthanna Formation) and ASMW 3 (J-K aquifer) in the centre of the basin, possibly as a result of localised secondary permeability.

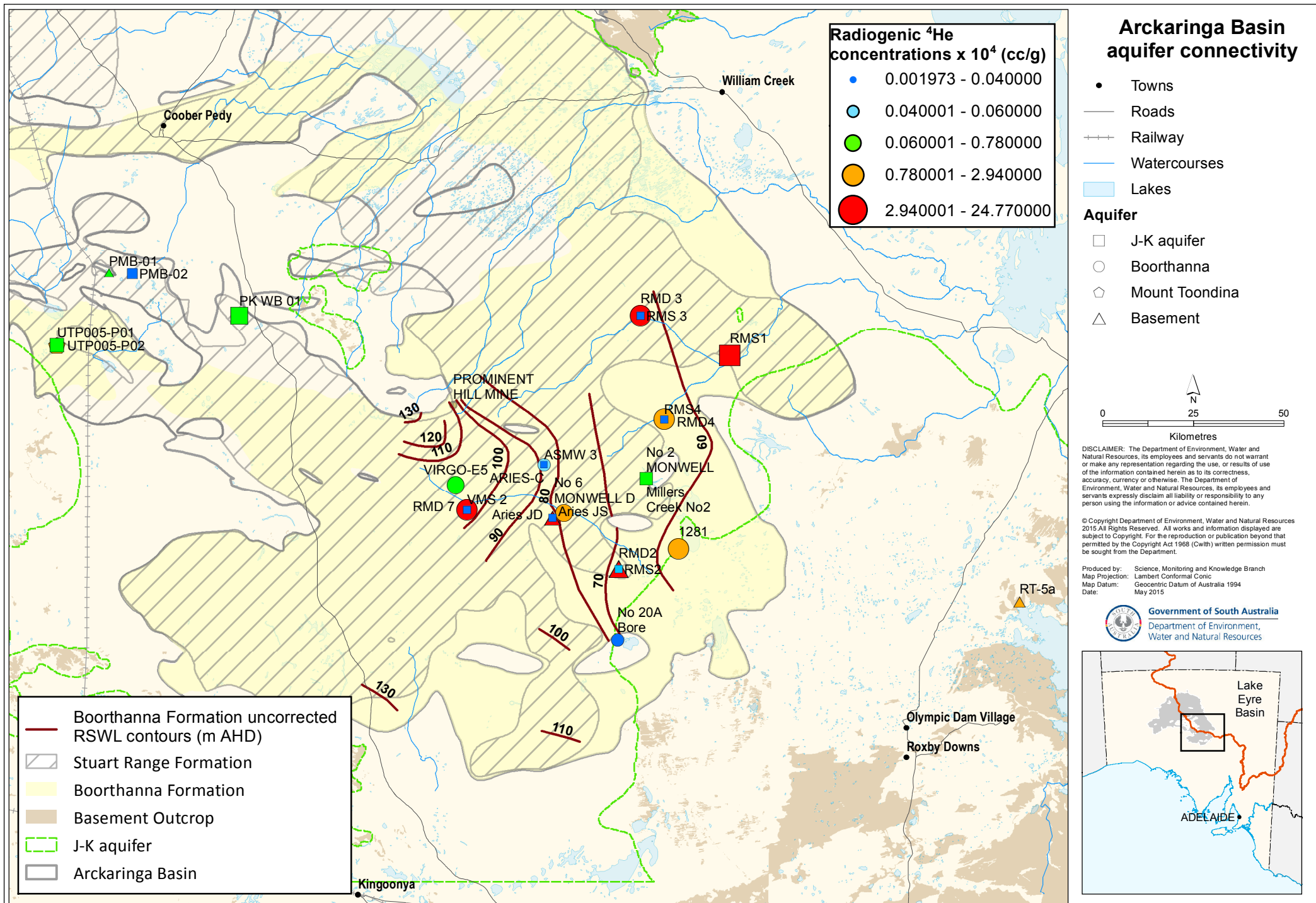


Figure 5-4 Radiogenic ^4He concentrations in the Arckaringa sub-region

6 Conclusions

The Arckaringa Basin connectivity investigation involved evidence from multiple investigation techniques to reveal that there is a low degree of connectivity between the Boorthanna Formation (Arckaringa Basin) and overlying GAB (J-K aquifer).

The key findings in relation to the specific project objectives are:

Objective 1: *Continuously core a hole through the GAB and into the Arckaringa Basin sequence to provide an assessment of vertical flow in the Arckaringa Basin via hydraulic, hydrogeological, hydrochemical and geophysical analysis. Thus providing an improved understanding of inter-connectivity between the Permian sequence and overlying GAB aquifer (J-K aquifer) and the intra-connectivity within the Arckaringa Basin (i.e. between the Stuart Range and Boorthanna Formations)*

A borehole was successfully cored to 110.4 m through the GAB and into the Arckaringa Basin (Stuart Range Formation and Boorthanna Formation). Hydraulic, hydrogeological and hydrochemical analyses contributed to the understanding of intra- and inter-connectivity. Geophysical analysis was not able to be undertaken on the borehole due to hole integrity concerns. Inter-connectivity between the Boorthanna Formation and overlying J-K aquifer exists at the site, however connectivity can be considered to be low with flow (flux) through the aquitard small, in the order of millimetres to centimetres per 1000 years.

Objective 2: *Provide estimates of aquitard parameters for the Stuart Range Formation*

Aquitard (Stuart Range Formation) physical parameters were obtained via laboratory analysis. Porosities ranged from 12.1 to 26 % vol., particle size analysis resulted in sand proportions from 4 to 32 %, silt from 23 to 39 %, and clay ranged from 39 to 70 %, and permeability coefficients (K_v) ranged from 4×10^{-10} to 4×10^{-13} m/s (median of 4.5×10^{-12} m/s). One-dimensional analytical modelling indicated a possible range of K_v 's of 4.8×10^{-13} to 5.3×10^{-12} m/s. One-dimensional numerical modelling of the chloride profile suggested a K_v of 1×10^{-12} m/s. The similarity of results from multiple techniques suggest that the physical and chemical techniques may be approaching a K_v value representative of the regional-scale.

Objective 3: *Evaluate site specific connectivity findings in the context of the greater Arckaringa Basin*

There was a lack of connectivity between the Boorthanna Formation and J-K aquifer at the majority of the well nest locations. One location, well nest 9, provided evidence for inter-aquifer connectivity between the Boorthanna Formation and J-K aquifer. Evidence from the hydraulics and hydrochemistry, particularly the Sr isotopes and noble gases, suggests localised connectivity between the Boorthanna Formation and J-K aquifer most likely due to secondary permeability in the Stuart Range Formation.

There was evidence for connectivity between the Boorthanna Formation and basement at one location which likely represents a wider area considering the Boorthanna Formation and basement are in contact throughout the basin.

Recharge may be entering the J-K aquifer and Boorthanna Formation at multiple locations in the south-east Arckaringa sub-region. The J-K aquifer receives recharge from adjacent surface water features such as ephemeral rivers and creeks. Where the Boorthanna Formation borders basement highs recharge appears to be occurring.

Objective 4: *Provide an assessment of aquifer connectivity using a robust methodology that is transferable across this and other basins, including through deep coal bearing units*

Multiple approaches (hydraulic, environmental tracer methods, analytical modelling and numerical modelling) were utilised in this investigation to constrain aquifer connectivity (flux) estimates and increase confidence in the assessment of aquifer connectivity. These methods have provided a reliable range of estimates for aquitard hydraulic conductivity, enabling the determination of diffuse flux at the site.

Additionally, vertical profiles of aquitard porewater chloride, and to a lesser extent stable isotopes of water, indicate a complex palaeohydrology and associated salinity variability. Chloride profiles were more easily interpreted (than stable isotopes of water), suggesting long-term changes in salinity of aquifers within the Quaternary. The environmental tracer profiles (in this case Cl^-) and associated 1D numerical and analytical modelling were useful for understanding regional palaeohydrogeological conditions in arid areas, which have not been glaciated for hundreds of millions of years. It is thought that this was one of the few investigations in Australia that has undertaken this type of aquitard assessment.

Further work is recommended using the regional Arckaringa Basin numerical model, to test the impact of K_v 's which are around four orders of magnitude less than K_v 's previously assigned to the Stuart Range Formation. Additional investigation of aquitard porewater chemistry is warranted, with regard to an apparent decoupling of Cl^- and stable isotopes of water signatures, and the differences observed between the δ^2H and $\delta^{18}O$ profiles.

Several lines of evidence (porewater chemistry, porewater potential, lithology) indicated aquitard variability and provided justification to simulate profile development using a two-layer analytical solution. Contrary to the overall hydraulic potential for downward flux and Peclet number suggesting a diffusion dominant system at the investigation site; the two-layer analytical solution provided evidence for an upward flux component from the upper portion of the profile, and implied that advection dominates over diffusion. Further work is suggested to investigate the potential for advective flow in the aquitard including; analysis of apparent porewater age and implications for ancient aquitard/aquifer Cl^- concentrations to constrain our regional conceptualisation of groundwater and porewater flow paths, and test this conceptualisation through setting of appropriate boundary conditions for analytical or numerical solutions; and implement and test an advection-dominant solution scheme in MT3DMS for future 1D numerical modelling of the aquitard.

7 Appendices

A. Composite log: unit number 6038-519



LOCATION: Mt Eba Station

EASTING: 560152
GDA 94 Zone 53

LOGGED BY: T Kleinig

CASING HEIGHT (m AGL):

DRILLER: Underdale Drillers Oz

NORTHING: 6686404
GDA 94 Zone 53

DRILL DEPTH (m): 110.4

Outer steel: 0.5

Inner steel: 1.45

DATE COMPLETED: 18/03/2015

ELEVATION (m AHD): ~154

CONSTRUCTED DEPTH (m): 110.4

Data logger: 1.75



Diameter: 95mm

B. The transport equation

Consider a single aquitard layer with coordinate, z , defined downwards from the top towards the bottom at depth $z = L$. It is assumed that the solute, Cl^- , moves by diffusion and advection, with a constant porewater velocity, V , and with respect to time, t , and also just the single space coordinate, z . With a concentration of Cl^- denoted by $C = C(x, t)$ and an effective diffusion coefficient, D_e , diffusive (J_d) and advective fluxes (J_v) are defined respectively by equation (B1).

$$J_d = -D_e \frac{\partial C}{\partial z} \quad \text{and} \quad J_v = VC \quad (\text{B1})$$

and a combined total flux (equation (B2)):

$$J = J_d + J_v = -D_e \frac{\partial C}{\partial z} + VC \quad (\text{B2})$$

positive in the downward z direction.

A mass balance, assuming constant geological matrix properties, then provides the 1D diffusion equation (B3):

$$-\frac{\partial J}{\partial z} = \frac{\partial C}{\partial t}, \quad \text{i.e.} \quad D_e \frac{\partial^2 C}{\partial z^2} - V \frac{\partial C}{\partial z} = \frac{\partial C}{\partial t} \quad (\text{B3})$$

where it is assumed that D_e is constant. In non-dimensional form this equation can be written as (B4):

$$\frac{\partial^2 C}{\partial (z/L)^2} - \frac{VL}{D_e} \frac{\partial C}{\partial (z/L)} = \frac{L^2}{D_e} \frac{\partial C}{\partial t} \quad (\text{B4})$$

which provides three quantities of interest (equation (B5)), Peclet number P_e , diffusion length, α_d , and time constant t_0 :

$$P_e = \frac{|V|L}{D_e}, \quad \alpha_d = \frac{D_e}{|V|}, \quad t_0 = \frac{D_e}{L^2} \quad (\text{B5})$$

Without considering any initial or boundary quantities, these three quantities can be used as a rough guide to the general behaviour of a solution for $C(z,t)$. When $t \gg t_0$, conditions of steady state prevail, and $t = t_0 \text{ --- } 3t_0$ may suffice. When $P_e = 1$ then diffusion dominates advection, and it is often stated that diffusion is dominant for $P_e < 5$ but advection dominant for $P_e > 9$. The diffusive length is a measure of how diffusion can modify the behaviour near a particular point, a small α_d having only a very local effect. This is often useful when considering the impact of altering boundary conditions.

The next step involves solving the transport under particular initial and boundary conditions. In principle these can be general with respect to z for an initial condition C_0 and boundary conditions involving both z and t , C_1 at $z = 0$ and C_2 at $z = L$. However, without any guiding information it will be assumed that all of C_0 , C_1 , C_2 are constant so that the initial (equation (B6)) and boundary conditions (equation (B7)) adopted are:

Initial condition:

$$C(z, 0) = C_0 \quad (\text{B6})$$

Boundary conditions at $z = 0$ and $z = L$:

$$C(0, t) = C_1, \quad C(L, t) = C_2 \quad (\text{B7})$$

The method of solution used is the Laplace transform and its analytical inversion (see, e.g. Carslaw and Jaeger, 1959).

With the definition of the Laplace transform of $C(z,t)$ as equation (B8):

$$U = U(z, p) = L \{C(z, t)\} = \int_0^{\infty} e^{-pt} C(z, t) dt \quad (B8)$$

and its inversion as equation (B9):

$$C = C(z, t) = L^{-1} \{U\} = \frac{1}{2\pi i} \int_{\gamma-i\infty}^{\gamma+i\infty} e^{pt} U(z, p) dp \quad (B9)$$

where γ is small but sufficiently large that all singularities lie to the left of the integration line in the complex p -plane, then the differential equation becomes (equation (B10)):

$$D_e \frac{d^2 U}{dz^2} - V \frac{dU}{dz} - pU = -C_0 \quad (B10)$$

and boundary conditions become equation (B11):

$$U = \frac{C_1}{p} \quad \text{at } z = 0 \quad \text{and} \quad U = \frac{C_2}{p} \quad (B11)$$

The solution can now be written in the form (equations (B12), (B12a) and (B12b)):

$$U = e^{Vz/(2D_e)} \left[A e^{\beta z} + B e^{-\beta z} \right] + \frac{C_0}{p}, \quad \beta = \sqrt{V^2/(4D_e^2) + p/D_e} \quad (B12)$$

$$A = \frac{(C_2' - C_1' e^{-\beta L}) e^{-\beta L}}{p(1 - e^{-2\beta L})} \quad B = \frac{(C_1' - C_2' e^{-\beta L})}{p(1 - e^{-2\beta L})} \quad (B12a)$$

$$C_1' = C_1 - C_0, \quad C_2' = e^{-VL/2D_e} (C_2 - C_0) \quad (B12b)$$

which leads to (equation (B13)):

$$U = e^{Vz/2D_e} \left[\frac{C_1' \sinh \beta(L-z) + C_2' \sinh \beta z}{p \sinh \beta L} \right] + \frac{C_0}{p} \quad (B13)$$

The first form of the solution given by equations (B12), (B12a) and (B12b) are useful for application of numerical methods or by expansion of the denominator into a power series of terms $\exp(-2z\beta L)$ and then to inversion of U into a series of error functions. This is useful for small times, which was not the case here. Examples of such evaluations can be found in Carslaw and Jaeger (1959). Carslaw and Jaeger (1959) also provide evaluations of expressions such as equation (B13) which may done by residue analysis to provide series representations more suitable for large times. In this way the residues arise from $p = 0$ and the zeros of $\sinh \beta L$ in the denominator of equation (B13) to provide the series (equation (B14)):

$$C(z, t) = C_\infty(z) + C_i(z, t) \quad (B14)$$

Where $p = 0$ produces the steady state (equation (B15)):

$$C_{\infty} = \frac{C_1 \left(1 - e^{-V(L-z)/D_e}\right) + C_2 \left(e^{-V(L-z)/D_e} - e^{-VL/D_e}\right)}{\left(1 - e^{-VL/D_e}\right)} \quad (\text{B15})$$

and from $\sinh \beta L = 0$, the transient component (equation (B16)):

$$C_i = 2e^{Vz/2D_e} \sum_{m=1}^{\infty} (-1)^m \frac{m\pi \left[C_1' \sin m\pi((L-z)/L) + C_2' \sin m\pi z/L \right]}{\left(m^2\pi^2 + P_e^2/4\right)} e^{-(m^2\pi^2 + P_e^2/4)t/t_0} \quad (\text{B16})$$

When $V = 0 = P_e$, equations (B15) and (B16) reduce to the solution given in Carslaw and Jaeger (1959).

For subsequent use the diffuse flux component arising from the steady state solution is given by equation (B17):

$$J_{d\infty} = -D_e \frac{dC_{\infty}}{dz} = \frac{V(C_1 - C_2)e^{-V(L-z)/D_e}}{\left(1 - e^{-VL/D_e}\right)} \quad (\text{Bb17})$$

and the total flux, using C_{∞} from equation (B15), is (equation (B18)):

$$J = \frac{V(C_1 - C_2 e^{-VL/D_e})}{\left(1 - e^{-VL/D_e}\right)} \quad (\text{B18})$$

It is noted that the steady solution is obtained easily by directly solving the steady state form of equation (B3) or by multiplying equations (B12) or (B13) by p and then setting $p = 0$.

C. Core descriptions and photographs



Bulldog Shale (12.4-14.4 m): CLAY, dark grey-brown with increased yellow and red-brown mottling, medium to high plasticity, friable, but becoming less friable with depth, blocky, less frequent white gypsum crystal veining < 3 mm, trace sand.



J-K aquifer (18-19.4 m): SAND, grey with orange-brown mottling, increase in fine to medium grain, some coarse grains (fining downwards), poorly sorted, trace clay, trace sub-rounded quartz gravel < 25 mm.



J-K aquifer (31.4-31.8 m): SAND, light grey with orange-brown mottling, medium to coarse grained quartz sand, sub-angular quartz and sandstone gravels < 50 mm.



J-K aquifer (41-44 m): SAND, white-light grey, medium to coarse grained, trace sub-angular quartz gravels < 20 mm, trace clay.



Stuart Range Formation (47-48.5 m): CLAYSTONE, grey with trace orange-brown mottling, consolidated, trace sand, trace sub-rounded to sub-angular quartz and sandstone gravels < 10 mm.



Stuart Range Formation (59.5-62.4 m): CLAYSTONE, grey, consolidated, trace fine to medium grained sand, trace sub-rounded to sub-angular quartz and sandstone gravels < 50 mm.



Stuart Range Formation (65.4-66.1 m):
CLAYSTONE, grey to dark grey, little consolidation, softer, medium to high plasticity, fine to medium grained sand, trace sub-rounded to sub-angular quartz and sandstone gravels < 50 mm.



Stuart Range Formation (77.4-80.4 m):
CLAYSTONE, grey, consolidated, harder, natural fracturing apparent, increase in coarse grained sand, trace possibly granitic gravels < 15 mm.



Stuart Range Formation (90.2-90.8 m):
CLAYSTONE, dark grey, consolidated, < 1 mm interbeds of clays and sands/sandstone with micaceous gravels < 3 mm, variably trace fine to coarse grained sand and sub-rounded to sub-angular quartz and possibly granitic gravels < 30 mm, vitreous in appearance, very fine layering and flaking apparent (possibly indicative of fining sequence), swirls visible.



Stuart Range Formation (93-93.2 m):
CLAYSTONE, dark grey, fine to medium
grained sand, 50 mm thick sandstone
interbeds, brown bands 20 mm thick.



Stuart Range Formation (97.4-97.6 m):
CLAYSTONE, grey with variable brown,
possibly sub-vertical sandstone and
claystone interbeds; sandstone has fine to
coarse grained sand, trace clay and silt;
claystone has trace fine to coarse grained
sand, trace gravel < 3 mm, wavy/swirly
depositional features, poorly sorted.



Stuart Range Formation (100.5-103.5 m):
CLAYSTONE, dark brown-grey, trace fine
to coarse grained sand, trace sub-rounded
to rounded gravels < 40 mm, wavy/swirly
depositional features, poorly sorted.



Boorthanna Formation (106.6-107 m): SANDSTONE, grey, fine to coarse grained sand, moderate percentage of sub-rounded to sub-angular granitic gravels < 15 mm, pyritic inclusions adjacent to gravels, pyritic gravels, poorly sorted.

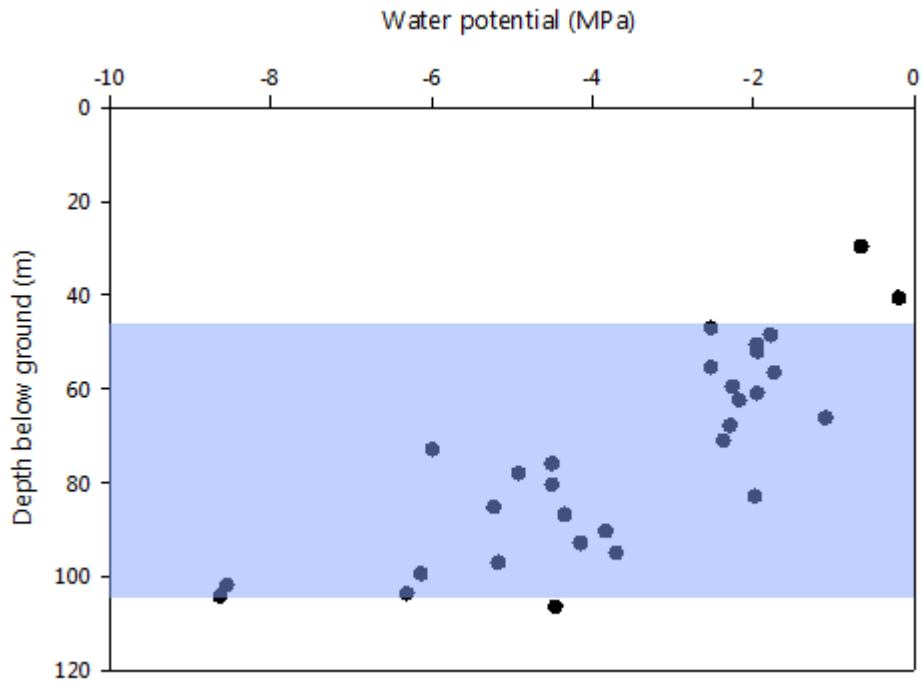


Boorthanna Formation (107.4-110.4 m): SANDSTONE, light grey with white sand, medium to coarse grained sand lenses of variable and uncertain thickness, light grey and grey wavy bedding, trace dark grey claystone 10 mm thick interbeds, fine to coarse grained sand, moderate percentage of sub-rounded to sub-angular granitic gravels < 15 mm, pyritic inclusions adjacent to gravels, pyritic gravels, poorly sorted.

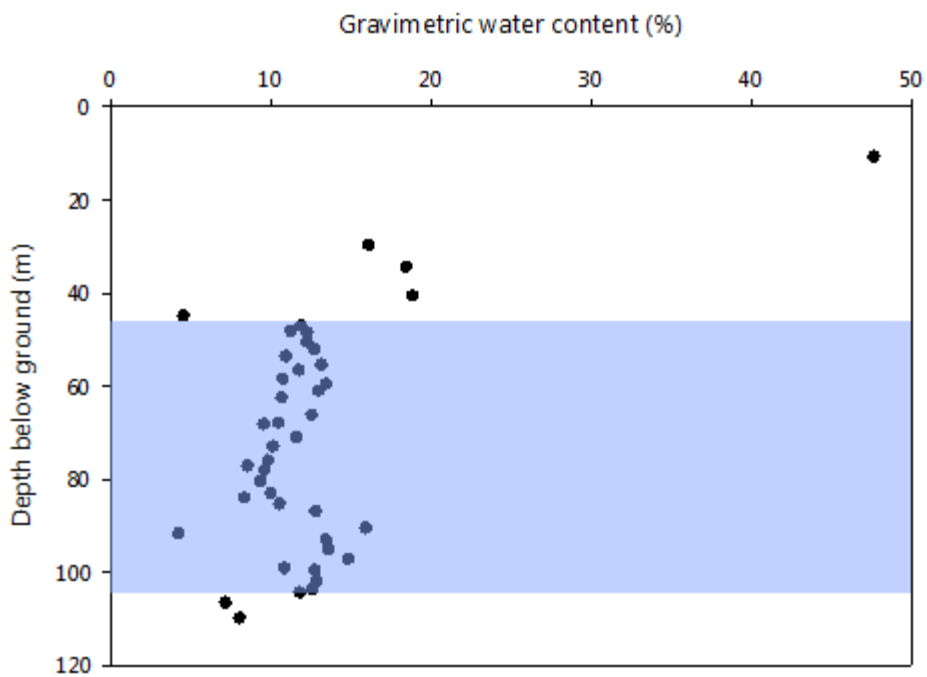
D. Physical parameter plots

Shaded zone corresponds to the interval of the Stuart Range Formation.

Water potential



Gravimetric water content



8 Units of measurement

8.1 Units of measurement commonly used (SI and non-SI Australian legal)

Name of unit	Symbol	Definition in terms of other metric units	Quantity
day	d	24 h	time interval
gigalitre	GL	10^6 m^3	volume
gram	g	10^{-3} kg	mass
hectare	ha	10^4 m^2	area
hour	h	60 min	time interval
kilogram	kg	base unit	mass
kilolitre	kL	1 m^3	volume
kilometre	km	10^3 m	length
litre	L	10^{-3} m^3	volume
megalitre	ML	10^3 m^3	volume
metre	m	base unit	length
microgram	μg	10^{-6} g	mass
microliter	μL	10^{-9} m^3	volume
milligram	mg	10^{-3} g	mass
millilitre	mL	10^{-6} m^3	volume
millimetre	mm	10^{-3} m	length
minute	min	60 s	time interval
second	s	base unit	time interval
tonne	t	1000 kg	mass
year	y	365 or 366 days	time interval

8.2 Shortened forms

AGS	above ground surface
~	approximately equal to
AHD	Australian Height Datum
BP	before present
BGS	below ground surface
BTOC	below top of casing
K	hydraulic conductivity (m/s)
K_v	vertical hydraulic conductivity (m/s)
SMOW	Standard mean ocean water
VSMOW	Vienna standard mean ocean water

9 Glossary

Aquifer — An underground layer of rock or sediment that holds water and allows water to percolate through

Aquifer, confined — Aquifer in which the upper surface is impervious (see 'confining layer') and the water is held at greater than atmospheric pressure; water in a penetrating well will rise above the surface of the aquifer

Aquifer test — A hydrological test performed on a well, aimed to increase the understanding of the aquifer properties, including any interference between wells, and to more accurately estimate the sustainable use of the water resources available for development from the well

Aquifer, unconfined — Aquifer in which the upper surface has free connection to the ground surface and the water surface is at atmospheric pressure

Aquitard — A layer in the geological profile that separates two aquifers and restricts the flow between them

Artesian — An aquifer in which the water surface is bounded by an impervious rock formation; the water surface is at greater than atmospheric pressure, and hence rises in any well which penetrates the overlying confining aquifer

Basin — The area drained by a major river and its tributaries

Bore — See 'well'

¹⁴C — Carbon-14 isotope (percent modern Carbon; pmC)

Confining layer — A rock unit impervious to water, which forms the upper bound of a confined aquifer; a body of impermeable material adjacent to an aquifer; see also 'aquifer, confined'

δD — Hydrogen isotope composition, measured in parts per thousand (‰)

DEWNR — Department of Environment, Water and Natural Resources (Government of South Australia)

EC — Electrical conductivity; 1 EC unit = 1 micro-Siemen per centimetre (μS/cm) measured at 25°C; commonly used as a measure of water salinity as it is quicker and easier than measurement by TDS

Evapotranspiration — The total loss of water as a result of transpiration from plants and evaporation from land, and surface water bodies

Floodout — An area where channelised flow ceases and floodwaters spill across adjacent alluvial plains

GAB — Great Artesian Basin

Geological features — Include geological monuments, landscape amenity and the substrate of land systems and ecosystems

GIS — Geographic Information System; computer software linking geographic data (for example land parcels) to textual data (soil type, land value, ownership). It allows for a range of features, from simple map production to complex data analysis

Groundwater — Water occurring naturally below ground level or water pumped, diverted and released into a well for storage underground; see also 'underground water'

δ²H — Hydrogen isotope composition (deuterium), measured in parts per thousand (‰)

Hydraulic conductivity (K) — A measure of the ease of flow through aquifer material: high K indicates low resistance, or high flow conditions; measured in metres per day

Hydrogeology — The study of groundwater, which includes its occurrence, recharge and discharge processes and the properties of aquifers; see also 'hydrology'

Inter-connectivity — Groundwater interaction between formations from the same basin

Intra-connectivity — Groundwater interaction between formations from different basins

Land — Whether under water or not, and includes an interest in land and any building or structure fixed to the land

LMWL — Local meteoric water line

m AHD — Defines elevation in metres (m) according to the Australian Height Datum (AHD)

Model — A conceptual or mathematical means of understanding elements of the real world that allows for predictions of outcomes given certain conditions. Examples include estimating storm run-off, assessing the impacts of dams or predicting ecological response to environmental change.

Monitoring — (1) The repeated measurement of parameters to assess the current status and changes over time of the parameters measured (2) Periodic or continuous surveillance or testing to determine the level of compliance with statutory requirements and/or pollutant levels in various media or in humans, animals and other living things

$\delta^{18}\text{O}$ — Oxygen isotope composition, measured in parts per thousand (‰)

Observation well — A narrow well or piezometer whose sole function is to permit water level measurements

Palaeochannels — Ancient buried river channels in arid areas of the state. Aquifers in palaeochannels can yield useful quantities of groundwater or be suitable for ASR

Peclet number — ratio of advection to diffusion

Permeability — A measure of the ease with which water flows through an aquifer or aquitard, measured in m^2/d or millidarcies

Potentiometric head — The potentiometric head or surface is the level to which water rises in a well due to water pressure in the aquifer, measured in metres (m); also known as piezometric surface

Production well — The pumped well in an aquifer test, as opposed to observation wells; a wide-hole well, fully developed and screened for water supply, drilled on the basis of previous exploration wells

Recharge area — The area of land from which water from the surface (rainfall, streamflow, irrigation, etc.) infiltrates into an aquifer. See also artificial recharge, natural recharge

Specific storage (S_s) — Specific storativity; the amount of stored water realised from a unit volume of aquifer per unit decline in head; it is dimensionless

Specific yield (S_y) — The volume ratio of water that drains by gravity, to that of total volume of the porous medium. It is dimensionless

Sustainability — The ability of an ecosystem to maintain ecological processes and functions, biological diversity, and productivity over time

TDS — Total dissolved solids, measured in milligrams per litre (mg/L); a measure of water salinity

Tertiary aquifer — A term used to describe a water-bearing rock formation deposited in the Tertiary geological period (1–70 million years ago)

Transmissivity (T) — A parameter indicating the ease of groundwater flow through a metre width of aquifer section

Underground water (groundwater) — Water occurring naturally below ground level or water pumped, diverted or released into a well for storage underground

Vienna Standard Mean Ocean Water (VSMOW) — a water standard defining the isotopic composition of fresh water

Water quality data — Chemical, biological, and physical measurements or observations of the characteristics of surface and groundwaters, atmospheric deposition, potable water, treated effluents, and wastewater, and of the immediate environment in which the water exists

Water quality monitoring — An integrated activity for evaluating the physical, chemical, and biological character of water in relation to human health, ecological conditions, and designated water uses

Water quality standard — A law or regulation that consists of the beneficial designated use or uses of a water body, the numerical and narrative water quality criteria that are necessary to protect the use or uses of that particular water body, and an anti-degradation statement

Well — (1) An opening in the ground excavated for the purpose of obtaining access to underground water. (2) An opening in the ground excavated for some other purpose but that gives access to underground water. (3) A natural opening in the ground that gives access to underground water

10References

- Althaus, R., Klump, S., Onnis, A., Kipfer, R., Purtschert, R., Stauffer, F. and Kinzelbach, W. 2009. Noble gas tracers for characterisation of flow dynamics and origin of groundwater: A case study in Switzerland. *Journal of Hydrology*, 370, 64-72.
- Aquaterra 2009. Prominent Hill Mine regional groundwater model. Prepared for OZ Minerals. Ref. No. A24C7-R001b
- Aquaterra REM 2005. Conceptual hydrogeological model of the Prominent Hill Mine Project. Prepared for Oxiana Ltd. Project No. (BJ)\02
- Aubertin, M., Bussière, B. and Chapuis, R. P. 1996. Hydraulic conductivity of homogenized tailings from hard rock mines, *Canadian Geotechnical Journal*, 33, 470-482.
- Ballentine, C. J., Burgess, R. and Marty, B. 2002. Tracing fluid origin, transport and interaction in the crust. In: Porcelli, D., Ballentine, C. J. and Wieler, R. (eds.) *Noble Gases in Geochemistry and Cosmochemistry*.
- Belperio, AP 2005, Water in Permian palaeochannels draining the Mount Woods Block, Minotaur Exploration Ltd., Adelaide.
- Beyerle, U., Aeschbach-Hertig, W., Imboden, D. M., Baur, H., Graf, T. and Kipfer, R. 2000. A mass spectrometric system for the analysis of noble gases and tritium from water samples. *Environmental Science and Technology*, 34, 2042-2050.
- Boggs, P.T., Donaldson, J.R. and Schnabel, R.B. 1989. Algorithm 676: ODRPACK: software for weighted orthogonal distance regression. *ACM Transactions on Mathematical Software*, 15, 348-364.
- Carslaw, H.S. and Jaeger, C.J. 1959. *Conduction of Heat in Solids*, Oxford University Press, Oxford.
- Cherry, J. A. and Parker, B. L. 2004. Role of Aquitards in the Protection of Aquifers from Contamination: A "State of Science" Report, Denver, USA, Awwa Research Foundation.
- Clark, J. F., Stute, M., Schlosser, P. and Drenkard, S. 1997. A tracer study of the Floridan aquifer in southeastern Georgia: Implications for groundwater flow and paleoclimate. *Water Resources Research*, 33, 281-289.
- Commonwealth of Australia. 2014. Aquifer connectivity within the Great Artesian Basin, and the Surat, Bowen and Galilee Basins, Background review, Commonwealth of Australia 2014, Canberra.
- CRAE 1987. Arkeeta No. 1 Well completion report. CRAE Report No. 302889.
- Crosbie, R., Morrow, D., Cresswell, R., Leaney, F., Lamotagne, S., and Lefournour, M. 2012. New insights to the chemical and isotopic composition of rainfall across Australia, CSIRO Water for a Healthy Country Flagship, Australia
- Department of Manufacturing, Innovation, Trade, Resources and Energy (DMITRE) 2011. Arckaringa Basin. Petroleum and Geothermal in South Australia.
http://www.pir.sa.gov.au/petroleum/prospectivity/basin_and_province_information/prospectivity_arckaringa
- Domenico, P. A. and Schwartz, F. W. 1998. *Physical and Chemical Hydrogeology*, New York, USA, John Wiley & Sons, Inc.
- Dogramaci, S. S. and Herczeg, A. L. 2002. Strontium and carbon isotope constraints on carbonate-solution interactions and inter-aquifer mixing in groundwaters of the semi-arid Murray Basin, Australia. *Journal of Hydrology*, 262, 50-67.
- Drexel, J.F. and Preiss, W.V. (eds). 1995. *The geology of South Australia: Volume 2, The Phanerozoic*, South Australia Department of Mines and Energy Resources, Adelaide
- Freeze, R. A. and Cherry, J. A. 1979. *Groundwater*, Englewood Cliffs, N.J. USA, Prentice-Hall.

- Gardner, P. M. and Heilweil, V. M. 2014. A multiple-tracer approach to understanding regional groundwater flow in the Snake Valley area of the eastern Great Basin, USA. *Applied Geochemistry*, 45, 33-49.
- Gee, G.W. and Bauder, J.W. 1986. *Methods of Soil Analysis: Part 1-Physical and Mineralogical Methods*, SSSA Book Series 5.15.1:383-411. doi:10.2136/sssabookser5.1.2ed.c15
- Habermehl, MA 1980. 'The Great Artesian Basin, Australia', *BMR Journal of Geology and Geophysics*, vol. 5, pp. 9–37.
- Hantush, M. S. 1966. Analysis of data from pumping tests in anisotropic aquifers. *Journal of Geophysical Research*, 71, 421-426.
- Hantush, M. S. 1967. Flow of groundwater in relatively thick leaky aquifers. *Water Resources Research*, 3, 583-590.
- Harbaugh, A.W., 2005, MODFLOW-2005, The U.S. Geological Survey modular ground-water model—the Ground-Water Flow Process: U.S. Geological Survey Techniques and Methods 6-A16, variously p.
- Harrington, G. A., Gardner, W. P., Smerdon, B. D. and Hendry, M. J. 2013. Palaeohydrogeological insights from natural tracer profiles in aquitard porewater, Great Artesian Basin, Australia, *Water Resources Research*, 49, 4054-4070
- Heaton, T. H. E. and Vogel, J. C. 1979. Gas concentrations and ages of groundwaters in beaufort group sediments, South Africa, *Water SA*, 5, 160-170.
- Heaton, T. H. E. and Vogel, J. C. 1981. Excess air in groundwater. *Journal of Hydrology*, 50, 201-216.
- Hendry, M. J., Kelln, C. J., Wassenaar, L. I. and Shaw, J. 2004. Characterizing the hydrogeology of a complex clay-rich aquitard system using detailed vertical profiles of the stable isotopes of water. *Journal of Hydrology*, 293, 47-56.
- Hendry, M.J. and Wassenaar, L.I. 1999. Implications of the distribution of δD in porewaters for groundwater flow and the timing of geologic events in a thick aquitard system. *Water Resources Research*, 35, 1751-1760.
- Hendry, M.J. and Wassenaar, L.I. 2011. Millennial-scale diffusive migration of solutes in thick clay-rich aquitards: evidence from multiple environmental tracers. *Hydrogeology Journal*, 19, 259-270.
- Herczeg, A. L., Love, A. J., Allan, G., Fifield, L. K. and Int Atom Energy, A. 1996. Uranium-234/238 and chlorine-36 as tracers of inter-aquifer mixing: Otway Basin, South Australia. *Isotopes in Water Resources Management*, Vol 2.
- Howe, P. E., Baird, D. J. and Lyons, D. J. 2008. Hydrogeology of the Southeast Portion of the Arckaringa Basin and Southwest Portion of the Eromanga Basin, South Australia. *Water Down Under*. Adelaide.
- International Atomic Energy Association (IAEA)/World Meteorological Organisation (WMO) (2015). *Global Network of Isotopes in Precipitation*. The GNIP Database. Accessible at: <http://www.iaea.org/water>
- Jack, RL 1923. The composition of the waters of the Great Australian Artesian Basin in South Australia and its significance. *Transactions of the Royal Society of South Australia*, pp. 316–321.
- Kellett, J, Veitch, S, McNaught, I and van der Voort, A 1999. Hydrogeological Assessment of a Region in Central Northern South Australia, BRS Australia, Canberra.
<http://www.ret.gov.au/resources/documents/radioactive_waste/hydrogeological_assessment_of_a_region_1999.pdf>
- Keppel, M., Wohling, D., Jensen-Schmidt, B. and Sampson, L., 2015, A hydrogeological characterisation of the Arckaringa Basin, DEWNR Technical report 2015/03, Government of South Australia, through Department of Environment, Water and Natural Resources, Adelaide
- Kipfer, R., Aeschbach-Hertig, W., Peeters, F. and Stute, M. 2002. Noble gases in lakes and ground waters. In: Porcelli, D., Ballentine, C. J. and Wieler, R. (eds.) *Noble Gases in Geochemistry and Cosmochemistry*. Chantilly: Mineralogical Society of America.

- Konikow, L. F. and Arevalo, J. R. 1993. Advection and diffusion in a variable-salinity confining layer. *Water Resources Research*, 29, 2747-2761.
- Love, A. J., Herczeg, A. L., Armstrong, D., Stadter, F. and Mazor, E. 1993. Groundwater-flow regime within the Gambier Embayment of the Otway basin, Australia - evidence from hydraulics and hydrochemistry. *Journal of Hydrology*, 143, 297-338.
- Love, A. J., Herczeg, A. L., Leaney, F. W., Stadter, M. F., Dighton, J. C. and Armstrong, D. 1994. Groundwater residence time and paleohydrology in the Otway Basin, South Australia - H-2, O-18 and C-14 data. *Journal of Hydrology*, 153, 157-187.
- Love, A. J., Wohling, D., Fulton, S., Rousseau-Guetin, P. and De Ritter, S. (eds) 2013a, *Allocating Water and Maintaining Springs in the Great Artesian Basin, Volume II: Groundwater Recharge, Hydrodynamics and Hydrochemistry of the Western Great Artesian Basin*, National Water Commission, Canberra.
- Love, A. J., Shand, P., Crossey, L., Harrington, G. A. and Rousseau-Guetin, P. (eds) 2013b, *Allocating Water and Maintaining Springs in the Great Artesian Basin, Volume III: Groundwater Discharge of the Western Great Artesian Basin*, National Water Commission, Canberra.
- Lyons, D and Hulme, K 2010. Hydrogeology of the south-eastern Arckaringa Basin and overlying south-western Eromanga Basin, and the implications for sustainable water supply development in central South Australia. Handbook, National Groundwater Conference. 31st October – 4th November, Canberra. Pg 207.
- Magee, J. W., Miller, G. H., Spooner, N. A. and Questiaux, D. 2004. Continuous 150 ky monsoon record from Lake Eyre, Australia: Insolation-forcing implications and unexpected Holocene failure. *Geology*, 32, 885-888.
- Marty, B., Dewonck, S. and France-Lanord, C. 2003. Geochemical evidence for efficient aquifer isolation over geological timeframes. *Nature*, 425, 55-58.
- Mazor, E. and Bosch, A. 1987. Noble gases in formation fluids from deep sedimentary basins: a review. *Applied Geochemistry*, 2, 621-627.
- Mazor, E., Jaffé, F. C., Fluck, J. and Dubois, J. D. 1986. Tritium corrected ¹⁴C and atmospheric noble gas corrected ⁴He applied to deduce ages of mixed groundwaters: Examples from the Baden region, Switzerland. *Geochimica et Cosmochimica Acta*, 50, 1611-1618.
- Mazurek, M., Alt-Epping, P., Bath, A., Gimmi, T., Waber, H. N., Buschaert, S., De Cannière, P., De Craen, M., Gautschi, A., Savoye, S., Vinsot, A., Wemaere, I. and Wouters, L. 2011. Natural tracer profiles across argillaceous formations. *Applied Geochemistry*, 26, 1035-1064.
- Meyboom, P. 1966. Unsteady groundwater flow near a willow ring in hummocky moraine. *Journal of Hydrology*, 4, 38-40, IN5-IN6, 41-62.
- Neuman, S. P. and Witherspoon, P. A. 1969. Applicability of current theories of flow in leaky aquifers. *Water Resources Research*, 5, 817-829.
- Neuman, S. P. and Witherspoon, P. A. 1972. Field determination of hydraulic properties of leaky multiple aquifer systems. *Water Resources Research*, 8, 1284-1298.
- Neuzil, C. E. 1986. Groundwater-flow in low-permeability environments. *Water Resources Research*, 22, 1163-1195.
- Osenbruck, K., Lippmann, J. and Sonntag, C. 1998. Dating very old porewaters in impermeable rocks by noble gas isotopes. *Geochimica Et Cosmochimica Acta*, 62, 3041-3045.
- Post, V., Kooi, H. and Simmons, C. 2007. Using hydraulic head measurements in variable-density ground water flow analyses. *Ground Water*, 45, 664-671

- Post, V. E. A. and von Asmuth, J. R. 2013. Review: Hydraulic head measurements-new technologies, classic pitfalls. *Hydrogeology Journal*, 21, 737-750
- Purczel C, 2015, Arckaringa Basin Numerical Groundwater Model 2014, DEWNR Technical report 2015/05, Government of South Australia, through Department of Environment, Water and Natural Resources, Adelaide
- REM 2007. Prominent Hill region conceptual hydrogeological model. Prepared for Oxiana Limited. Resource and Environmental Management Pty Ltd.
- Sampson, L., Wohling, D., Jensen-Schmidt, B. and Fulton, S. 2012, South Australian and Northern Territory Great Artesian Basin (Eromanga Basin) Hydrogeological Map. Department of Environment, Water and Natural Resources, South Australian Government.
- Sampson L, Wohling D, Jensen-Schmidt B and Keppel M, 2014, South Australia Arckaringa Basin Hydrogeological Map – Part 1 and Part 2. Department of Environment, Water and Natural Resources, South Australian Government.
- Shand, P., Darbyshire, D. P. F., Love, A. J. and Edmunds, W. M. 2009. Sr isotopes in natural waters: Applications to source characterisation and water-rock interaction in contrasting landscapes. *Applied Geochemistry*, 24, 574-586.
- Sinclair Knight Merz (SKM) 2009. Prominent Hill Regional Conceptual Hydrogeological Model. Prepared for OZ Minerals. Project No. VE23235
- Sultenfuss, J., Purtschert, R. and Fuhrboter, J. F. 2011. Age structure and recharge conditions of a coastal aquifer (northern Germany) investigated with Ar-39, C-14, H-3, He isotopes and Ne. *Hydrogeology Journal*, 19, 221-236.
- Tucker, L.R. 1997. Correlation of Permian sandstones in the Officer, Arckaringa and Pedirka Basins. Department of Mines and Energy Resources South Australia, Adelaide Report No. DME 493/96.
- van der Kamp, G. 2001. Methods for determining the in situ hydraulic conductivity of shallow aquitards – an overview. *Hydrogeology Journal*, 9, 5-16.
- Wohling, D., Keppel, M., Fulton, S., Costar, A., Sampson, L. and Berens, V. 2013. Australian Government Initiative on Coal Seam Gas and Large Coal Mining - Arckaringa Basin and Pedirka Basin Groundwater Assessment Projects. Adelaide: Government of South Australia, through Department of Environment, Water and Natural Resources.

